UNIVERSIDADE FEDERAL DE SANTA CATARINA
CENTRO DE CIÊNCIAS DA SAÚDE
PROGRAMA DE PÓS-GRADUAÇÃO EM FARMÁCIA

TECHNISCHE UNIVERSITÄT BERLIN
FACULTY III PROCESS SCIENCES

Louise Rubia Probst Purnhagen

Role of zinc in the tryptophan pathway: *in vivo* and *in vitro* studies

Florianópolis/Berlin
2021

Role of zinc in the tryptophan pathway: *in vivo* and *in vitro* studies

vorgelegt von:

M. Sc. Louise Rubia Probst Purnhagen

von der Fakultät III – Prozesswissenschaften
der Technischen Universität Berlin
zur Erlangung des akademischen Grades

Doktor der Naturwissenschaften

- Dr. rer. nat. –

genehmigte Dissertation

Promotionsausschuss:

Vorsitzender:

Gutachterin: Dr. Claudia Keil - TU Berlin

Gutachterin: Prof. Dr. Tânia Beatriz Creczynski Pasa - UFSC

Gutachterin: Prof. Dr. Elaine Hatanaka - Cruzeiro do Sul University

Tag der wissenschaftlichen Aussprache: 29. Januar 2021

Florianópolis/Berlin 2021

Louise Rubia Probst Purnhagen

Role of zinc in the tryptophan pathway: *in vivo* and *in vitro* studies

Tese submetida ao Programa de Pós-graduação em Farmácia da Universidade Federal de Santa Catarina e pela Instituição Technische Universität Berlin em regime de cotutela para a obtenção do título de doutor.
Orientadores: Prof.(a) Dr.(a) Fabíola Branco Filippin Monteiro (UFSC) e Prof. Dr. Hajo Haase (TU Berlin)
Coorientador: Dr.(a) Adny Henrique Silva (UFSC)

Florianópolis/Berlin
2021

Louise Rubia Probst Purnhagen

Role of zinc in the tryptophan pathway: *in vivo* and *in vitro* studies

Doctoral thesis submitted to the Federal University of Santa Catarina and Technische Universität Berlin as a final requirement for obtaining the Doctor degree under the agreement between the two universities.

Supervisor: Prof. Dr. Fabíola Branco Filippin Monteiro (UFSC) and Prof. Dr. Hajo Haase (TU Berlin)

Co-Supervisor: Dr. Adny Henrique Silva (UFSC)

Florianópolis/Berlin

2021

Ficha de identificação da obra elaborada pelo autor,
através do Programa de Geração Automática da Biblioteca Universitária da UFSC.

Purnhagen, Louise Rubia Probst
Role of zinc in the tryptophan pathway: *in vivo* and *in vitro* studies / Louise Rubia Probst Purnhagen ; orientadora, Fabíola Branco Filippin Monteiro , orientador, Hajo Haase , coorientadora, Adny Henrique Silva , 2021.
138 p.

Tese (doutorado) - Universidade Federal de Santa Catarina, Centro de Ciências da Saúde, Programa de Pós Graduação em Farmácia, Florianópolis, 2021.

Inclui referências.

Trabalho elaborado em regime de co-tutela.

1. Farmácia. 2. Obesidade e Tecido Adiposo. 3. Deficiência de Zinco. 4. Via do Triptofano. 5. Distúrbios Neurocomportamentais. I. Monteiro , Fabíola Branco Filippin . II. Haase , Hajo . III. Silva , Adny Henrique . IV. Universidade Federal de Santa Catarina. Programa de Pós Graduação em Farmácia. V. Título.

Louise Rubia Probst Purnhagen

Role of zinc in the tryptophan pathway: *in vivo* and *in vitro* studies

This work at the doctoral level was evaluated and approved by examining members composed of the following members:

Prof. Dr. Tânia Beatriz Creczynski Pasa

UFSC

Dr. Claudia Keil

TU Berlin

Prof. Dr. Elaine Hatanaka

Cruzeiro do Sul University

We certify that this is the original and final version of the final work, which was deemed appropriate to obtain the title of Doctor.

Documento assinado digitalmente
Fabiola Branco Filippin
Data: 21/05/2021 11:59:15-0300
CPF: 027.645.219-44
Verifique as assinaturas em https://v.ufsc.br

Postgraduate Program in Pharmacy UFSC

_____

Prof. Dr. Aleksander Gurlo

Dean of Faculty III Process Sciences Program TU Berlin

Documento assinado digitalmente
Fabiola Branco Filippin
Data: 21/05/2021 12:00:48-0300
CPF: 027.645.219-44
Verifique as assinaturas em https://v.ufsc.br

Prof. Dr. Fabíola Branco Filippin Monteiro (UFSC – Supervisor)

_____

Prof. Dr. Hajo Haase (TU Berlin – Supervisor)

Florianópolis/Berlin, 2021

ACKNOWLEDGMENTS

This thesis is the outcome of the work of a considerable number of people who contributed to the development of this study. Now, it is time that I have the opportunity to demonstrate my gratitude to those who contributed during my doctoral journey.

First, I would like to acknowledge my two advisors, Dr. Fabíola B. F. Monteiro and Dr. Hajo Haase, for all their support and guidance during the formulation and conclusion of this project and throughout my entire post-graduate school career. Both of them are my sources of inspiration, wisdom, knowledge, and understanding. I demonstrate my gratitude to my co-supervisor. Dr. Adny H. Silva, for her guidance and instruction. I would like to thank Dr. Claudia Keil for her immense support. Her help was crucial to the development of this thesis. I am speechless and will always be thankful for her support.

I would also like to thank my qualification committee members, Prof. Dr. Maria Luiza Bazzo, Prof. Dr. Áurea Elizabeth Linder, Prof. Dr. Dirleise Colle, and Prof. Dr. Manuella Pinto Kaster for their thoughtful critiques and helpful insights. In particular, my examiners Dr. Tânia Beatriz Creczynski Pasa, Dr. Claudia Keil, and Dr. Elaine Hatanaka, who kindly accepted to be part of the final evaluation.

I also thank our collaborators Prof. Dr. Beatriz Garcia Mendes Borba for HPLC analyses, Prof. Dr. Ana Carolina Rabello de Moraes for statistical analyses, Laura S. Assunção and Marjorie G. P. Marin for *in vivo* assays, and Najla A. Saleh and Caroline D. Siqueira for ELISA analyses. I am also grateful to Michele P. Rode and Júlia Cisilotto for sharing their RT-PCR expertise and Dr. Cristiane Ribeiro de Carvalho for sharing her behavioral neuroscience expertise. I thank them for their time, engagement, and genuine interest in my research topic. I am also indebted to the LAMEB team for their assistance in histological analyses. Moreover, I am so grateful to have worked in the laboratories of Prof. Dr. Tânia Beatriz Creczynski-Pasa and Prof. Dr. Roger Walz. I would like to thank Prof. Nils Cordes, who provided A172 cells, and Anna Happe-Kramer, who provided T98G cells. I acknowledge my friends and colleagues who made my laboratory journey memorable: my Brazilian lab mates Carol, Laura, Marjorie, Bianca, Tamara, Daiane, Ícaro, Najla, Michele, Júlia, Tânia, Rafael, Anne, Leônidas, Alex, and Gabriela. My German lab mates, Wiebke, Thomas, Chris, Natascha, Cathrin, and Madlen. And all my colleagues who were willing to listen, offer me suggestions, and share their knowledge. Special thanks to Maria, she is wonderfully motivated, dedicated who never faltered or complained when I asked about many doubts that I had. Her interest, support, and encouragement helped me maintain momentum and stay on track to accomplish this project in

one year and three months in Germany. Your contribution to my life is immeasurable, you are ever my friend. My office mates Frau Lohmann, who kindly invited me to have some social moments, Dr. Güdog Yücesan, and lab technicians Timo, Susanne, and Constanze.

On a personal note, I thank my daughter for understanding the period that we stayed separated, but at that time she showed me how she is turning into such a brave and strong woman. I am so proud of her. I would also like to thank, Alex, my boyfriend, for his entire patience, mainly support and understanding throughout this study and my entire postgraduate school career. Always making me laugh when I needed and always helped me keep things in perspective. I am also greatly indebted to my family, my oma, my father and his wife, my cousin Cibele and Patricia, my uncle César, and my relatives for their support and prayers. My JJ friends who went to Germany with me to do our Ph.D.: Gustavo, Paula, Ana Paula, Renata, Natan, Everton, Larissa, and Victor. I would like to say thank you to my best friends, who I met during my Ph.D. course: Patrícia, Tamila, Valdelúcia, Nádia, and Gabriela for their endless encouragement.

Above all, I cannot forget to express my gratitude to the Pharmacy Postgraduate Program of the Federal University of Santa Catarina and the Faculty III Process Sciences Program of the Technische Universität Berlin.

I am grateful to the Brazilian Federal Agency for Support and Evaluation of Graduate Education (CAPES, *Coordenação de Aperfeiçoamento de Pessoal de Nível Superior*), the Brazilian National Council for Scientific and Technological Development (CNPq, *Conselho Nacional de Desenvolvimento Científico e Tecnológico*), and Deutscher Akadesmischer Austauschdienst (DAAD) for funding this project.

Finally, I thank God for the numerous blessings that He has bestowed upon me throughout my thesis journey.

RESUMO

A obesidade é um distúrbio multifatorial que envolve fatores hereditários e ambientais e estilo de vida; seus efeitos adversos não são apenas sociais ou psicológicos, mas também relacionados a presença de comorbidades como diabetes tipo 2 e distúrbios neurológicos, sendo considerado pela Organização Mundial da Saúde como uma epidemia global. Nos últimos anos, vários trabalhos relatam uma relação entre deficiência de zinco (Zn) e obesidade em humanos. A obesidade denota expansões desproporcionais do tecido adiposo branco com hipertrofia adipocitária e está associada à inflamação crônica de baixo grau, caracterizada por concentrações significativas de citocinas pró-inflamatórias circulantes. A produção de citocinas pró-inflamatórias provenientes do tecido adiposo hipertrofiado pode resultar na expressão e ativação periférica ou central da enzima indoleamina 2,3-dioxigenase (IDO) na via do triptofano (Trp), levando à um aumento nas concentrações de quinurenina (Quin), promovendo alterações neurocomportamentais. Nesse contexto, o presente estudo examina *in vivo* e *in vitro* o papel do Zn em certos aspectos da conversão metabólica do Trp. No primeiro estudo, foram utilizados camundongos Swis albino expostos a uma dieta padrão (SD), dieta padrão deficiente em Zn (SD-ZD), dieta hiperlipídica (HFD) e dieta hiperlipídica deficiente em Zn (HFD-ZD) por oito semanas. Demonstrou-se que os grupos HFD e HFD-ZD tiveram um aumento na adiposidade, bem como na circunferência abdominal, apresentando hipertrofia do tecido adiposo e apresentaram um aumento nas concentrações de leptina sérica. Em relação à conversão de Trp em Quin periférica, não houve alterações significativas nos grupos expostos as dietas hiperlipídicas. Foram investigados os efeitos das dietas hiperlipídicas em modelo comportamental como o teste de respingo (splash test). Enquanto o grupo HFD não demostrou alterações comportamentais, o grupo HFD-ZD demonstrou comportamentos anedônicos no teste de respingo. Esses resultados sugerem que, pelo menos em camundongos, a obesidade em combinação com a deficiência de Zn desacelera os impulsos de autocuidado e comportamentos motivacionais. O tratamento com fluoxetina foi capaz de reverter o comportamento anedônico no teste de respingo e diminuir as concentrações de leptina sérica e aumentar as concentrações de adiponectina sérica em animais que receberam HFD-ZD. O papel do Zn livre na regulação da via das Quin foi investigado no estudo *in vitro*. Houve um aumento nas concentrações de Quin e uma diminuição nas concentrações de Trp nos sobrenadantes de células de glioma cerebral T98G e A172 mantidas sob condições de Zn suficiente ou deficiente sendo tratadas com sobrenadante de macrófagos THP-1 estimulados por lipopolissacarídeo (LPS). Concluiu-se que o Zn não tem efeito direto no catabolismo do Trp. No entanto, efeitos indiretos foram observados em um experimento diferente. Quando as células T98G foram tratadas com sobrenadante de macrófagos THP-1 deficientes em Zn estimulados por LPS, houve um aumento nos níveis de Quin e na razão Quin/Trp no sobrenadante da cultura celular T98G. Como descrito na literatura, o LPS ativa a cascata de sinalização NF-κB, resultando na produção e secreção de citocinas pró-inflamatórias no meio de cultura em THP-1 macrófagos. De fato, a RT-PCR revelou que os genes que codificam citocinas pró-inflamatórias (*IL6*, *TNFA* e *IFNG*) foram expressos em macrófagos THP-1 estimulados por LPS, tanto em condições de Zn suficiente quanto deficiente. Os resultados mostraram concentrações aumentadas de IL-6 no sobrenadante e uma expressão aumentada de *IFNG* em macrófagos THP-1 deficientes em Zn estimulados por LPS em comparação com células adequadas em Zn. Por fim, é sugerido que uma combinação de citocinas pró-inflamatórias podem estar significativamente envolvidas na potencialização da conversão do triptofano pela via das Quin em células T98G. Estes resultados fornecem evidências adicionais que implicam a deficiência de Zn e inflamação de baixo grau associado à obesidade no desenvolvimento de distúrbios neurológicos.

Palavras-chave: Obesidade. Deficiência de Zinco. Distúrbios Neurocomportamentais.

RESUMO EXPANDIDO

Introdução

A abundância de alimentos de alta densidade energética e o estilo de vida cada vez mais sedentário das sociedades ocidentais modernas estão intimamente relacionados à epidemia de obesidade (LEISEGANG, 2019). A obesidade também está associada à deficiência de Zn (DI MARTINO *et al*., 1993; MARREIRO *et al*., 2002; 2004). O Zn pode estar implicado no metabolismo adiposo, contribuindo para a exacerbação da resistência à insulina e o desenvolvimento de um estado pró-inflamatório (TALLMAN e TAYLOR 2003; LIU *et al*., 2013). A obesidade está associada a um estado crônico de inflamação de baixo grau caracterizado por secreção anormal de mediadores pró-inflamatórios, como fator de necrose tumoral-alfa (TNF-α) e interleucina (IL)-6 tanto no tecido adiposo como no soro de animais e humanos (CINTI, 2005). Pacientes obesos com baixa ingestão de Zn na dieta apresentaram uma condição inflamatória sistêmica marcada por um aumento de IL-1α, IL-1β e IL-6 em células mononucleares do sangue periférico (COSTARELLI *et al.*, 2010). A obesidade é um fator de risco para várias comorbidades, incluindo diabetes, doenças cardiometabólicas e distúrbios neurológicos. Os sintomas depressivos aparecem com uma taxa de prevalência mais elevada quando comparados com outros transtornos observados em indivíduos obesos (COHEN, 2010). Os mecanismos fisiopatológicos da obesidade e da função cognitiva ainda precisam ser totalmente compreendidos. Recentemente, Mangge *et al*. (2014) demonstraram uma relação entre o catabolismo do triptofano (Trp) e a inflamação imuno-mediada relacionada à obesidade. Trp é convertido pela indoleamina 2,3-dioxigenase-1 (IDO) resultando em quinurenina (Quin) como um produto intermediário (SAINIO *et al*., 1996; BADAWY, 2017). O aumento da expressão/ativação da IDO por citocinas pró-inflamatórias periféricas ou centrais pode causar uma mudança para a via das quinureninas, aumentando a produção de Quin e, consequentemente, levando à depleção de serotonina; esses efeitos são provavelmente responsáveis por alterações emocionais e cognitivas relevantes em pacientes obesos (JENKINS *et al*., 2016). De acordo com a literatura, indivíduos com deficiência dietética de Zn estão sujeitos a alterações comportamentais. Há uma relação entre o catabolismo do Trp e a inflamação imunomediada associada à obesidade, que, por sua vez, pode aumentar a expressão e ativação da IDO. A presente tese teve como objetivo realizar estudos *in vivo* e *in vitro* para avaliar o papel do Zn na conversão metabólica do Trp pela via das quinureninas e investigar até que ponto a deficiência de Zn associada a obesidade pode desencadear distúrbios comportamentais.

Objetivos

Esta tese teve como objetivo investigar a influência da deficiência de Zn associada a obesidade e o desenvolvimento de alterações comportamentais. A pesquisa foi dividida em dois subestudos, como segue: um estudo *in vivo* investigando a influência da deficiência de Zn na conversão metabólica do Trp pela via das quinureninas em camundongos obesos alimentados com uma dieta hiperlipídica (HFD) ou uma dieta hiperlipídica deficiente em Zn (HFD-ZD); e um estudo *in vitro* avaliando os efeitos da deficiência de Zn na conversão metabólica do Trp pela via das quinureninas em uma combinação de dois subconjuntos de linhagens celulares humanas, macrófagos THP-1 e células de glioblastoma A172 / T98G.

Metodologia

Para o estudo *in vivo*, os animais (n = 10 por grupo) foram aleatoriamente designados a uma das quatro diferentes dietas por 8 semanas: dieta padrão (SD), dieta padrão deficiente em Zn (SD-ZD), dieta hiperlípidica (HFD), dieta hiperlípidica deficiente em Zn (HFD-ZD). O peso corpóreo, comprimento naso-anal e circunferência abdominal foram registrados uma vez por

semana. Ao final do período experimental, os camundongos (n = 5 por grupo) foram submetidos ao teste de respingo (splash test) para avaliação comportamental e o sangue foi coletado para avaliação dos parâmetros bioquímicos e hematológicos. Na segunda parte do estudo *in vivo*, os camundongos remanescentes (n = 5 por grupo) foram mantidos com suas respectivas dietas e foram submetidos a tratamento com cloridrato de fluoxetina (antidepressivo). Após duas semanas os camundongos foram submetidos a avaliação comportamental pelo teste de respingo (splash test) e as amostras de sangue foram coletadas para análise bioquímica.
Para o estudo *in vitro* avaliou-se os efeitos da deficiência de Zn na conversão metabólica do Trp pela via das Quin. Os ensaios *in vitro* de estimulação de glioblastoma humano foram realizados em diferentes condições de incubação. Primeiro regime de incubação: células A172 e T98G foram tratadas com diferentes concentrações com sobrenadante de macrófagos THP-1 estimulados por LPS. Segundo regime de incubação: as células T98G foram pré-incubadas com TPEN em por 2, 4 ou 24 h. Após o período de pré-incubação, os sobrenadantes da cultura foram substituídos por sobrenadantes de macrófagos THP-1 estimulados por LPS mantidos sob condições adequadas de Zn ou deficientes em Zn (TPEN) por 24 h. Terceiro regime de incubação: as células T98G foram tratadas com (i) sobrenadante de macrófagos THP-1 não estimulados, (ii) sobrenadante de macrófagos THP-1 estimulados por LPS, (iii) sobrenadante de macrófagos THP-1 tratados com TPEN, ou (iv) sobrenadante de macrófagos THP-1 incubados em meio LPS/TPEN por 24 h. Todos os sobrenadantes obtidos foram submetidos à quantificação de Trp e Quin por HPLC-UV.

Resultados e Discussão
Os resultados do estudo *in vivo*, demonstrou-se que os grupos HFD e HFD-ZD tiveram um aumento na adiposidade, bem como na circunferência abdominal, apresentando hipertrofia do tecido adiposo e apresentaram um aumento nas concentrações de leptina sérica. Em relação à conversão de Trp em Quin periférica, não houve alterações significativas nos grupos expostos as dietas hiperlipídicas. Foram investigados os efeitos das dietas hiperlipídicas em modelo comportamental como o teste de respingo (splash test). Enquanto o grupo HFD não demostrou alterações comportamentais, o grupo HFD-ZD demonstrou comportamentos anedônicos no teste de respingo. Esses resultados sugerem que, pelo menos em camundongos, a obesidade em combinação com a deficiência de Zn até certo ponto desacelera os impulsos de autocuidado e comportamentos motivacionais. Em animais que receberam HFD-ZD o tratamento com fluoxetina foi capaz de reverter o comportamento anedônico no teste de respingo e diminuir as concentrações de leptina sérica e também aumentar as concentrações de adiponectina sérica.
O papel do Zn livre na regulação da via das quinureninas foi investigado no estudo *in vitro*. Houve um aumento nas concentrações de Quin e uma diminuição nas concentrações de Trp nos sobrenadantes de células de glioma cerebral T98G e A172 mantidas sob condições de Zn suficiente ou deficiente sendo tratadas com sobrenadante de macrófagos THP-1 estimulados por lipopolissacarídeo (LPS). Concluiu-se que o Zn não tem efeito direto no catabolismo do Trp. No entanto, efeitos indiretos foram observados em um experimento diferente. Quando as células T98G foram tratadas com sobrenadante de macrófagos THP-1 deficientes em Zn estimulados por LPS, houve um aumento nas concentrações de Quin e na razão Quin/Trp no sobrenadante da cultura celular T98G. Como descrito na literatura, o LPS ativa a cascata de sinalização NF-κB, resultando na produção e secreção de citocinas pró-inflamatórias no meio de cultura. De fato, a RT-PCR revelou que os genes que codificam citocinas pró-inflamatórias (*IL6*, *TNFA* e *IFNG*) foram expressos em macrófagos THP-1 estimulados por LPS, tanto em condições de Zn suficiente quanto deficiente. Os resultados mostraram concentrações aumentadas de IL-6 no sobrenadante e uma expressão aumentada de *IFNG* em macrófagos THP-1 deficientes em Zn estimulados por LPS em comparação com células adequadas em Zn.

Considerações Finais

Essas descobertas sugerem que, pelo menos em camundongos, a obesidade em combinação com a deficiência de Zn até certo ponto desacelera os impulsos de autocuidado e comportamentos motivacionais. Em animais que receberam HFD-ZD o tratamento com fluoxetina foi capaz de reverter o comportamento anedônico no teste de respingo e diminuir as concentrações de leptina sérica e também aumentar as concentrações de adiponectina sérica.
Além disso, o estudo *in vitro* revelou um aumento na conversão de Quin/Trp em células T98G induzida por sobrenadante obtido de macrófagos THP-1 estimulados por LPS mantidos sob condições deficientes de Zn. Os resultados destes estudos fornecem evidências de que a obesidade associada à deficiência de Zn pode aumentar a vulnerabilidade aos sintomas depressivos imunomediados.

Palavras-chave: Obesidade. Deficiência de Zinco. Distúrbios Neurocomportamentais.

ABSTRACT

Obesity, a multifactorial disorder associated with lifestyle, hereditary, and environmental factors, has been described by the World Health Organization as a global epidemic. Its adverse effects are not only social and psychological but also related to the development of comorbidities such as cardiovascular disease, type 2 diabetes, and neurological disorders. In recent years, several studies reported a relationship between zinc (Zn) deficiency and obesity in humans. Obesity denotes excessive white adipose tissue expansion and adipocyte hypertrophy, conditions that may lead to chronic low-grade inflammation and increased levels of circulating proinflammatory cytokines. Excessive production of proinflammatory cytokines may promote the expression and activation of indoleamine 2,3-dioxygenase (IDO), in both the central nervous system and peripheral organs, resulting in tryptophan (Trp) depletion and increased kynurenine (Kyn) levels, which ultimately leads to neurobehavioral alterations. This study used *in vivo* and *in vitro* assays to examine the role of Zn in different aspects of metabolic Trp conversion. In the first experiment, Swiss albino mice were fed a standard diet (SD), standard Zn-deficient diet (SD-ZD), high-fat diet (HFD), or high-fat Zn-deficient diet (HFD-ZD) for 8 weeks. It was found that HFD groups had increased adiposity markers, abdominal circumference, white adipocyte hypertrophy, and serum leptin levels. Peripheral Kyn–Trp breakdown was not altered in HFD groups. The effect of HFD on behavior was investigated using the splash test. Whereas HFD mice did not show behavioral alterations, HFD-ZD mice showed anhedonic behaviors in the splash test. These findings suggest that, at least in mice, obesity combined with Zn deficiency decelerates impulses for self-care and motivation behaviors to a certain extent. Fluoxetine treatment was able to reverse anhedonic behavior in the splash test, decrease serum leptin, and increase serum adiponectin levels in animals receiving HFD-ZD. The role of free Zn in regulating the Kyn–Trp pathway was investigated *in vitro*. There was an increase in Kyn and a decrease in Trp levels in supernatant from T98G and A172 brain glioma cells maintained under Zn-sufficient or -deficient conditions and treated with supernatant from lipopolysaccharide (LPS)-stimulated THP-1 macrophages. Thus, it was concluded that Zn does not have a direct effect on Kyn/Trp breakdown. However, indirect effects were observed in a different experiment. When T98G cells were treated with supernatant from LPS-stimulated Zn-deficient THP-1 macrophages, there was an increase in Kyn levels and Kyn/Trp ratio in culture supernatant. As described in the literature, LPS activates the NF-κB signaling cascade, resulting in the production and secretion of proinflammatory cytokines into the culture medium. Indeed, RT-PCR revealed that genes encoding proinflammatory cytokines (*IL6*, *TNFA*, and *IFNG*) were expressed in LPS-stimulated THP-1 macrophages, under both Zn-sufficient and -deficient conditions. The results showed increased IL-6 supernatant levels and increased *IFNG* expression in LPS-stimulated Zn-deficient THP-1 macrophages as compared with Zn-adequate cells. It is suggested that a combination of proinflammatory cytokines were significantly involved in potentiating Kyn/Trp breakdown in T98G cells. Overall, these results provide further evidence implicating Zn deficiency and low grade-inflammation in the development of obesity-associated neurological disorders.

Keywords: Obesity. Zinc deficiency. Behavioral disturbance.

ZUSAMMENFASSUNG

Fettleibigkeit, eine multifaktorielle Störung, die mit Lebensstil-, Erb- und Umweltfaktoren verbunden ist, wurde von der Weltgesundheitsorganisation als globale Epidemie beschrieben. Die nachteiligen Auswirkungen sind nicht nur sozial und psychisch, sondern hängen auch mit der Entwicklung von Komorbiditäten wie Herz-Kreislauf-Erkrankungen, Typ-2-Diabetes und neurologischen Störungen zusammen. In den letzten Jahren wurde in mehreren Studien ein Zusammenhang zwischen Zinkmangel (Zn) und Fettleibigkeit beim Menschen festgestellt. Fettleibigkeit bedeutet eine übermäßige Expansion des weißen Fettgewebes und eine Hypertrophie der Adipozyten, Zustände, die zu einer chronischen, leicht entzündlichen Erkrankung und einem erhöhten Spiegel an zirkulierenden proinflammatorischen Zytokinen führen können. Eine übermäßige Produktion von proinflammatorischen Zytokinen kann die Expression und Aktivierung von Indoleamin-2,3-Dioxygenase (IDO) sowohl im Zentralnervensystem als auch in den peripheren Organen fördern, was zu einer Tryptophan (Trp) -Verarmung und erhöhten Kynurenin (Kyn) -Spiegeln führt, was letztendlich dazu führt zu neurobehavioralen Veränderungen. Diese Studie verwendete In-vivo- und In-vitro-Tests, um die Rolle von Zn in verschiedenen Aspekten der metabolischen Trp-Umwandlung zu untersuchen. Im ersten Experiment erhielten Schweizer Albino-Mäuse eine Standarddiät (SD), eine Standarddiät mit Zn-Mangel (SD-ZD), eine Diät mit hohem Fettgehalt (HFD) oder eine Diät mit hohem Fettgehalt mit Zn-Mangel (HFD-ZD) für 8 Wochen. Es wurde festgestellt, dass HFD-Gruppen erhöhte Adipositas-Marker, Bauchumfang, Hypertrophie der weißen Adipozyten und Serum-Leptin-Spiegel aufwiesen. Der periphere Kyn-Trp-Abbau wurde in HFD-Gruppen nicht verändert. Der Einfluss von HFD auf das Verhalten wurde mit dem Splash-Test untersucht. Während HFD-Mäuse keine Verhaltensänderungen zeigten, zeigten HFD-ZD-Mäuse im Splash-Test anhedonisches Verhalten. Diese Ergebnisse legen nahe, dass zumindest bei Mäusen Fettleibigkeit in Kombination mit Zn-Mangel die Impulse für das Selbstpflege- und Motivationsverhalten bis zu einem gewissen Grad verlangsamt. Die Behandlung mit Fluoxetin war in der Lage, das anhedonische Verhalten im Spritztest umzukehren, das Serum-Leptin zu senken und die Serum-Adiponektin-Spiegel bei Tieren zu erhöhen, die HFD-ZD erhielten. Die Rolle von freiem Zn bei der Regulierung des Kyn-Trp-Signalwegs wurde in vitro untersucht. Es gab eine Zunahme von Kyn und eine Abnahme der Trp-Spiegel im Überstand von T98G- und A172-Hirngliomzellen, die unter Zn-ausreichenden oder defizienten Bedingungen gehalten und mit Überstand von Lipopolysaccharid (LPS) -stimulierten THP-1-Makrophagen behandelt wurden. Daher wurde der Schluss gezogen, dass Zn keinen direkten Einfluss auf den Kyn / Trp-Abbau hat. In einem anderen Experiment wurden jedoch indirekte Effekte beobachtet. Wenn T98G-Zellen mit Überstand von LPS-stimulierten Zn-defizienten THP-1-Makrophagen behandelt wurden, gab es einen Anstieg der Kyn-Spiegel und des Kyn/Trp-Verhältnisses im Kulturüberstand. Wie in der Literatur beschrieben, aktiviert LPS die NF-κB-Signalkaskade, was zur Produktion und Sekretion von proinflammatorischen Zytokinen in das Kulturmedium führt. Tatsächlich zeigte die RT-PCR, dass Gene, die für proinflammatorische Zytokine (*IL6*, *TNFA* und *IFNG*) kodieren, in LPS-stimulierten THP-1-Makrophagen sowohl unter ausreichenden als auch unter unzureichenden Zn-Bedingungen exprimiert wurden. Die Ergebnisse zeigten erhöhte IL-6-Überstandsspiegel und erhöhte *IFNG*-Expression in LPS-stimulierten Zn-defizienten THP-1-Makrophagen im Vergleich zu Zn-adäquaten Zellen. Es wird vermutet, dass eine Kombination von proinflammatorischen Zytokinen signifikant an der Potenzierung des Kyn/Trp-Abbaus in T98G-Zellen beteiligt war. Insgesamt liefern diese Ergebnisse weitere Hinweise auf einen Zn-Mangel und eine niedriggradige Entzündung bei der Entwicklung von mit Fettleibigkeit verbundenen neurologischen Störungen.

Schlüsselwörter: Fettleibigkeit. Zinkmangel.Verhaltensstörungen.

LIST OF FIGURES

LIST OF TABLES

LIST OF SUPPLEMENTAL TABLES

LIST OF ABBREVIATIONS AND ACRONYMS

AgRP – Agouti-related protein

ANOVA – Analysis of variance

BAT – Brown adipose tissue

BBB – Blood brain barrier

BMI – Body mass index

BSA – Bovine serum albumin

CART – Cocaine and amphetamine-regulated transcript

CNS – Central Nervous System

DIO – Diet-induced obesity

DMEM – Dulbecco's modified Eagle's medium

EDTA – Ethylenediaminetetraacetic acid

ELISA – Enzyme-linked immunosorbent assay

FCS – Fetal calf serum

FluoZin-3AM – 4-(6-Acetoxymethoxy-2,7-dichloro-3-oxo-9-xanthenyl)-4′-methyl-2,2′(ethylenedioxy)dianiline-*N*,*N*,*N*′,*N*′-tetraacetic acid tetrakis(acetoxymethyl) ester

HFD – High-fat diet

HFD-ZD – Zinc-deficient high-fat diet

HPLC – High-performance liquid chromatography

IDO 1/IDO 2 – Indoleamine 2,3-dioxygenase 1/2

IKK – IκB kinase

IL – Interleukin

IFN – Interferon

IRAK – IL-1 receptor-associated kinase

IRF3 – Interferon-responsive factor 3

JAK2 – Janus kinase 2

Kyn – Kynurenine

Kyn/Trp ratio – Kynurenine/tryptophan ratio

KYNA – Kynurenic acid

LPS – Lipopolysaccharides

MCP-1 – Monocyte chemoattractant protein-1

MD-2 – Myeloid differentiation factor 2

MyD88 – Adaptor protein myeloid differentiation factor

MTT – 3-(4,5-dimethylthiazolyl-2)-2,5-diphenyltetrazolium bromide

NF-κB – Nuclear factor κB

NMDA – *N*-methyl-D-aspartate

NPY – Neuropeptide Y

ObRb – Long leptin receptor

PMA – Phorbol 12-myristate-13-acetate

POMC – Pro-opiomelanocortin

P/S – Penicillin/streptomycin

QUIN – Quinolinic acid

RT-PCR – Reverse transcription polymerase chain reaction

SOCS3 – Supressor of cytokine signaling 3

SD – Standard diet

SD-ZD – Zinc-deficient standard diet

SFA – Saturated fatty acids

STAT3 – Signal transducer and activation of transcript 3

TDO – Tryptophan 2,3-dioxygenase

TLR2/4 – Toll-like receptor 2/4

TNF-α – Tumor necrosis factor-alpha

TPEN – *N*,*N*,*N*′,*N*′-Tetrakis(2-pyridylmethyl)-1,2-ethanediamine

Trp – Tryptophan

WAT – White adipose tissue

WHO – World Health Organization

Zinpyr-1 – 2-[4,5-*bis*[[*bis*(Pyridin-2-ylmethyl)azaniumyl]methyl]-2,7-dichloro-3-oxido-6-oxoxanthen-9-yl]benzoate

Zn – Zinc

TABLE OF CONTENTS

1 INTRODUCTION

The abundance of energy-dense foods and the increasingly sedentary lifestyle of modern Western societies are closely related to the obesity epidemic (LEISEGANG, 2019). Obesity has also been associated with Zn deficiency (DI MARTINO *et al*., 1993; MARREIRO *et al*., 2002; 2004). Zn was found to be implicated in altered adipose metabolism, contributing to the exacerbation of insulin resistance and the development of a proinflammatory state (TALLMAN and TAYLOR 2003; LIU *et al*., 2013).

Obesity is associated with a chronic state of low-grade inflammation characterized by abnormal secretion of proinflammatory mediators such as tumor necrosis factor-alpha (TNF-α) and interleukin (IL)-6 in adipose tissue and serum (CINTI, 2005). Obese patients with low dietary Zn intake display a systemic inflammatory condition marked by upregulation of IL-1α, IL-1β, and IL-6 in peripheral blood mononuclear cells. Costarelli *et al.* (2010) suggested that hypozincemia can aggravate obesity-related disturbances, such as insulin resistance and inflammation, thereby worsening the preexisting obesity status.

Obesity is a risk factor for several comorbidities, including diabetes, cardiometabolic diseases, and neurological disorders. Depressive symptoms appear at a higher prevalence rate when compared with other disorders observed in obese subjects (COHEN, 2010). The pathophysiological mechanisms of obesity and cognitive function remain to be fully understood. Recently, Mangge *et al.* (2014) demonstrated the relationship between L-Trp catabolism and obesity-related immune-mediated inflammation.

Trp is an essential amino acid. It is catabolized through four distinct pathways: (1) the serotonergic pathway, which leads to the formation of the neurotransmitter serotonin in the brain and melatonin in the pineal gland, (2) the tryptamine pathway (decarboxylation), (3) the indole pyruvic acid pathway (transamination) (RICHARD *et al.*, 2009; BADAWY, 2017), and (4) the Kyn pathway. The first three routes are of minor quantitative importance. The fourth accounts for 95% of Trp catabolism, whereby Trp is converted by indoleamine 2,3-dioxygenase-1 (IDO) and Trp 2,3-dioxygenase (TDO) to give Kyn as an intermediate product (SAINIO *et al.*, 1996; BADAWY, 2017). The increase in IDO expression/activation by peripheral or central proinflammatory cytokines can cause a shift in the Kyn pathway, increasing Kyn production and consequently leading to serotonin depletion; these effects are likely responsible for relevant emotional and cognitive alterations in obese patients (JENKINS *et al*., 2016). Increased Kyn levels can also stimulate the production of other neurotransmitters, such as 3-hydroxykynurenine and quinolinic acid, which have neurotoxic effects because of

their ability to generate oxidative radicals and act as *N*-methyl-D-aspartate (NMDA) receptor agonists. 3-Hydroxykynurenine and quinolinic acid (QUIN) are well known to be involved in neuropsychiatric and neurodegenerative diseases (CASTANON *et al*., 2014; CHAVES FILHO *et al*., 2018).

Zn acts as a cofactor in the rate-limiting step of serotonin synthesis catalyzed by L-amino acid decarboxylase (BEDIZ, 2003). Previous studies showed that Zn deficiency exerts depressant-like effects, and may induce depressive behaviors, in which case Zn supplementation can produce anxiolytic and antidepressant-like responses, as demonstrated in animal models (SWARDFAGER *et al.*, 2013).

According to the literature, individuals with dietary Zn deficiency are more prone to behavioral alterations. There is a relationship between Trp catabolism and obesity-related immune-mediated inflammation, which, in turn, can enhance IDO expression and activation in the Kyn–Trp pathway in the periphery and central nervous system (CNS), thereby increasing the levels of neurotoxic catabolites. The present thesis, therefore, aimed to perform *in vivo* and *in vitro* studies to assess the role of Zn in the Kyn–Trp pathway and investigate the extent to which Zn deficiency causes behavioral disturbances associated with obesity.

2 LITERATURE REVIEW

2.1 OBESITY

2.1.1 The concept of obesity and its epidemiology

Obesity is associated with a sedentary lifestyle and excessive intake of high-energy foods and; its prevalence is higher in women than in men (SCHOETTL *et al*., 2018). The disease has a complex etiology. Factors such as socioeconomic status, environment, personal behavior, and genotype–phenotype interactions must be considered (GONZÁLEZ-MUNIESA *et al*., 2017). This multifactorial phenomenon is implicated in the development of several comorbidities, including insulin resistance, type 2 diabetes, hyperlipidemia, atherosclerosis, and cardiovascular diseases, in addition to a variety of effects on the CNS (BHAT *et al*., 2017).

Overweight and obesity are recognized worldwide as health problems that reduce life expectancy. Their rates have increased rapidly in recent decades, leading the World Health Organization (WHO) to formally recognize the global nature of the obesity epidemic in 1997 (CABALLERO, 2007). WHO describes obesity as an excessive fat accumulation that can impair health and defines obese individuals as those with a body mass index (BMI) of 30 kg/m^2 or higher (WHO, 2019). BMI, calculated as weight in kilograms divided by the square of height in meters, is generally well accepted in epidemiological studies, public health services, and clinical practice as a defining criterion for the disease (OKORODUDU *et al*., 2010). Obesity can be subdivided into class 1 ($30 \leq BMI < 35$ kg/m^2), class 2 ($35 \leq BMI < 40$ kg/m^2), and class 3 ($BMI \geq 40$ kg/m^2), with commensurate rates of disability and mortality (FRUH, 2017).

Despite the fact the BMI is the most widely used index for classifying obesity, other parameters have been suggested for the definition of obesity and metabolic risk factors, such as waist circumference, waist/hip ratio, and waist/height ratio (SOHN, 2014; QIAN *et al*., 2019). Waist/hip and waist/height ratios reflect the distribution of body fat, whereas waist circumference indicates abdominal adiposity. Abdominal adiposity is a primarily visceral, metabolically active fat associated with metabolic dysregulation, which predisposes individuals to comorbidity development (HRUBY and HU, 2015). These three obesity indices are possibly correlated with morbidity and mortality in obese individuals (GU *et al*., 2018).

There are various physicochemical methods to assess adiposity that are complementary to obesity diagnosis. One of them is hydrostatic underwater weighing, a specific

type of densitometry that derives body composition from body density and volume using the Archimedes principle (NIHR, 2020). Dual-energy X-ray absorptiometry is a validated method for the determination of soft tissue composition and bone mineral density through the generation of two X-ray beams at different energy levels (LASKEY, 1996). Body fat composition can be determined by the difference between lean soft tissue and total soft tissue mass (WANG *et al*., 2010). Computed tomography and magnetic resonance imaging have been successfully applied to investigate the distribution of subcutaneous and visceral adipose tissues (PESCATORI *et al*., 2019).

Worldwide prevalence of obesity increased from 3.2 to 10.8% in adult men and from 6.4 to 14.9% in adult women between 1975 and 2014 (BLÜHER, 2019). According to recent global data (WHO, 2016), more than 650 million adults were obese in 2016, corresponding to 13% of the adult population (11% of adult men and 15% of adult women aged 18 years and older). In Brazil, according to Gomes *et al.* (2019), obesity prevalence increased from 7.5 to 17% in adults aged 20–39 years and from 14.7 to 25.7% in adults aged 40–59 years between 2002 and 2013, with a slightly higher prevalence in young women. From 2008 to 2013, a substantial increase in prevalence was observed among women with secondary (90%) and pre-primary (42%) education (GOMES *et al*., 2019). The role of socioeconomic status and education level in obesity will be discussed in Section 2.1.2. Recent reports of the Brazilian Association for the Study of Obesity and Metabolic Syndrome (ABESO, *Associação Brasileira para o Estudo da Obesidade e da Síndrome Metabólica*) revealed that 110 million adults are overweight (52.5%) and 38 million are obese (17.9%) (VIGITEL, 2014). These findings are consistent with the latest data provided by the 2016 Surveillance of Risk and Protective Factors for Chronic Diseases by Telephone Survey showing that 53.8% of Brazilian adults are overweight and 18.9% are obese (BRASIL 2016).

Obesity has a significant impact on healthcare costs (CAWLEY and MEYERHOEFER, 2012). In a systematic review of 32 articles (published between 1990 and 2009) about the direct treatment costs of obesity worldwide, Withrow and Alter (2011) found that the disease accounts for 0.7 to 2.8% of a country's total healthcare expenditures. Obese individuals were found to have about 30% higher medical costs than normal-weight individuals (WITHROW and ALTER, 2011). In Brazil, the direct costs of obesity in the public health system in 2011 were estimated at US$ 269.6 million, demonstrating that the prevalence and costs are gradually increasing in the country, a fact that can have severe implications for the financial sustainability of the public health system (de OLIVEIRA *et al*., 2015).

In summary, obesity has been associated with an increase in morbidity and mortality of the worldwide population, and the costs of obesity have had a significant economic impact. To better deal with these problems, we need a comprehensive understanding of the biology and physiopathology of adipose tissue. In particular, it is crucial to elucidate the mechanisms underlying the role of white adipose tissue (WAT) in the development of obesity and related disorders.

2.1.2 Causes of obesity

The fundamental cause of obesity is the energy imbalance between consumption and expenditure of calories, leading to WAT accumulation (BLÜHER, 2019). However, the etiology of obesity is highly complex, associated with interactions between genetics and epigenetics, the environment, and human behavior (NGUYEN and EL-SERAG, 2010; McGILL, 2011; WRIGHT and ARONNE, 2012; MELDRUM *et al*., 2017).

The human genome sequence has not been substantially altered in the last centuries; thus, it is believed that the rapid rise in obesity prevalence is linked to a profound shift in lifestyle, characterized by excessive food consumption and physical inactivity (MILAGRO *et al.*, 2020). The level of physical activity has decreased with the increased use of labor-saving devices, mechanization of work, and pursuit of sedentary leisure activities (e.g., cell phone, television, and computer use) (BAQAI and WILDING, 2014). Nevertheless, it is important to recognize the contribution of hereditary factors to weight gain in humans.

Several genes associated with weight gain were identified in nonhuman animals, as well in humans. The most common obesity-related mutations occur in genes encoding melanocortin-4 receptor, long leptin receptor (ObRb), and pro-opiomelanocortin (POMC), expressed mainly in the hypothalamus (NGUYEN and EL-SERAG, 2010). Other genes related to obesity include the peroxisome proliferator activator receptor gene and prohormone convertase-1 gene (FAROOQI and O'RAHILLY, 2006; SELASSIE and SINHA, 2011).

Studies have reported that low education level and socioeconomic status are risk factors for obesity (PAERATAKUL *et al*., 2002; NOCON *et al.*, 2007). One explanation could be that food and nutrition education is not sufficiently taught at school, at either primary or secondary levels (NICOLAIDIS, 2019). As a result, food choices are generally driven by taste preferences, convenience, and price instead of healthiness (DREWNOWSKI and SPECTER, 2004).

With the advances in food technology, food innovations have been directed toward ready-to-eat and ready-to-use products. Energy-dense foods are frequently available in large portions and are easily found in grocery stores, fast-food restaurants, food machines, and other retail food establishments (SELASSIE and SINHA, 2011; McGILL, 2011; MYLES, 2014; STATOVCI *et al*., 2017). Packaged foods are generally highly palatable and rich in saturated fat, refined sugar, and sodium, contributing greatly to daily energy intake but poorly to satiety (WRIGHT and ARONNE, 2012; MAHER and CLEGG, 2018). Palatable foods are a powerful source of neurobiological rewards, as they produce feelings of comfort that can lead to positive emotional reactions, thereby playing a crucial role in overeating and obesity development (DREWNOWSKI and SPECTER, 2004; FULTON, 2010). Several authors have suggested that high consumption of palatable foods can induce addiction-like behaviors (PANDIT *et al*., 2012). Palatable foods frequently lack dietary fibers (which exert important satiating effects) and are poor in micronutrients (McGILL, 2008). These facts explain why micronutrient deficiency is frequently observed in obese individuals (VIA, 2012).

Obese individuals have lower blood levels of selenium, iron, folate, vitamin B12, vitamin A, vitamin E, 25-hydroxyvitamin D, and Zn than normal-weight controls (GARCÍA *et al*., 2009). There are some hypotheses to describe the etiology of micronutrient deficiencies in obese individuals. For example, 25-hydroxyvitamin D can be sequestered by WAT as a consequence of increased fat deposition, thereby decreasing 25-hydroxyvitamin D bioavailability. Iron deficiency in obese individuals results from reduced iron intake and absorption; moreover, in the chronic low-grade inflammatory state of obesity, macrophages may sequester iron (GARCÍA *et al*., 2009; TUSSING-HUMPHREYS and NGUYEN, 2014). The implications of Zn deficiency in obesity will be discussed in Section 2.3.1

2.1.2.1 Diet-induced obesity (DIO) models

Given the rapid increase in the prevalence of obesity and related comorbidities worldwide, animal models have become indispensable for the study of the physiopathological mechanisms of this disease (CASTANON *et al*., 2014; LANG *et al*., 2019). Preclinical animal models can provide important information about obesity and neuropsychiatric alterations. Laboratory mice and rats represent a suitable model for translational research because their physiology is similar to that of humans. Compared with other laboratory animals, rats and mice are small, have high fecundity and short life cycle (KLEINERT *et al.*, 2018).

Over the years, a wide variety of genetic and nongenetic animal models have been used in obesity studies. Genetic models can be monogenic, polygenic, or transgenic and seem to be better suited for drug testing (SULEIMAN *et al.*, 2020). There are over 200 mouse models of monogenic obesity with mutations in the leptin pathway; other genetically engineered mutants include alterations in glucose transporter subtype 4, neuropeptide Y (NPY)-1 receptor, and insulin receptor knockout mice (BARRETT *et al.*, 2016; LUTZ and WOODS, 2012). Although studies with monogenic mouse models have made considerable advances in the mechanistic understanding of obesity, they have some limitations. A common argument against these models is the deficiency in the leptin system, a condition that is not entirely representative of obesity pathogenesis in humans. DIO rats and mice have been commonly used in obesity research and are believed to mimic the various physiological conditions observed in obese humans (BUETTNER *et al*., 2007; NILSSON *et al*., 2012).

Inbred (isogenic) mouse strains are mainly used as DIO models, such as the inbred strain C57BL/6J, which gains weight progressively, develops severe obesity, and shows elevated adiposity. Their homogeneity reduces variability in experimental settings (KLEINERT *et al*., 2018; MAREI *et al*., 2020). However, inbreeding may increase genetic drift and the occurrence of undiscovered mutations, leading to the misunderstanding of experimental variables. Consequently, extrapolation of data obtained with inbred models to human physiology is practically impossible. On the other hand, outbred strains, such as Swiss mice, have wide genetic variability, are metabolically sensitive to high-fat diets (HFDs), and develop obesity and insulin resistance (MAREI *et al*., 2020).

DIO rodent models have been used to assess the effects of switching from a low energy-dense, low-fat, and high complex-carbohydrate diet to high-fat, high-sugar diets. HFDs are designed to provide 40–60% of energy from fat, and animals receive diets for 12 to 20 weeks (BARRETT *et al.*, 2016; AVTANSKI *et al*., 2019). An important factor contributing to the development of obesity in animal models is the type of fat used in the diet. According to a literature review carried out by Buettner *et al.* (2007), the best method to induce obesity in animals is to use HFDs containing saturated fatty acids (SFA) of animal origin (e.g., lard). HFD containing SFA was more effective in inducing obesity and insulin resistance than HFD containing polyunsaturated fat (BUETTNER *et al*., 2007), in agreement with the findings of Hariri and Thibault (2010) showing that SFA is more obesogenic than polyunsaturated fatty acids. The higher body weight and prominent body fat accumulation in animals fed SFA can be explained by the fact that SFA is inadequately used for energy production, resulting in acylation to triglycerides and storage in adipose tissue. The development of chronic low-grade

inflammation and SFA-induced neuroinflammation in obesity will be discussed in Sections 2.2.3 and 2.4.2, respectively.

2.2. ADIPOSE TISSUE

The adipose tissue is considered the largest endocrine organ, recognized as a significant player in systemic metabolic homeostasis (LUO and LIU, 2016; STOLARCZYK, 2017). This organ is involved in the regulation of glucose and lipid metabolism, insulin sensitivity, and inflammatory responses (KWOK *et al*., 2016).

Adipose tissue exists in two functionally and morphologically distinct forms: brown adipose tissue (BAT), comprising 1-2% of the total body fat in human adults, and WAT, which stores 95% of body fat (LEE *et al*., 2013; SAITO, 2013). Brown adipocytes are specialized for energy expenditure and heat production. These cells are rich in mitochondria expressing uncoupling protein 1, whose function is to uncouple oxidative phosphorylation, resulting in the dissipation of chemical energy as heat. BAT is found in cervical-supraclavicular, perirenal, and paravertebral regions (SCHOETTL *et al*., 2018; LUO and LIU, 2016; CYPESS *et al*., 2009; LEE *et al*., 2011).

In most mammals, including rodents and humans, WAT adipocytes are organized in anatomically distinct depots, classified as visceral (omental, mesenteric, retroperitoneal, pericardial, and gonadal) and subcutaneous fat. Most of the body fat (80-90%) is stored in subcutaneous adipose tissues in the abdominal, subscapular, gluteal, and femoral regions, and a smaller portion (10-20%, depending on sex and individual factors) resides viscerally in the abdominal cavity (HEINONEN, 2016; SCHOETTL *et al*., 2018). WAT is primarily constituted of adipocytes, although other cell types are present, including preadipocytes, endothelial cells, fibroblasts, mast cells, and immune cells (LEE *et al.*, 2011; OUCHI *et al*., 2011). White adipocytes have a unique morphology of unilocular lipid droplets with high capacity to store triglycerides (BERRY *et al*., 2013).

The apparent simplicity of WAT, both histologically and metabolically, might make this fatty tissue seem like a passive organ of energy storage. Until recently, this view led researchers to ignore the metabolic importance of fatty tissues (ROSEN and SPIEGELMAN, 2006). A closer examination of WAT at the cellular level reveals an underestimated complexity. Adipocytes express and secrete a variety of factors collectively known as adipokines, which act at local (autocrine and paracrine) and systemic (endocrine) levels to modulate systemic metabolism (ROSEN and SPIEGELMAN, 2014).

2.2.1 Relationship between energy homeostasis, integration of satiety signals, and adiposity

Energy homeostasis refers to the balance between energy intake, energy storage, and energy expenditure, whose effects are primarily associated with the maintenance of body weight. Body weight, however, is the result of several metabolic processes controlled by a complex physiological system (ENRIORI *et al*., 2006). It involves, for instance, interactions between peripheral neuron and hormone signals that have short-term effects on substrate supply (pancreas and gastrointestinal system), long-term effects on energy availability (WAT), and a modulatory action on the CNS, particularly in the hypothalamus (WILSON and ENRIORI, 2015; KOLIAKI *et al*., 2020). The hypothalamus regulates body temperature, circadian rhythms, fatigue, sleep and in particular feeding behavior and energy homeostasis through neuronal circuits that project into the brainstem and other brain regions (BENOMAR and TAOUIS, 2019; KOLIAKI *et al*., 2020; MURPHY and BLOOM, 2006). In the median eminence, a small region at the inferior part of the hypothalamus, fenestrated capillaries lacking a blood–brain barrier (BBB) facilitate the transport of peripheral hormones and nutrients from the blood (RODRÍGUEZ *et al*., 2010). At the base of the hypothalamus and adjacent to the median eminence, there is an aggregation of neuronal cells known as the arcuate nucleus, comprising orexigenic neurons expressing NPY and agouti-related protein (AgRP) as well as anorexigenic neurons that express POMC and cocaine- and amphetamine-regulated transcript (CART) (MURPHY and BLOOM, 2006; KOLIAKI *et al*., 2020). Neuronal connections extend from the arcuate nucleus to other hypothalamic sites, including paraventricular, ventromedial, dorsomedial, and lateral nuclei (AMITANI *et al*., 2013). Both the arcuate nucleus and vagal sensory terminals are known to express receptors for peptides involved in metabolic regulation (YI and TSCHÖP, 2012).

Peripheral metabolic signals can be categorized as long- or short-acting. Several hormones have a short-term effect on food intake, whereas others, such as insulin and leptin, have long-lasting effects on energy stores (WILSON and ENRIORI, 2015). In the gastrointestinal tract, food digestion and absorption trigger the release of short-acting factors in a nutrient-sensitive manner. The majority of peripheral signaling molecules are anorexigenic, including cholecystokinin, whose magnitude of secretion is proportional to energy intake. Cholecystokinin activates specific receptors on sensory nerves in the duodenum that send satiety information to the brain via the vagus nerve (MURPHY and BLOOM, 2006; WOODS and D'ALESSIO, 2008). Peptide YY, glucagon-like peptides 1 and 2, and oxyntomodulin are

released from the large intestine after a meal and, through the vagus nerve, stimulate anorectic pathways in the hypothalamus and brainstem (MURPHY and BLOOM, 2006). Ghrelin, on the other hand, is secreted by the stomach during starvation and binds to growth hormone secretagogue receptors on the vagus nerve and hypothalamus (WILSON and ENRIORI, 2015; ZANCHI *et al*., 2017). This stimulus leads to activation of NPY/AgRP neurons in the paraventricular nucleus and suppression of POMC neuronal activity, culminating in increased food intake, a positive energy balance, and, ultimately, weight gain (AMITANI *et al*., 2013; KOLIAKI *et al*., 2020).

Some peripheral signaling molecules, such as insulin and leptin, play an important role in the hypothalamic control of energy homeostasis (SUZUKI *et al*., 2012; WILSON and ENRIORI, 2015). Insulin is secreted by pancreatic β-cells in response to food intake to modulate energy and glucose homeostasis. Circulating levels of insulin are directly related to body fat content. Insulin crosses the BBB via a receptor-mediated transport mechanism to the hypothalamus, reaching POMC/CART and NPY/AgRP neurons in the arcuate nucleus, which contain high levels of insulin receptors (SUZUKI *et al*., 2012; TIMPER and BRÜNING, 2017). Central levels of insulin enhance CART and inhibit NPY/AgRP expression, resulting in a decrease in food intake and body weight (BENOMAR and TAOUIS, 2019).

WAT releases both anti-inflammatory (adiponectin) and proinflammatory (leptin) adipokines. Adiponectin is functionally analogous to insulin in its antiobesity, antiatherogenic, and antidiabetic effects; it enhances insulin sensitivity in skeletal muscle while increasing fatty acid oxidation and reducing glucose production in the liver (STOLARCZYK, 2017). Leptin is considered the most crucial peripheral signal for long-term energy homeostasis, as it is sensitive to the levels of triglycerides stored in adipocytes (LUO and LIU, 2016). The hormone is also implicated in autonomic regulation of the cardiovascular system, reproductive function, and immune system (YI and TSCHÖP, 2012; PAZ-FILHO *et al*., 2012; CUI *et al*., 2017).

Leptin relays information about peripheral energy storage to the CNS (TIMPER and BRÜNING, 2017). Circulating leptin is transported across the BBB and acts on POMC neuronal excitability and CART and POMC expression (AL-SUHAIMI and SHEHZAD, 2013; AMITANI *et al*., 2013; de GIT and ADAN, 2015; TIMPER and BRÜNING, 2017). The peptide regulates neuronal activity by binding to and activating ObRb in multiple regions of the hypothalamus, including the arcuate, ventromedial, and paraventricular nuclei (ZHOU and RUI, 2013). Upon binding to ObRb, leptin activates Janus kinase 2 (JAK2). JAK2, in turn, phosphorylates ObRb at Tyr985, Tyr1077, and Tyr1138, triggering the initiation of several signal transduction pathways (ZHOU and RUI, 2013). Suppressor of cytokine signaling 3

(SOCS3) then binds to phospho-Tyr985 and inhibits ObRb signaling in a negative feedback manner. Transduction of leptin signaling is also marked by increased phosphorylation of signal transducer and activator of transcript 3 (STAT3), which binds to phospho-Tyr1138 and activates target genes coding for anorexigenic effectors (MOORIS and RUI, 2009; de GIT and ADAN, 2015). In summary, the brain responds to peripheral leptin levels by increasing energy expenditure and reducing food intake to maintain energy homeostasis and body weight (de GIT and ADAN, 2015).

2.2.2 Dysregulation of energy metabolism in obesity

Obesity results from dysregulation of energy metabolism in association with chronic systemic low-grade inflammation, a hypothalamic inflammatory state, and resistance to hormone signals, such as leptin and insulin, not only in the periphery but also in the CNS (TIMPER and BRÜNING, 2017; SAMODIEN *et al*., 2019).

Circulating leptin levels are abnormally higher in obese humans and rodents than in controls. Leptin resistance is linked to endogenous hyperleptinemia evoked by the inability to decrease food intake or increased energy expenditure, being a primary risk factor for obesity (MORRIS and RUI, 2009; CUI *et al*., 2017). Various mechanisms are responsible for the development of leptin resistance. The mechanisms include impaired leptin transport, altered leptin signaling, hypothalamic inflammation, and endoplasmic reticulum stress (MORRIS and RUI, 2009; ZHOU and RUI, 2013; AMITANI *et al.*, 2013). The BBB is a specialized interface between the blood and the brain that promotes active transport and controls exchanges with the periphery (LAMPRON *et al.*, 2013; GUILLEMOT-LEGRIS and MUCCIOLI, 2017). Leptin and insulin can cross the BBB via specific transporters. In situations of increased hormone levels, the sensitivity of transporters may be affected, impairing transport across the BBB and decreasing hypothalamic uptake (BENOMAR and TAOUIS, 2019).

Hyperleptinemia and hyperinsulinemia downregulate receptor expression in the CNS and stimulate that of regulators, such as SOCS3 and STAT3. Chronic activation of STAT3 leads to increased SOCS3 activation, which, in turn, inhibits STAT3 signaling, resulting in leptin and insulin resistance (TIMPER and BRÜNING, 2017). In addition to the brain, multiple peripheral tissues respond to leptin. ObRb is also present in pancreatic β-cells, where leptin directly inhibits insulin expression and secretion (AMITANI *et al.*, 2013; MORRIS and RUI, 2009). Conversely, insulin has a stimulatory action on leptin secretion from adipose tissue. Thus, hyperleptinemia disrupts the adipo-insular crosstalk (AMITANI *et al.*, 2013).

Long-term ingestion of HFD may increase SFA levels in the periphery. After crossing the BBB, SFA may induce inflammatory responses in hypothalamic neurons, particularly in microglia. Hypothalamic inflammation (involving activation of NK-κB by SFA and/or proinflammatory cytokines) promotes endoplasmic reticulum stress in neurons, contributing to insulin and leptin resistance (CUI *et al*., 2017; TIMPER and BRÜNING, 2017). More details regarding hypothalamic inflammation will be provided in Section 2.4.2.

2.2.3 Chronic low-grade inflammation in obesity

When energy intake exceeds energy expenditure, there is increased storage of triglycerides in adipose cells. This can be accomplished by adipocyte hypertrophy (cell expansion) or hyperplasia (cell number increase); the latter only occurs at the early stages of adipose tissue development (GUSTAFSON *et al*., 2009; JO *et al*., 2009). Hypertrophied adipocytes eventually reach a threshold at which cell and tissue expansion are no longer possible (REILLY and SALTIEL, 2017). Excessive storage of triglycerides causes mechanical stresses that may reduce oxygen tension and restrict blood flow in WAT, leading to hypoxia. These stresses trigger inflammatory cascades that regulate cell death (CINTI *et al*., 2005; REILLY and SALTIEL, 2017).

Obesity is associated with a chronic state of low-grade inflammation characterized by abnormal secretion of proinflammatory mediators, macrophage-dependent immune responses, and activation of inflammatory signaling pathways in adipose tissues (SCHÄFFLER and SCHÖLMERICH, 2010; OUCHI *et al*., 2011; BAI and SUN, 2015). These associations were first observed by Hotamisligil *et al*. (1993), who found elevated levels of the proinflammatory cytokine TNF-α in the blood and adipose tissue of obese rats. In 2003, Weisberg *et al*. demonstrated that adipocyte volume is a strong predictor of the percentage of macrophages in adipose tissues, both in humans and mice.

Macroscopic changes in WAT weight are indicative of hypertrophy, fibrosis, neovascularization, and alterations in tissue cell composition, such as monocytic infiltration (SCHÄFFLER and SCHÖLMERICH, 2010). Hypertrophic adipocytes secrete chemokines (such as leukotriene B4, monocyte chemotactic protein-1, and C–C motif chemokine receptors-2 and -5) in a manner that creates a chemotactic gradient for the recruitment of monocytes (SUN *et al*., 2010; CASTOLDI *et al*., 2015; SHI *et al*., 2006; OSBORN and OLEFSKY, 2012). After entering WAT, more than 90% of infiltrated monocytes differentiate into classically activated macrophages (M1). The condition can be further aggravated by inflammatory mediators, such

as lipopolysaccharides (LPS) and IFN-γ, which promote the switch of resident M2 macrophages wich secretes IL-10 and adiponectin (anti-inflammatory environment) to the M1-like phenotype, characterized by CD11c surface expression and production of proinflammatory cytokines (pro-inflammatory environment) (CASTOLDI *et al*., 2015). This crosstalk between hypertrophic adipocytes and macrophages generates a sustained inflammatory state, continually recruiting more macrophages/monocytes from circulation (BAI and SUN, 2015).

In obesity, macrophages adopt a metabolic activation state with prominent lysosomal activity, with the main purpose of eliminating apoptotic/dead adipocytes in an immunologically specific manner to prevent the release of detrimental substances (RUSSO and LUMENG, 2018). Histological examination of hypertrophic WAT reveals crown-like structures formed by accumulation of macrophages around hypertrophic/necrotic adipocytes, suggesting impairment of macrophage-mediated phagocytic processes, as depicted in Fig. 1 (OUCHI *et al*., 2011).

Figure 1. Lean and obese dysfunctional adipose tissue

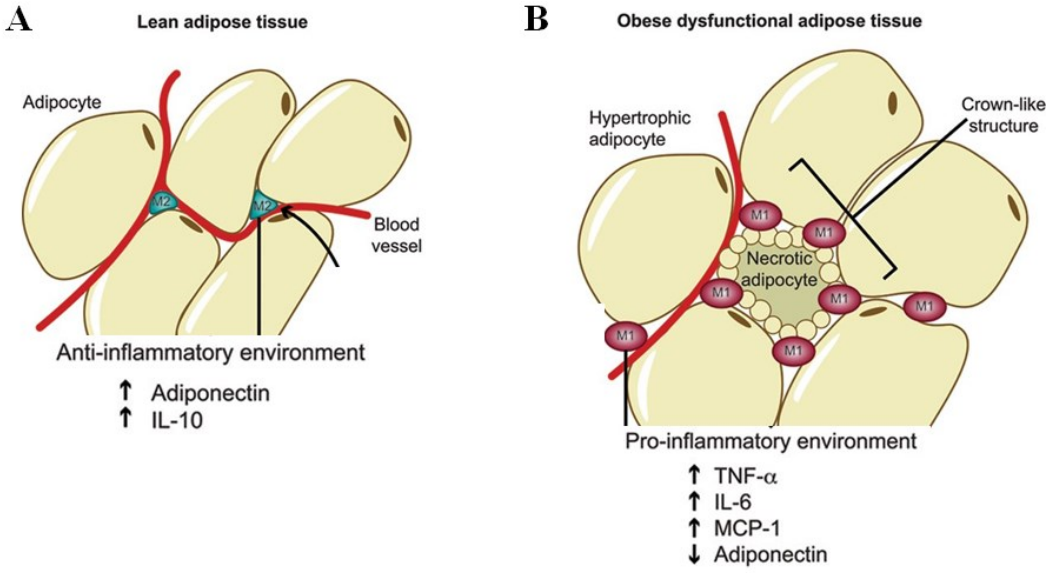

(A) Lean WAT composed of adipocytes and M2 macrophages that secret IL-10 and adiponectin. This panel exemplifies an anti-inflammatory environment. (B) Enlarged adipocytes storing triglycerides that accumulate during excess energy intake. WAT is hypertrophic and infiltrated by proinflammatory M1 macrophages. This panel exemplifies a pro-inflammatory environment. Tumor necrosis factor-alpha (TNF-α) and interleukin (IL)-6 and -10, monocyte chemoattractant protein–1 (MCP-1). Source: adapted from Bijland *et al*. (2013).

Although the precise triggers of obesity-associated inflammation are not fully understood, some potential inducers have been suggested, such as gut-derived antigens and dietary or endogenous lipids (REILLY and SALTIEL, 2017). For instance, endotoxemia, defined as elevated levels of LPS (a cell wall component of Gram-negative bacteria) in blood, is a trigger of chronic inflammation in obese individuals. HFD results in increased circulating

levels of LPS by inducing changes in the composition of the gut microbiota and/or affecting the integrity of the gastrointestinal barrier (PENDYALA *et al*., 2012; SCHACHTER *et al*., 2017). These effects may promote the growth of toxigenic bacteria and increase LPS absorption through chylomicron-driven transport; the increased intestinal permeability syndrome is commonly known as "leaky gut" (RADILLA-VÁZQUEZ *et al*., 2016; GUILLEMOT-LEGRIS and MUCCIOLI, 2017; SCHACHTER *et al*., 2017).

In obese individuals, WAT cells overexpress toll-like receptors (TLR) 2 and 4, a finding that may be associated with obesity-related inflammatory signaling (REILLY and SALTIEL, 2017). The inflammatory cascade can be activated by the binding of gut-derived LPS to TLR4 and by the interaction of SFA with the TLR2 or TLR4 complex, inducing NF-κB activation in monocytes, macrophages, and adipocytes, thereby leading to proinflammatory cytokine production (SCHÄFFLER and SCHÖLMERICH, 2010).

Upon binding to free fatty acids or LPS, TLR4 complexes with CD-14 and myeloid differentiation factor 2 (MD-2) and triggers the initiation of two pathways, one dependent and the other independent of myeloid differentiation primary response 88 (MyD88) (ZHOU *et al*., 2020). Induction of the MyD88-dependent pathway involves phosphorylation and activation of IL-1 receptor-associated kinase (IRAK). IRAK-1, together with TNF receptor-associated factor 6, activates the IκB kinase (IKK) complex, which phosphorylates NF-κB. NF-κB forms a heterodimer with p65/p50 and is translocated to the cell nucleus, where it binds to promoters of inflammatory genes, increasing the expression and release of inflammatory cytokines such as IL-6 and TNF-α (JIALAL *et al*., 2014). MyD88-independent signaling, also known as the TRIF related-adaptor molecule pathway, involves activation of interferon-responsive factor 3 (IRF3) and late phase activation of NF-κB, culminating in increased expression of inflammatory genes and secretion of type I IFNs, as depicted in Fig. 2 (IFN-α and IFN-β) (WANG *et al*., 2014).

Figure 2. Obese dysfunctional adipose tissue and activation of TLR2 and TLR4 complexes in M1 macrophages by inflammatory factors inducing the release of proinflammatory cytokines

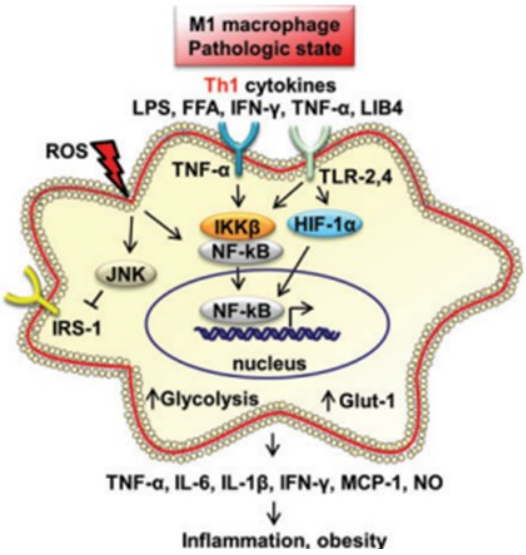

M1 macrophages are activated by inflammatory inducers such as lipopolysaccharides (LPS), free fatty acids (FFA), or proinflammatory factors, leading to the expression and release of proinflammatory cytokines. Tumor necrosis factor-alpha (TNF-α), interleukins (IL)-6 and 1β, interferon gamma (IFN-γ), nitric oxide (NO), nuclear factor-kappa B (NF-κB), reactive oxygen species (ROS), signal transducer and activator of transcription 6 (STAT6), toll-like receptor (TLR), monocyte chemoattractant protein–1 (MCP-1). Source: adapted from Appari *et al*. (2018).

Thus, obesity is characterized by dysregulation of energy metabolism and chronic low-grade inflammation. Systemic inflammation arises from inflammatory inducers, including SFA and LPS, which bind to the TLR2 or TLR4 complex, thereby activating NF-κB in macrophages and WAT adipocytes and increasing peripheral levels of proinflammatory cytokines (COPE *et al*., 2018). Peripheral circulating proinflammatory cytokines, SFA, and immune cells then cross the BBB and reach the hypothalamus, causing neuroinflammation (TAN and NORHAIZAN, 2019). The role of peripheral proinflammatory cytokines and CNS inflammation will be explored in Section 2.4.2.

2.3 ZINC

Zn is an essential micronutrient with numerous structural, biochemical, and regulatory functions. Second only to iron, Zn is the most abundant micromineral in the human body, found in large quantities in all tissues (ROOHANI *et al*., 2013). In 1961, Zn was identified as an essential micronutrient for humans (PRASAD *et al*., 1961). Zn ions act as catalytic, structural, and regulatory cofactors. There are 2800–3000 proteins encoded in the human genome that require Zn for physiological function (MARET, 2013A). The sequency of events in the research

of Zn biology demonstrates an ever-increasing range of functions. Three phases of discovery can be observed: (i) recognition that Zn is essential for all forms of life, (ii) comprehension of Zn in enzymes and other proteins as a basis of their catalytic and structural functions, and (iii) identification of the role of Zn(II) ions in cellular regulation (MARET, 2013B).

The total amount of Zn within the body is 2–3 g (JACKSON, 1989; KAMBE *et al*. 2015). Humans do not have the capacity to store Zn, thereby requiring sufficient daily intake and/or reabsorption to maintain adequate levels and prevent Zn deficiency (KING *et al*., 2015). Rich dietary Zn sources are meat, legumes, eggs, fish, grains, and grain-based products (OLZA *et al*., 2017; KLOUBERT and RINK, 2015). Regarding the bioavailability of Zn from foods, it is known that plant-based foods are rich in phytates, which severely decrease intestinal Zn absorption; thus, Zn from animal-based foods is better absorbed (HAASE *et al*., 2020). Phytates effectively bind to Zn and form stable and insoluble complexes in the duodenum, consequently impairing Zn absorption and leading to excretion in the feces (MIQUEL and FARRÉ, 2007). Recommendations for Zn intake are divided into three levels to account for endogenous Zn losses (sweat, menstrual bleeding, renal, and intestinal losses) and phytate intake. The recommended Zn intake is 11 mg/day for adult men with a low phytate intake, 14 mg/day for adult men with a moderate phytate intake, and 16 mg/day for adult men with a high phytate intake; for adult women, the recommended intake levels are 7, 8, and 10 mg/day, respectively (HAASE *et al*., 2020).

Zn is found in all tissues and secretions at relatively high concentrations, with 80–90% of whole-body Zn in bone and skeletal muscle and 5% in the skin and liver. The remaining Zn is distributed in other tissues, with the highest concentrations in the prostate and parts of the eye (TAPIERO and TEW, 2003; CHASAPIS *et al*., 2012; KAMBE *et al*., 2015). Less than 1% of total Zn is found in the serum, from where it is distributed to the body to maintain biological processes. Of this small fraction, 80–90% of the serum Zn pool is bound to serum albumin and 10–20% is strongly bound to α2-macroglobulin (KAMBE *et al*., 2015). A small fraction of the serum pool is free Zn, which is relatively weakly bound to low molecular weight ligands. The free Zn pool is also known as labile, mobile, bioavailable, or rapidly exchangeable Zn (ZALEWSKI *et al*., 2006; MARET, 2015; ALKER *et al*., 2019). At the cellular level, 30–40% of intracellular Zn is located in the nucleus, 50% in the cytoplasm, 10% in cell membranes, and the remainder in organelles and specialized vesicles (TAPIERO and TEW 2003; KAMBE *et al*. 2015). Cytoplasmic Zn comprises three main pools: protein-bound Zn, Zn stored in vesicles (known as zincosomes), and free Zn, which is bound to low molecular weight ligands (MARET, W. 2017). This pool of free Zn is biologically active, as shown by its involvement

in numerous signaling pathways (FUKADA *et al*., 2011; CARTER *et al*., 2014). Intracellular free Zn acts as an intracellular molecule and second messenger, transmitting information between cells. Changes in its homeostasis can lead to diverse types of abnormalities in humans and animal models (FUKADA *et al*., 2011).

Zn ions play essential roles in numerous intracellular signaling pathways. For instance, free Zn acts as a signaling molecule in immune cells and as a neurotransmitter in synaptic vesicles (FREDERICKSON *et al.*, 2005; FUKADA *et al.*, 2011 WELLENREUTHER *et al.*, 2009; FUKADA and KAMBE, 2018). In brain cells, free Zn is released from presynaptic terminals and modulates various receptors. It inhibits the glutamatergic NMDA receptor and activates signaling pathways via GPR39 receptors (MŁYNIEC *et al*., 2013; WANG *et al*., 2018). Disruption of Zn homeostasis in the hippocampus and cortex has been implicated in behavioral cognition and emotional disturbances (WANG *et al*., 2018). Numerous preclinical and clinical studies demonstrated the role of Zn deficiency in the development of depressive symptoms (MAES *et al*., 1994; 1997; SWARDFAGER *et al*., 2013; NGUYEN *et al*., 2009; STYCZEŃ *et al*., 2017). Zn ions also play an important role in the regulation of immune system and inflammatory processes (MAARES and HAASE, 2016). The relationship between Zn and inflammatory signaling is based particularly on TLR-4 signaling in monocytes and macrophages (MAARES and HAASE, 2016; GAO *et al*., 2018). Zn ions have the ability to regulate the signaling pathway of TLR receptors, which, in turn, and can inhibit or induce NF-κB activation, influencing the expression and production of proinflammatory cytokines, such as IL-6, TNF-α, and IL-1β (FOSTER and SAMMAN, 2012).

Given the biological importance of intracellular free Zn, its precise determination is crucial and of current interest (CARTER *et al*., 2014; KAMBE *et al*. 2015). Free Zn determination can be achieved using fluorescent probes. The analytes (metal ions) recognize the site and bind to metal ion chemosensors; as a result, the complex emits intense fluorescence (LIM *et al*., 2004; CARTER *et al*., 2014; ALKER and HAASE, 2020). The most common cell-permeable and Zn-selective dyes used for free Zn determination are Zinpyr-1 and FluoZin3-AM (WALKUP *et al*., 2000; BURDETTE *et al*., 2001; KRĘŻEL and MARET, 2006; ALKER and HAASE, 2020). The formula introduced by Grynkiewicz and coworkers (GRYNKIEWICZ *et al*. 1985) allows estimation of the concentration of labile Zn, when Zn and TPEN (*N*,*N*,*N*′,*N*′-tetrakis(2-pyridylmethyl)-1,2-ethanediamine) are used to determine the maximal and minimal fluorescence, respectively (HAASE *et al*., 2006). Whereas EDTA (ethylenediaminetetraacetic acid) is a membrane-impermeable chelator (RICHARDSON and BAKER, 1994), TPEN is a

well-known membrane-permeable chelating agent that primarily depletes intracellular free Zn, which has a femtomolar affinity of 15.6 L/mol (pH 7.2) (MARET, W. 2015).

2.3.1 Zinc deficiency in obesity

The relationship between Zn deficiency and obesity in humans was established in the 1970s (ATKINSON *et al*., 1978). In the past decades, numerous epidemiological studies have supported that obesity is associated with hypozincemia, which might have implications in the development of obesity-related diseases (CHEN *et al*., 1988; SINGH *et al*., 1998). A study conducted by de Luis *et al.* (2013) showed a high prevalence (73.9%) of micronutrient deficiencies in obese women before bariatric surgery. Other studies reported reduced serum Zn levels in obese individuals both before and after bariatric surgery (MADAN *et al*., 2006; XANTHAKOS, 2009). In India, a probable association was observed between hypozincemia and increased body fat in adults (SINGH *et al.*, 1998).

In a systematic review of 17 articles (published up to April, 2018) about the association between serum Zn level and overweight/obesity, Gu *et al*. (2018) found that serum Zn levels were significantly decreased in obese children and adults. The authors also described some of the possible mechanisms underlying the association between hypozincemia and obesity (GU *et al*., 2018). One explanation for Zn deficiency in obesity is that chronic low-grade inflammation can affect cortisol metabolism and increase proinflammatory cytokine levels. Glucocorticoids and proinflammatory cytokines may stimulate the expression of genes encoding Zn transporters and metallothionein. Such proteins increase cytoplasmatic concentrations of Zn by increasing influx and release in intracellular organelles, thereby decreasing serum Zn levels (MOTA MARTINS *et al*., 2014; GU *et al*., 2018). Schmidt *et al*. (2007) observed that Zn transporter proteins were more expressed in subcutaneous WAT. The authors suggested that obesity may increase the transport of Zn in WAT, favoring hypozincemia in obese individuals.

Ozata *et al.* (2002) found low plasma levels of Zn and alterations in plasma antioxidant defense mechanisms in obese adult men; the authors suggested that obesity leads to oxidative stress. Rodent studies demonstrated that Zn deficiency in obesity causes increased oxidative stress and altered adipose metabolism (TALLMAN and TAYLOR, 2003; LIU *et al*., 2013). Tallman and Taylor (2003) demonstrated that C57BL/6J mice fed diets rich in SFA and low in Zn had reduced fatty acid content in adipose triglycerides than mice fed HFDs. The authors proposed that Zn status influences fatty acid accumulation in WAT (TALLMAN and TAYLOR, 2003). Interestingly, Liu *et al*. (2013) showed that C57BL/6J mice fed an HFD low

in Zn had increased circulating leptin levels and altered leptin signaling in the liver. The results further showed an increase in the infiltration of activated macrophages into visceral WAT of Zn-deficient obese mice. The authors suggested that leptin acts as a chemoattractant that recruits monocytes and macrophages into WAT, contributing to exacerbation of the proinflammatory state (LIU *et al*., 2013). Furthermore, decreased dietary Zn intake in obesity can contribute to a chronic inflammatory state. IL-1α, IL-1β, and IL-6 were upregulated in peripheral blood mononuclear cells of overweight and obese Zn-deficient adults (with low dietary Zn intake) compared with overweight and obese subjects with normal dietary Zn intake (COSTARELLI *et al.*, 2010). In the referred study, micronutrient dietary intakes were estimated using a semiquantitative food frequency questionnaire. The authors suggested that hypozincemia can aggravate obesity-related disturbances, such as insulin resistance and inflammation, thereby worsening the preexisting obesity status (COSTARELLI *et al.*, 2010).

Zn is an important regulator of zinc-α-2-glycoprotein activity. The protein mediates lipolysis and adiponectin production. The low Zn serum levels associated with obesity appear to inhibit zinc-α-2-glycoprotein, leading to a decrease in serum adiponectin and an increase in leptin levels (GU *et al*., 2018; SEVERO *et al*., 2020). Leptin enhances the expression of proinflammatory cytokines, such as IL-6, IL-8, and TNF-α, contributing to the persistence of inflammation in obese individuals (GU *et al*., 2018). Evidence has shown that alterations in immune–inflammatory responses and oxidative stress are linked to several types of psychiatric disorders, for instance, the pathophysiology of depression (WANG *et al*., 2018). Clinical and experimental studies have demonstrated that dietary Zn insufficiency is associated with depressive behaviors and that plasma Zn levels are lower in depressive patients (SWARDFAGER *et al*., 2013; GRØNLI *et al*., 2013). Tassabehji *et al*. (2008) reported that rats fed Zn-deficient diets for 3 weeks developed depression-like symptoms, including anorexia, anhedonia, and increased anxiety-like behavior. Treatment with the antidepressant drug fluoxetine (10 mg/kg) was ineffective in Zn-deficient rats. Interestingly, low serum Zn in depressed patients was correlated with immune–inflammatory responses and neuroprogression (MAES *et al*., 1997). A possible hypothesis for the relationship between hypozincemia and depression is that Zn deficiency exacerbates low-grade systemic inflammation, which stimulates IDO expression and activation. The increase in IDO expression/activation by peripheral or central proinflammatory cytokines can cause a shift in the Kyn pathway, increasing Kyn production and consequently leading to serotonin depletion; these effects are likely responsible for relevant emotional and cognitive alterations in obese patients (SWARDFAGER *et al*., 2013; JENKINS *et al*., 2016). The effect of proinflammatory cytokines

on IDO expression/activation in the Kyn–Trp pathway and the development of depression-like symptoms will be explored in Sections 2.4.3 and 2.4.4.

Despite all clinical and experimental studies demonstrating the relationship between Zn deficiency, obesity, and neuropsychiatric disorders, the physiopathological mechanism connecting these factors still not completely understood and needs to be clarified at cellular and tissue levels.

2.4 OBESITY AND NEUROPSYCHIATRIC COMORBIDITIES

Obesity is associated with comorbidities such as diabetes, cardiovascular disease, and several neurological disorders, particularly sleep disturbance, as well as psychiatric and psychosocial problems. Depressive symptoms are observed in obese individuals at a higher rate than symptoms of other disorders observed in obese subjects (COHEN, 2010). Obesity significantly contributes to the development of neuropsychiatric comorbidity, and there is a bidirectional association between depression and obesity. Depressed individuals are more likely to gain weight and increase abdominal adiposity because of poor diet quality and reduced physical activity (PAN *et al*., 2012; ZHAO *et al*., 2011).

Mood and anxiety disorders, depressive symptoms, cognitive impairment, and binge eating are some of the neuropsychiatric comorbidities frequently seen in obese individuals, often leading to a reduction in quality of life (CASTANON *et al*., 2014). The major depression symptoms experienced by obese individuals are low self-esteem, anhedonia (hyposensitivity to pleasure), hopelessness, altered appetite, sleep disturbance, lack of energy, self-destructive behavior, and suicidal ideation (SMITH and JAKOBSEN, 2013).

The development of functional neuroimaging techniques such as magnetic resonance imaging, single-photon emission computed tomography, and positron emission tomography, has allowed investigation of brain regions involved in the pathophysiology of obesity (TATARANNI and DELPARIGI, 2003; PALAZIDOU, 2012; WHITTEN, 2012) and *in vivo* characterization of anatomy, physiology, and neurochemistry in human subjects with mood disorders. Neuronal atrophy was observed in the medial prefrontal cortex and hippocampus of individuals with such disorders (PRICE and DREVETS, 2012).

A previous study investigated the effects of high BMI and regional cerebral blood flow in healthy subjects using single-photon emission computed tomography (WILLEUMIER *et al.*, 2011). The findings revealed that overweight is associated with lower blood flow in the brain, particularly in the prefrontal cortex and anterior cingulate gyrus, which may impair brain

functions (WILLEUMIER *et al.*, 2011). In another study, positron emission tomography indicated an increase in cerebral metabolic activity in obese women, particularly in the posterior cingulate gyrus, attributed to functional compensation (MARQUES *et al*., 2014).

2.4.1 Neurobiology of depression

Over the past decades, the pathophysiology of depression has been explained by the monoamine hypothesis. This theory suggests that depression results from a decrease in the synthesis of biogenic amine neurotransmitters (noradrenaline and/or serotonin) in the CNS (LÓPEZ-MUÑOZ and ALAMO, 2009). Serotonin, a catabolite of Trp formed by the action of Trp hydroxylase, has important functions, including appetite suppression, energy expenditure, and behavior regulation (YABUT *et al.*, 2019). After several clinical experiments, researchers concluded that serotonin metabolism is reduced in depressed subjects, giving way to the development of a class of antidepressants known as selective serotonin reuptake inhibitors (e.g., citalopram, fluoxetine, paroxetine, and sertraline). These antidepressant drugs were shown to increase serotonin neurotransmission (WOHLEB *et al*., 2016; LILLY, 2017); however, despite the advances in depression treatment, one-third of depressed patients fail to respond to conventional antidepressant medication, revealing limitations in the monoaminergic hypothesis of depression.

Modern theories have been proposed to better explain the pathophysiology of mental disorders (RUSH *et al*., 2006; CHAVES FILHO *et al*., 2018). The pathophysiological mechanisms of obesity and cognitive function remain to be fully understood. It is possible that multiple biological systems are involved and interconnected (COHEN, 2010; ARNONE *et al*., 2018). Therefore, it is important to identify the mechanisms underlying neuropsychiatric symptoms in obesity. Some clinical studies reported strong evidence of the role of inflammatory processes in obesity development. After administration of cytokines as therapeutic agents for cancer or viral disease treatment, patients began to experience depressive symptoms (CAPURON *et al.*, 2002). Recent reports showed that depression is associated with increased levels of proinflammatory cytokines in peripheral blood and the CNS (BAUNE *et al*., 2012; PAPAKOSTAS *et al*., 2013).

2.4.2 Obesity and neuroinflammation

Obese individuals display hypertrophied WAT and resident immune cells that cause an elevation of the peripheral inflammatory response, affecting the organism as a whole and producing neuroinflammation, particularly in the hypothalamus (GUILLEMOT-LEGRIS and MUCCIOLI, 2017). Peripheral circulating proinflammatory cytokines, SFA, and immune cells can cross the BBB and reach the hypothalamus, where they activate cytokine receptors that initiate and modulate inflammatory cascades (TAN and NORHAIZAN, 2019).

The CNS is a complex organ composed of numerous cell types. Examples are neurons, glial cells, and endothelial cells. Some resident brain cells lie in close contact with the BBB (LAMPRON *et al.*, 2013; GUILLEMOT-LEGRIS and MUCCIOLI, 2017). Because most peripheral cytokines are large molecules, they cannot freely cross the BBB. However, there is evidence that proinflammatory cytokines such as TNF-α and IL-6 increase BBB permeability (ROCHFORT and CUMMINS, 2015). Moreover, proinflammatory cytokines can gain access to the brain through leaky regions of the BBB (seen, for instance, in the choroid plexus and circumventricular organs) via volume diffusion or through cytokine transporters known as saturable transport systems (DANTZER *et al*., 2008). It has also been proposed that receptors for IL-1β, IL-6, and TNF-α, which are expressed on the cerebral endothelium, could induce the synthesis of these and other proinflammatory cytokines (VARATHARAJ and GALEA, 2017).

Elevated SFA levels induced by HFD can also disrupt BBB integrity (NGUYEN *et al.*, 2014). Evidence indicates that HFD consumption produces a decrease in the mRNA expression of tight junction proteins in the choroid plexus and BBB of rodents, consequently increasing blood-to-brain permeability in the hypothalamus (KANOSKI *et al*., 2010). Some observations indicate that BBB breakdown in obesity impairs cognition by allowing the traffic of peripheral macrophages into the brain parenchyma (STRANAHAN *et al*., 2016).

The mechanisms responsible for HFD-induced neuroinflammation were investigated by de Souza *et al.* (2005). The authors demonstrated that HFDs induce the expression of proinflammatory cytokines and activation of NF-κB in the hypothalamus of rodents. Subsequent studies showed that HFDs high in SFA cause hypothalamic inflammation in DIO rodent models (MILANSKI *et al.*, 2009; MARIC *et al*. 2014; THALER *et al*., 2012). Milanski *et al.* (2009) revealed that SFA could enter the brain and act as a molecular target for the TLR4 receptor, triggering intracellular inflammatory signaling in the hypothalamus of rats. Further data from a study conducted by Maric *et al*. (2014) suggested that different fat sources can induce different proinflammatory profiles. The researchers found a higher TLR4 mRNA

expression, followed by a more pronounced upregulation of IL-6, IL-1β, and TNF-α, in the hypothalamus of rats fed diets rich in SFA from butter compared with those fed diets rich in SFA from coconut oil. It has been shown that markers of hypothalamic inflammation such as IL-1β and IL-6 increase within 24 h of feeding on an HFD in rodent models; these effects occur before any substantial weight gain can be detected (THALER *et al*., 2012).

Clinical and experimental studies have demonstrated that overproduction of central and/or peripheral proinflammatory cytokines can enhance the expression or activate IDO, an enzyme that catabolizes Trp into Kyn and neuroactive derivatives of Kyn (BRANDACHER *et al.*, 2006; CAPURON and MILLER, 2011). Recently, Mangge *et al.* (2014) demonstrated the relationship between Trp catabolism and obesity-related immune-mediated inflammation.

2.4.3 Kyn–Trp pathway

Trp is one of the nine essential amino acids for humans. In the body, it follows complex metabolic pathways. About 90–95% of the circulating Trp is complexed with albumin and cannot cross the BBB. However, the remaining fraction exists in its free form in the blood and has access to the brain (RUDDICK *et al.*, 2006; BADAWY, 2016; REFAEY *et al*., 2017).

Trp can be metabolized via four pathways, three of which are of minor quantitative relevance, namely the hydroxylation (serotonin), decarboxylation (tryptamine), and transamination (indole-pyruvic acid) pathways. The major pathway is the Kyn route, which accounts for 95% of Trp catabolism (BADAWY, 2016). Trp is converted to *N*-formylkynurenine by TDO (EC 1.13.11.11). This reaction occurs mainly in the liver (an organ rich in enzymes necessary for NAD^+ synthesis), kidney, and immune cells and is responsible for 90% of peripheral Trp metabolism under physiological conditions (AGUDELO *et al.*, 2014; BADAWY, 2017).

Trp can also be converted to *N*-formylkynurenine by IDO (EC 1.13.11.17) and further hydrolyzed to Kyn by *N*-formylkynurenine formamidase (BADAWY, 2016). IDO is broadly distributed in peripheral tissues and immune cells and, more importantly, in the brain, particularly in astrocytes, infiltrating macrophages/microglia, and dendritic cells (BADAWY, 2016; CHAVES FILHO *et al*., 2018). IDO exists in two forms: IDO 1 and IDO 2. Human IDO 2 has a much higher K_m for Trp than IDO 1 but exhibits reduced catalytic activity. Thus, the Kyn pathway is controlled mainly by circulating free Trp, TDO activity in the liver, and IDO activity elsewhere (BADAWY, 2016). The Kyn/Trp ratio can be used to estimate IDO activity/expression and as a readout for peripheral or central Trp catabolism (ARNONE *et al.*,

2018). In physiological situations, the control of plasma Trp availability is exerted mainly by hepatic TDO. However, when the immune system is activated, IDO takes center stage in Trp catabolism, being expressed and activated by several proinflammatory cytokines, alone or in combination, such as IFN-γ, IL-6, TNF-α, IL-2, and IL-1β. TDO may also play an important part under immune-stimulatory conditions (CAMPBELL *et al.*, 2014; BADAWY, 2016).

Kyn is degraded through three specific pathways to generate different neuroactive metabolites. (1) Kyn hydroxylase (monooxygenase) converts Kyn into anthranilic acid. (2) Irreversible transamination by Kyn aminotransferases in astrocytes, oligodendrocytes, and neurons metabolizes Kyn into kynurenic acid (KYNA) (CAPURON and MILLER 2011; QIN *et al.*, 2018; HAROON *et al.*, 2020). (3) Kyn-3-monooxygenase converts Kyn into 3-hydroxykynurenine. Only Trp, Kyn, and 3-hydroxykynurenine efficiently cross the BBB, as these molecules can be actively transported to the CNS by L-type amino acid transporter 1, the large neutral amino acid carrier system (GOSTNER *et al*., 2020). Further cleavage of 3-hydroxykynurenine by kynureninase B yields 3-hydroxyanthranilic acid, which is then oxidized by 3-hydroxyanthranilic acid oxidase into 2-amino-3-carboxymuconic-6-semialdehyde. After production of 2-amino-3-carboxymuconic-6- semialdehyde, there are two possible degradation routes. One branch leads to the formation of small quantities of picolinic acid, and the other produces QUIN. In the brain, QUIN is synthesized by infiltrating macrophages and microglial cells (BADAWY, 2016; CAPURON and MILLER 2011; CHAVES FILHO *et al.*, 2018; HAROON *et al.*, 2020).

All of the aforementioned Kyn catabolites exert different biological and neurobehavioral effects. For example, KYNA and picolinic acid have neuroprotective properties, as they are able to block NMDA receptors. By contrast, 3-hydroxykynurenine and QUIN have neurotoxic effects as a result of their ability to generate oxidative radicals and act as NMDA receptor agonists (CHAVES FILHO *et al*., 2018). On the basis of these findings, studies proposed the use of the KYNA/QUIN ratio as a neuroprotective index, where low values indicate an inflammation-induced pathology (QIN *et al.*, 2018; ARNONE *et al.*, 2018). Recently, Bay-Richter *et al.* (2015) found an excessive production of QUIN concomitant with elevated levels of IL-6 and decreased levels of KYNA in cerebrospinal fluid of suicidal patients compared with healthy controls. The researchers reported a relationship of clinical vulnerability to severe depressive symptoms with inflammatory conditions and altered levels of Kyn catabolites, corroborating the inflammatory hypothesis that depression is associated with microglial Kyn pathway expression/activation in an inflammation-related state (DANTZER *et al*., 2011).

2.4.4 Effect of proinflammatory cytokines on IDO expression/activation in the Kyn–Trp pathway and the development of depression-like symptoms

Recent studies have proposed that imbalance of Kyn/Trp catabolites is a consequence of IDO expression/activation by proinflammatory cytokines. Such results suggest a link between increased neuroinflammation and behavioral alterations in obesity. Reininghaus *et al.* (2014) found increased Kyn levels and KYNA/QUIN ratio caused by inflammatory mediators in the blood of bipolar overweight individuals. A preclinical study demonstrated that DIO mice fed palatable energy-dense food had a significant behavioral change after 9 weeks and anxiety-like behavior after 18 weeks (ANDRÉ *et al*., 2014). At 20 weeks, DIO mice showed LPS-induced depressive-like behavior compared with LPS-treated lean mice, exhibiting elevated levels of TNF-α and IL-6 in plasma and increased Kyn/Trp ratio in the lungs and brain. Upregulation of IL-6 and IDO was observed in the hypothalamus and that of TNF-α, IFN-γ, and IDO in the hippocampus. The authors concluded that energy-dense diets alter cognition and anxiety and enhance activation of neurobiological mechanisms underlying depression after immune stimulation (ANDRÉ *et al*., 2014).

Overall, the findings of this literature review show that the obesity pandemic might be contributing to the increased prevalence of depression and vice-versa. Several epidemiologic studies revealed a relationship between Zn deficiency and obesity. Thus, obesity, Zn deficiency, and depression might share a crucial, pivotal mediator: the inflammatory process. Excessive production of proinflammatory cytokines from WAT can result in enhanced IDO expression and activation in the Kyn–Trp pathway in the CNS, thereby increasing the levels of neurotoxic catabolites. Questions arise about the impact of Zn deficiency in obesity and the onset of neuropsychiatric alterations. This study examines the role of Zn deficiency in certain aspects of Kyn–Trp metabolic conversion *in vivo* and *in vitro*.

3 AIMS

This thesis aimed to investigate the influence of Zn deficiency on obesity and the development of behavioral alterations. The research was divided into two substudies, as follows: an *in vivo* study investigating the influence of Zn deficiency in Kyn–Trp catabolism in obese mice fed an HFD or a Zn-deprived HFD and an *in vitro* study assessing the effects of Zn deficiency on Kyn–Trp catabolism in a combination of two human cell line subsets, THP-1 macrophages and A172/T98G glioblastoma cells.

In the *in vivo* study, we aimed to:

(1) induce obesity in experimental animals fed a restrictive HFD or a Zn-deprived HFD;

(2) evaluate morphometric parameters;

(3) subject animals to behavioral tests, such as the splash test;

(4) analyze the effect of obesity on biochemical, hematological, and histological parameters; and

(5) determine plasma levels of Kyn, Trp, Kyn/Trp ratio, adipokines such as leptin and adiponectin, as well as serum levels of Zn and the ability of fluoxetine to reverse these parameters.

The goals of the *in vitro* study were to:

(1) establish an *in vitro* cell culture model suitable for the investigation of the effects of Zn deficiency on Trp–Kyn pathway under proinflammatory conditions by combining two human cell line subsets: THP-1 macrophages, capable of synthesizing proinflammatory mediators upon LPS stimulation, and A172/T98G glioblastoma cells, active in the Trp–Kyn pathway cascade;

(2) measure Trp and Kyn levels and calculate the Kyn/Trp ratio in A172 and T98G culture media treated with supernatant from LPS-stimulated THP-1 macrophages;

(3) investigate the effect of Zn deficiency on Kyn/Trp breakdown by measuring total Kyn levels and Kyn/Trp ratio produced by T98G cells following treatment with supernatant from LPS-stimulated THP-1 macrophages;

(4) investigate the impact of Zn deficiency on Kyn/Trp breakdown by measuring total Kyn levels and Kyn/Trp ratio produced by T98G cells treated with supernatant from LPS-stimulated THP-1 macrophages cultivated under Zn-deficient conditions;

(5) determine intracellular labile Zn levels in THP-1 macrophages when post-treated with LPS, TPEN, or a combined LPS/TPEN treatment;

(6) determine LPS-induced gene expression of proinflammatory cytokines, such as TNF-α, IFN-α, IFN-β, and IFN-γ, in LPS-stimulated THP-1 macrophages cultivated under Zn-adequate and Zn-deficient conditions; and

(7) determine levels of proinflammatory cytokines IL-6 and TNF-α in supernatant from LPS-stimulated THP-1 macrophages cultivated under Zn-adequate and Zn-deficient conditions by an enzyme-linked immunosorbent assay.

4 MATERIALS AND METHODS

4.1 *IN VIVO* STUDY

4.1.1 Mice and diets

Adult female Swiss albino mice (8–9 weeks of age, 39.0 ± 2.0 g body weight) were obtained from the animal breeding center of the Federal University of Santa Catarina (UFSC). Experimental procedures were approved by the local animal ethics committee (CEUA/UFSC protocol PP00892) and are in accordance with animal ethics and welfare requirements of Brazilian legislation (Law no. 11.794/2008). The animals were maintained in standard polypropylene cages with stainless steel mesh cover under controlled temperature (22 ± 2 °C) and relative humidity (65–75%) conditions on a 12:12 h light/dark cycle with *ad libitum* access to food and water.

After 1 week of adaptation, the animals (n = 10 per group) were randomly assigned to one of four dietary groups for 8 weeks: standard diet (SD), standard Zn-deficient diet (SD-ZD), HFD, and high-fat Zn-deficient diet (HFD-ZD). Diets were formulated based on the American Institute of Nutrition (REEVES *et al*., 1993). HFDs contained 30% lard. The composition of experimental diets is presented in Table S1 (Supplementary Material), and vitamin and mineral contents are provided respectively in Tables S2 and S3 (Supplementary Material). Daily food intake was calculated by subtracting the weight of leftovers from the initial weight of feed (ASAKAWA *et al*., 2003). Energy intake (kcal/day) was calculated by multiplying the daily food intake by the energy value of each diet (SD and SD-ZD, 3.5 kcal/g; HFD and HFD-ZD, 5.2 kcal/g). Body weight, naso-anal length, and abdominal circumference were recorded once a week. Feed efficiency was estimated as weight gain (g) divided by energy intake (kcal) during the 8-week experimental period (NOVELLI *et al*., 2007; HEENEY *et al*., 2019). The Lee index was calculated as the cube root of body weight (g) divided by naso-anal length (cm) (NOVELLI *et al*., 2007).

At the end of the experimental period, mice (n = 5 per group) were subjected to the splash test for behavioral assessment, as described in Section 4.1.4. At 24 h after the splash test, blood was collected by decapitation into EDTA-containing tubes (BD Vacutainer®, Franklin Lakes, USA) for evaluation of hematological parameters and into no-additive tubes (No Additive Vacuette®, Greiner Bio-one, Monroe, USA) for biochemical analysis of serum leptin, adiponectin, total Zn, Trp, and Kyn levels. The experimental protocol is illustrated in Fig. 3.

For biochemical analysis, samples were allowed to coagulate for 30 min at room temperature and were then centrifuged at 3000 × *g* for 10 min. Serum was separated and stored at −80 °C until measurement (GOLDE *et al*., 2005). Organs (liver, lung, heart, spleen, kidney, brain, and WAT) were dissected, weighed, and stored in 70% ethanol (CHAURAND *et al*., 2008).

In the second part of this study, the remaining mice (*n* = 5 per group) were maintained on their respective feeding regimens while placed on antidepressant treatment with fluoxetine hydrochloride (Pharmanostra®, São Paulo, Brazil) for an additional 2 weeks (Fig. 3). Fluoxetine was freshly prepared in saline solution (0.9% NaCl) and administered orally by gavage at a dose of 10 mg/mL once a day (FREITAS *et al*., 2013). Following behavioral assessment by the splash test, mice were sacrificed by decapitation, and blood samples were collected for biochemical analysis.

Figure 3. *In vivo* experimental design

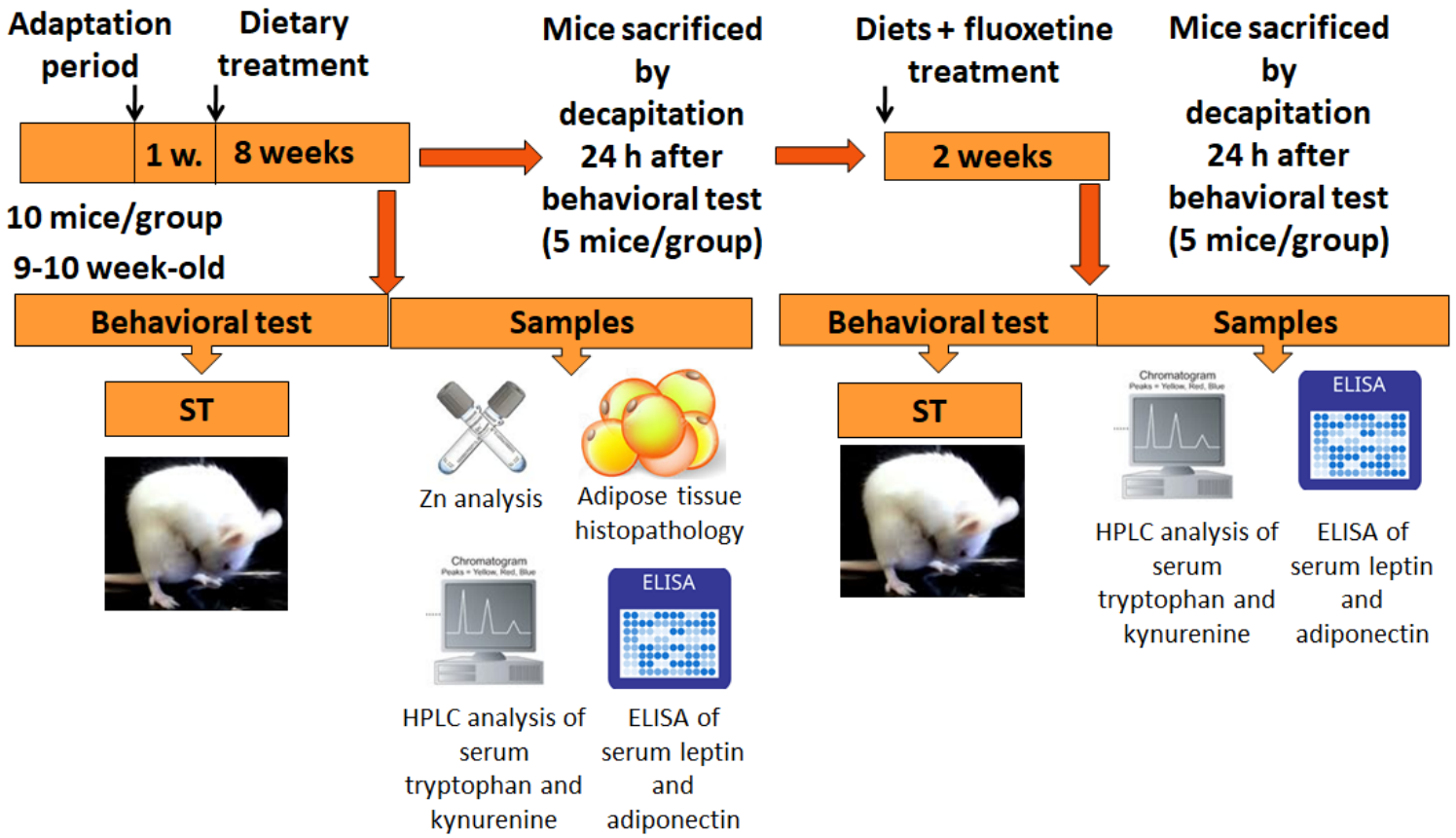

Schematic representation of the experimental protocol indicating the feeding period (8 weeks) and four dietary groups: standard diet, standard zinc (Zn)-deficient diet, high-fat diet, and high-fat Zn-deficient diet (n = 10 per group). The splash test (ST) was used to assess motivation behaviors. At 24 h after the behavioral test, the mice (n = 5 per group) were sacrificed by decapitation, blood samples were collected for hematological and biochemical analyses, and organs were dissected, weighed, and stored in preservation solution. In the second part of the experimental protocol, mice (n = 5 per group) were maintained on their respective diets, treated with fluoxetine for 2 weeks, subjected to the behavioral test, and sacrificed by decapitation. Blood samples were collected for biochemical analysis.

4.1.2 Measurement of adiposity and WAT morphology

Visceral (perigonadal region) and subcutaneous WAT fat pads were excised separately, weighed, and stored in 70% ethanol (CHAURAND *et al*., 2008). The adiposity index was calculated as total adipose tissue weight divided by total body weight (%) (TERRA *et al*., 2009). Adipose tissue morphology was analyzed in terms of adipocyte cell number and size distribution (volume) within the WAT compartment (TANDON *et al*., 2018). For histological analysis, small fragments (~0.5 g) of WAT were collected from SD, SD-ZD, HFD, and HFD-ZD mice and fixed in 4% paraformaldehyde solution for 24 h. The SD-ZD group samples were preserved in incorrect conditions therefore were not possible to be analyzed. After fixation, tissues were dehydrated (80% ethanol for 1 h, 90% ethanol for 1 h, 100% ethanol for 1.5 h, 1:1 (v/v) xylol/ethanol for 10 min, and xylol for 10 min) and embedded in paraffin at 52 °C using an automatic tissue processor (Leica TP 1020, Leica Biosystems, Nussloch, Germany). Paraffin blocks were cut into successive 5 μm thick sections (Leica RM 2255, Leica Biosystems, Nussloch, Germany). Sections were mounted on slides and subjected to automated staining (Leica Autostainer XL, Leica Biosystems, Nussloch, Germany) with hematoxylin/eosin or Prussian blue. Photomicrographs of WAT sections were captured at 100× and 200× magnification using an inverted microscope (Olympus IX83, Olympus Corporation, Tokyo, Japan) equipped with a digital camera and CellSens Dimension software version 1.12 (Olympus Corporation, Tokyo, Japan). Images of five slides containing three sections from each group were analyzed for mean relative cell number using ImageJ software (NIH, Bethesda, USA). Adipocyte volume (V) was calculated by the equation $V = 4\pi \times \text{radius}^3 \div 3$ (ROTONDO *et al*., 2016).

4.1.3 Biochemical and hematological analyses

Mice were sacrificed by decapitation, and blood samples were collected for total serum Zn analysis into no-additive tubes (No Additive Vacuette®, Greiner Bio-one, Monroe, USA). Samples were allowed to coagulate for 30 min at room temperature and were then centrifuged at 3000 × *g* for 10 min. Serum was separated and stored at −80 °C until measurement (GOLDE *et al*., 2005). All laboratory glassware and materials were washed with 1% chloridric acid to avoid any sources of contamination prior to analysis. Total serum Zn levels were determined using a Zn colorimetric assay kit (chromogen 2-(5-bromo-2-pyridylazo)-5-(*N*-propyl-*N*-sulphopropylamino)-phenol, catalogue number ZN2341, Randox Laboratories Ltd., Crumlin,

UK). Prior to Zn analysis, serum calibrators were obtained from Sigma–Aldrich (Mauá, Brazil), and samples were deproteinized with trichloroacetic acid at 8000 × *g* for 10 min. Zn colorimetric analysis were performed using a UV/Vis spectrophotometer (Pharmacia LKB, Ultrospec III, Biochrom, Holliston, USA) at a wavelength of 550 nm following the parameters outlined in the Randox protocol.

Serum leptin and adiponectin were quantified by an enzyme-linked immunosorbent assay (ELISA), according to the manufacturer's protocol (R&D Systems, Inc. Minneapolis, USA). Linear calibration curves were constructed for determination of leptin and adiponectin concentrations in the ranges of 0.06 to 4 ng/mL and 156 to 10,000 ng/mL, respectively, with a lower detection limit of 0.02 ng/mL for both leptin and adiponectin. Hematological parameters (red blood cell count, hemoglobin, hematocrit, mean corpuscular volume, mean corpuscular hemoglobin concentration, total and differential leukocyte, and platelet counts) were measured using a veterinary hematology analyzer (BC-2800 Vet, Mindray Bio-Medical. Electronics Co. Ltd, Shenzhen, China).

4.1.4 Splash test

The splash test, a behavioral assay used to assess self-care and motivation behaviors, was carried out as described by Isingrini *et al.* (2010), with minor modifications. Briefly, mice were placed individually in clear Plexiglas boxes, sprayed with 10% sucrose solution on the dorsal coat, and monitored for latency (time between spraying and grooming) and duration of grooming behavior (FREITAS *et al*., 2013). The high viscosity of sucrose solution is expected to induce grooming in mice; increased latency and decreased grooming duration are analogous to some symptoms of depression, such as anhedonia (WILLNER, 2005; YALCIN *et al*., 2005; d'AUDIFFRET *et al*., 2010). The apparatus was cleaned with 10% ethanol between each test to eliminate animal clues. All tests were video-recorded (GoPro HERO 3+, San Mateo, USA) for 5 min after spraying.

4.1.5 Determination of serum Trp and Kyn

Trp and Kyn standard solutions (analytical grade, >99% purity) were obtained from Sigma–Aldrich (Mauá, Brazil). Calibration curves were constructed by diluting Trp (5, 10, 25, 50, 100, and 150 µM) and Kyn (0.5, 1, 1.5, 2, 3, and 6 µM) in Milli-Q water. Trp and Kyn were quantified using a Shimadzu LC-20A high-performance liquid chromatography (HPLC)

apparatus (Shimadzu do Brasil Comércio Ltd., Barueri, Brazil), according to previously described methods (XIAO *et al*., 2014; VIGNAU *et al*., 2004), with modifications. The HPLC system was equipped with an SCL-10A VP controller, an SIL-10AF automatic injector, LC-10A VP pumps, and a DGV-14A degasser. Elution was achieved by using a C18 column (150 × 4.60 mm, 4 µm, 80 Å) and mobile phases A (5% acetonitrile in Milli-Q water) and B (95% acetonitrile in Milli-Q water). Linear gradient conditions were as follows: 100% A to 100% B during 20 min, followed by 100% B for 5 min to clean the system. The flow rate was set at 1 mL/min, and the column temperature at 35 °C. Trp was determined at 280 nm and Kyn at 365 nm by using SPDM 10A VP diode array detectors. Calibration curves were established by linear regression of peak area ratios (y-axis) *vs*. analyte concentrations (x-axis). The coefficients of determination (R^2) and regression equations of calibration curves were $R^2 = 0.9988$ and $y = 9654.4x + 5619$ for Trp and $R^2 = 0.999$ and $y = 111416x - 2441.8$ for Kyn.

Prior to HPLC analysis, serum samples (100 µL) were deproteinized by addition of an equal volume of 10% perchloric acid. The mixture was vortexed for 1 min and centrifuged for 10 s at 25 °C and 14,000 × *g*. Then, 40 µL of the supernatant was injected into the HPLC. Retention time and area under the curve were determined using Class VP software (Shimadzu LC-20A, Shimadzu Corporation, Prague, Czech Republic). Kyn and Trp concentrations were calculated using the regression equations of calibration curves. The Kyn/Trp ratio was determined by dividing serum Kyn levels (µM) by serum Trp levels (µM) and multiplying by 1000 (DARCY *et al*., 2011).

4.1.6 Statistical analysis

Results are present as mean and standard deviation. Data were analyzed using one-way analysis of variance (ANOVA) followed by Bonferroni *post hoc* test to compare effects of HFD or a Zn-deprived HFD or two-way ANOVA followed by Bonferroni *post hoc* test to determine if the interaction effects of diets and fluoxetine treatment were significant. The level of significance was set at $p < 0.05$. Statistical analyses were performed using GraphPad Prism software version 5 (GraphPad Software Inc., San Diego, USA).

4.2 *IN VITRO* STUDY

4.2.1 Cell lines

The human glioblastoma cell lines A-172 (ATCC® CRL-1620™) (GIARD *et al*., 1973) and T98G (ATCC® CRL-1690™) (STEIN, 1979) were kindly provided by Professor Nils Cordes (OncoRay, National Center for Radiation Research in Oncology, Technische Universität Dresden, Germany) and Anna Happe-Kramer (Translational Radiobiology & Radiooncology Research Laboratory, Department of Radiotherapy, Charité-Universitätsmedizin Berlin, Germany), respectively. The human monocytic cell line THP-1 (ATCC® TIB-202™) (TSUCHIYA *et al*., 1982) was obtained from the Leibniz Institute DSMZ (German Collection of Microorganisms and Cell Cultures GmbH, Germany). All cell lines were grown in Dulbecco's Modified Eagle's Medium (DMEM; PAN-Biotech, Aidenbach, Germany) supplemented with 10% heat-inactivated fetal calf serum (FCS; CCPro, Oberdorla, Germany) and 100 U/mL penicillin + 100 µg/mL streptomycin (P/S). Cells were maintained at 37 °C under a humidified atmosphere containing 5% CO_2.

4.2.2 *In vitro* experimental design

4.2.2.1 Stimulation of THP-1 macrophages

Culture supernatant containing proinflammatory cytokines was obtained by differentiating THP-1 cells into macrophages with phorbol 12-myristate-13-acetate (PMA) and then stimulating active macrophages with lipopolysaccharides (LPS) from *Escherichia coli* O111:B4, according to the method of Takashiba *et al.* (1999), with minor modifications. THP-1 cells were cultured at a density of 1×10^6 cells/mL in $DMEM_{FCS+P/S}$ premixed with 200 nM PMA in 75 cm^2 tissue culture flasks for 24 h. After incubation, unattached cells were removed by aspiration, and adherent cells were washed three times with fresh medium ($DMEM_{FCS+P/S}$). For cell stimulation, THP-1 cells were incubated in either (i) fresh medium (control), (ii) medium containing 100 ng/mL LPS, (iii) medium containing 3 µM TPEN (membrane-permeable Zn-chelator), or (iv) LPS/TPEN-premix (100 ng/mL and 3 µM, respectively) diluted in $DMEM_{FCS+P/S}$. After 4 h of incubation, cells were centrifuged at 300 × *g* and 4 °C for 5 min, and supernatants were collected and stored at −80 °C.

4.2.2.2 Stimulation of human glioblastoma cells

Human glioblastoma stimulation assays were performed under different incubation conditions. First, T98G and A172 cells were trypsinized from tissue culture flasks by 1 mM EDTA/0.25% (w/v) trypsin treatment and transferred to new 24-well plates in 500 µL of fresh medium. A172 and T98G cells were seeded at a density of 2×10^4 cells per well in early experiments, and T98G cells were seeded at 6×10^4 cells per well in later experiments. Plates were incubated for 24 h until reaching 60% confluency. Then, cells were subjected to three different incubation conditions, as described below.

First incubation regime: A172 and T98G cells were treated with different concentrations (0, 25%, 50%, and 100% v/v) of supernatant from LPS-stimulated THP-1 macrophages diluted in fresh medium. Fresh media containing 25, 50, or 100 ng/mL LPS were used as negative controls for proinflammatory effects of LPS on A172 and T98G cells. These LPS concentrations were similar to those used to activate THP-1 cells. All plates were incubated for 24 h.

Second incubation regime: T98G cells were preincubated with 3 µM TPEN in $DMEM_{FCS+P/S}$ for 2, 4, or 24 h. After the preincubation period, culture supernatants were replaced with supernatant from LPS-stimulated THP-1 macrophages maintained under Zn-adequate or Zn-deficient (3 µM TPEN) conditions for 24 h.

Third incubation regime: T98G cells were treated with (i) supernatant from nonstimulated THP-1 macrophages, (ii) supernatant from LPS-stimulated THP-1 macrophages, (iii) supernatant from TPEN-treated THP-1 macrophages, or (iv) supernatant from THP-1 macrophages incubated in LPS/TPEN medium for 24 h.

All the supernatants obtained were subjected to Trp and Kyn quantification by HPLC-UV.

4.2.3 Cytotoxicity assays

T98G and A172 cells were plated on 96-well plates at a density of 4×10^4/mL. On the following day, the culture medium was removed, and cells were exposed to serial dilutions of TPEN (0, 0.5, 1, 1.5, 2, 2.5, 3, 3.5, 4, 4.5, 5, and 7.5 µM) in supernatant from LPS-stimulated THP-1 macrophages incubated for 24 h under standard conditions. Cell viability was determined by the 3-(4,5-dimethylthiazol-2-yl)-2,5-diphenyltetrazolium bromide (MTT) assay, which is based on the metabolization of yellow tetrazolium salt to purple formazan crystals by

viable cells (MOSMANN, 1983). Cells were incubated with a 5 mg/mL MTT solution in DMEM (without phenol red or FCS) for 40 min. Next, the medium was removed, and 100 µL of MTT stop solution (50% dimethyl sulfoxide and 50% ethanol v/v) was added to each well. The product was quantified spectrophotometrically at 540 nm using an Infinite M200 microplate reader (Tecan, Männedorf, Switzerland).

T98G cells were seeded at a density of 4×10^4 cells/mL in early experiments and at 12×10^4 cells/mL in later experiments. Plates were incubated for 24 h until reaching 60% confluency. Cells were subjected to the second and third incubation conditions, as described in Section 4.2.2.2. Then, cell viability was determined by the MTT assay.

4.2.4 Determination of Trp and Kyn in cell supernatant

Trp and Kyn analytical standards (99% purity) were purchased from VWR International (Darmstadt, Germany). Other chemicals were of analytical grade and obtained from Sigma–Aldrich (Munich, Germany). Chromatographic-grade water was prepared using a Millipore water purification system (Milford, USA).

Trp and Kyn were quantified using HPLC system consisted of a Shimadzu LC-20A chromatograph (Shimadzu Europe Corporation, Duisburg, Germany), a variable wavelength UV detector (SPD 20A VP), a delivery pump (LC-10AD), a system controller (CBM-20A), and an automatic injector (SIL-10A), according to previously described methods (XIAO *et al*., 2014; VIGNAU *et al*., 2004), with modifications. Separation was achieved on a C18 column (150 × 4.60 mm, 4 µm, 80 Å) at 35 °C using 8% acetonitrile in ultrapure water at a flow rate of 1 mL/min in isocratic mode. The running time was 15 min. Elution of Trp and Kyn was monitored at 280 and 365 nm, respectively. Areas under the curves were calculated using Shimadzu LC Solution software.

Stock solutions of Trp and Kyn at 10 mM were prepared in ultrapure water and stored at −20 °C. A series of standard solutions of Trp and Kyn at different concentrations (0.5, 1, 2.5, 5, 7.5, 10, 25, 50, and 100 µM) were prepared by diluting stock solutions in 60 mg/mL bovine serum albumin (BSA) solution in Milli-Q water. The average protein content of standard solutions corresponds to that of $DMEM_{FCS+P/S}$.

For protein precipitation, 440 µL of standard solution or culture medium sample was mixed with 40 µL of 60% perchloric acid, vortex-mixed for 1 min, and centrifuged at 14,000 × *g* and 25 °C for 10 min. The supernatants were immediately diluted 1:10 (v/v) in Milli-Q water, and 20 µL of these solutions was directly injected into the HPLC system for analysis. Three

independent replicates were conducted to obtain the retention times and calibration curves for compound identification and quantification, respectively. Calibration curves were generated by linear regression of peak area ratios (*y*-axis) *vs*. analyte concentrations (*x*-axis). R^2 values and regression equations of calibration curves are presented in the Results section. Trp and Kyn concentrations in cell supernatant samples were determined from calibration curves. Then, the Kyn/Trp ratio was calculated by dividing the Kyn concentration (μM) by the Trp concentration (μM) and multiplying the result by 1000 (DARCY *et al*., 2011).

4.2.5 Intracellular Zn quantification

Intracellular labile Zn levels were analyzed using the fluorescent Zn probes Zinpyr-1 (Santa Cruz Biotechnology, Dallas, USA) (WALKUP *et al*., 2000) and FluoZin-3AM (Invitrogen, Karlsruhe, Germany) (HAUGLAND, 2000), according to the methods described by Maares *et al*. (2018), with minor modifications. THP-1 cells were seeded in DMEM enriched with 200 nM PMA in 96-well plates at a density of 1×10^6 cells/mL and incubated for 24 h to promote macrophage differentiation. Then, cells were loaded with 2.5 μM Zinpyr-1 or 1 μM FluoZin-3AM in incubation buffer (120 mM NaCl, 5.4 mM KCl, 5 mM glucose, 1 mM $CaCl_2$, 1 mM $MgCl_2$, 1 mM NaH_2PO_4, 10 mM HEPES, and 0.3% w/v BSA, pH 7.35) for 30 min at 37 °C. After incubation, the supernatants were removed, and the adherent cell monolayers were washed twice with assay buffer (incubation buffer without BSA) to remove extracellular Zinpyr-1 or FluoZin-3AM. Minimal (F_{min}) and maximal (F_{max}) fluorescence signals were determined by adding 100 μL of assay buffer containing 20 μM TPEN and 600 μM $ZnSO_4 \cdot 7H_2O$, respectively, to a subset of wells used for calibration. All other wells were filled with 100 μL of assay buffer. After 30 min of incubation at 37 °C, baseline Zinpyr-1 (λ_{ex} = 492 nm and λ_{em} = 527 nm) or FluoZin-3AM (λ_{ex} = 485 nm and λ_{em} = 516 nm) fluorescence was measured using a fluorescence plate reader (Infinite M200, Tecan, Zürich, Austria). Subsequently, 10 μL of 11-fold concentrated solutions containing either LPS, TPEN, or an LPS/TPEN mixture was added to the cells. Fluorescence was measured again after incubation for a further 50 min at 37 °C. Intracellular labile Zn concentration was calculated using the equation described by Grynkiewicz *et al*. (1985), $[Zn] = K_d \times [(F - F_{min})/(F_{max} - F)]$, assuming a dissociation constant (K_d) of 0.7 nM for the Zn–Zinpyr-1 complex (WALKUP *et al*., 2000; BURDETTE *et al*., 2001) and of 8.9 nM for the Zn–FluoZin-3AM complex (KRĘŻEL and MARET, 2006).

4.2.6 Quantitative RT-PCR and ELISA

THP-1 macrophages activated by the protocol described in Section 4.2.2.1 were washed with pre-cooled phosphate-buffered saline (PBS) and scratched on ice using a cell scraper. The cell suspension was transferred into fresh tubes and centrifuged (300 × *g* for 5 min at 4 °C). Pellets were stored at −80 °C until RNA isolation. Total RNA was extracted from THP-1 cells using the NucleoSpin II Kit (Takara, Tokyo, Japan) or TRIzol (Invitrogen, Carlsbad, USA), according to the manufacturers' instructions. Single-stranded complementary DNA (cDNA) was synthesized from 1 µg of total RNA using the iScript cDNA Synthesis Kit or High-Capacity cDNA Reverse Transcription Kit (Thermo Fisher Scientific, Waltham, USA), according to the manufacturer's protocols. Finally, RT-PCR was carried out using an iCycler iQ Multi-Color system (Bio-Rad Laboratories, Hercules, USA) or a StepOne system (Applied Biosystems, Beverly, USA). Each amplification reaction was carried out in a total volume of 10 µL, comprising 5 µL of the double-stranded DNA-binding dye SYBR^{TM} Green, 1 µL of cDNA (equivalent to 15–20 ng RNA), 0.45 µL of each primer stock solution at 10 µM, and 3.1 µL of water. Detailed information on the primers used is provided in Table 1. Thermal cycling conditions were 95 °C for 2 min, followed by 40 cycles of 95 °C for 15 s, 56 °C for 1 min, and 72 °C for 15 s. Quantitative values of gene expression were calculated by the ΔCt method and normalized to expression levels of the housekeeping β-actin gene. Relative quantification was performed by the $2^{-\Delta\Delta Ct}$ method (LIVAK and SCHMITTGEN, 2001).

Table 1. Primers used for quantitative real-time PCR

Gene target	**NCBI reference sequence**	**Primer sequences (5′-3′)**	**Reference**
IL-6	NM_000600.5	F: CCACACAGACAGCCACTCAC R: AGGTTGTTTTCTGCCAGTGC	(KATO *et al.*, 2004)
IFN-α	NM_024013.2	F: GACTCCATCTTGGCTGTGA R: TGATTTCTGCTCTGACAACCT	(COLAN-TONIO *et al*., 2011)
IFN-β	NM_002176.4	F: TGCTCTCCTGTTGTGCTTCTCC R: CATCTCATAGATGGTCAATGCGG	(KATO *et al.*, 2004)
IFN-γ	NM_000619.3	F: CTTGGCTTTTCAGCTCTGCA R: TCCGCTACATCTGAATGACCTG	(MASU-NAGA *et al*., 2018)
TNF-α	NM_000594.4	F: ATCTACTCCCAGGTCCTCTTCAA R: GCAATGATCCCAAAGTAGACCT	(KATO *et al.*, 2004)
β-actin	NG_007992.1	F: CGCCCCAGGCACCAGGGC R: GCTGGGGTGTTGAAGGT	(WOLF *et al.*, 2002)

F, forward; R, reverse.

Proinflammatory cytokines IL-6 and TNF-α were quantified in the supernatants obtained from THP-1 macrophages (as described in Section 4.2.2.1) using the BD Biosciences OptEIA™ Human IL-6 ELISA Kit II and OptEIA™ Human TNF-α ELISA Kit (Becton, Dickinson and Company, Franklin Lakes, USA), according to the manufacturer's protocol. IL-6 and TNF-α concentrations were determined against linear calibration curves both in the ranges of 15.6 to 1,000 pg/mL, with a lower detection limit of 2 pg/mL.

4.2.7 Statistical analysis

Statistical significance was analyzed by one-way ANOVA followed by Bonferroni *post hoc* test. The Shapiro–Wilk test was used to assess the normality of data distribution. Statistical analyses were performed using GraphPad Prism software version 5 (GraphPad Software Inc., San Diego, USA). Results are the mean and standard deviation of three independent experiments.

5 RESULTS

5.1 *IN VIVO* STUDY

5.1.1. Energy intake, feed efficiency, body parameters, and total serum Zn

Energy intake data revealed that the SD-ZD group had higher energy consumption than the other dietary groups (SD-ZD, 20.6 ± 1.2 kcal/day; SD, 15.6 ± 1.3 kcal/day; HFD, 15.9 ± 1.5 kcal/day; and HFD-ZD, 16.2 ± 2.2 kcal/day) (Fig. 4A). However, feed efficiency (calculated as weight gain in grams divided by kilocalories consumed) was significantly higher ($p < 0.001$) for HFD and HFD-ZD than for SD-ZD and SD (Fig. 4B). The high energy density of HFD treatments promoted a greater increase ($p < 0.001$) in body weight than that observed in SD treatments during the experimental period (HFD, 51.9 ± 6.9 g; HFD-ZD, 51.9 ± 6.4 g; SD, 42.2 ± 4.9 g; and SD-ZD, 41.3 ± 6.5 g) (Fig. 4C). Mice were also evaluated for abdominal circumference and Lee index. HFD and HFD-ZD groups showed significantly higher ($p < 0.001$) abdominal circumference and Lee index than SD and SD-ZD groups (Fig. 4E and F).

Blood biochemical analysis confirmed the presence of serum Zn deficiency in SD-ZD and HFD-ZD mice. Mice fed Zn-deficient diets showed significantly lower ($p < 0.05$) total serum Zn levels than those fed Zn-sufficient diets (SD-ZD, 40.9 ± 13.9 µg/dL; HFD-ZD, 37.8 ± 11.6 µg/dL; SD, 82.4 ± 18.8 µg/dL; and HFD, 99.6 ± 21.7 µg/dL) (Fig. 4F).

Figure 4. Effect of experimental diets on energy intake, feed efficiency, body parameters, and total serum zinc in mice

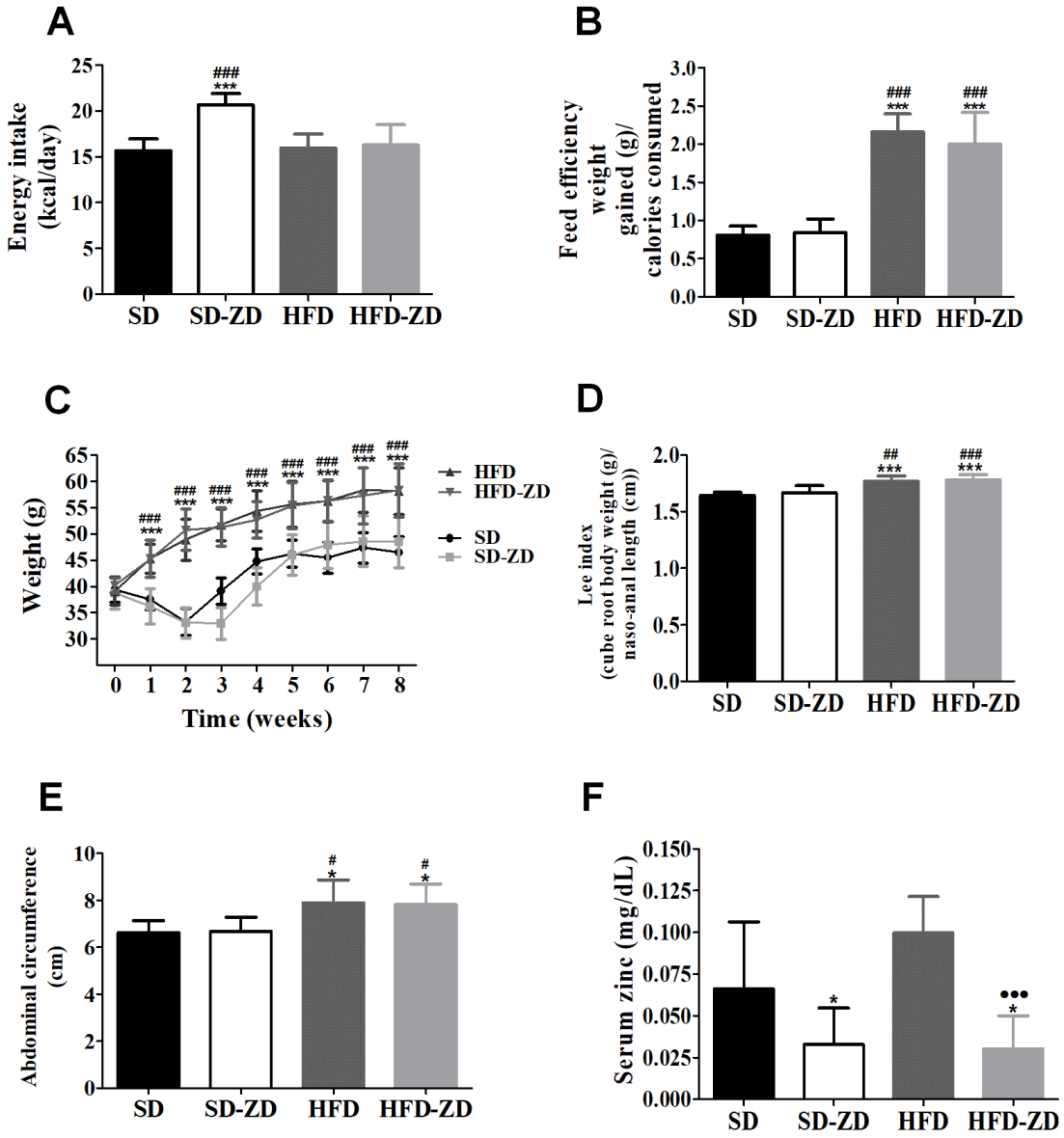

(A) Energy intake, (B) feed efficiency, (C) body weight, (D) Lee index, (E) abdominal circumference, and (F) serum zinc. SD, standard diet; SD-ZD, standard zinc-deficient diet; HFD, high-fat diet; HFD-ZD, high-fat zinc-deficient diet. Each column represents the mean ± standard deviation of five mice per group. * $p < 0.05$ and *** $p < 0.001$ compared with SD; # $p < 0.05$, ## $p < 0.01$, and ### $p < 0.001$ compared with SD-ZD; ••• $p < 0.001$ for HFD-ZD *vs.* HFD (one-way ANOVA, Bonferroni *post hoc* test).

5.1.2 WAT depots, organs weights, and WAT histology

HFD and HFD-ZD groups showed higher total WAT weight in relation to their respective controls (HFD *vs*. SD, $p < 0.001$; HFD-ZD *vs*. SD-ZD, $p < 0.001$) (Fig. 5A). Moreover, adiposity index data demonstrated that both HFD and HFD-ZD groups had a significant increase ($p < 0.001$) in adiposity percentage relative to body weight compared with

SD and SD-ZD groups. Interestingly, mice fed HFD had higher ($p < 0.05$) adiposity index than those fed HFD-ZD (Fig.5B). Analysis of WAT distribution within body compartments showed that HFD and HFD-ZD mice had higher ($p < 0.001$) subcutaneous WAT weight than SD and SD-ZD (Fig. 5C). It was also found that the HFD group had a 2-fold higher visceral WAT weight than the SD group ($p < 0.001$). However, no differences were observed between HFD-ZD and SD-ZD groups (Fig. 5D). Organ weights did not differ between any of the groups (Table 2).

Figure 5. Effect of experimental diets on white adipose tissue weights and adiposity index

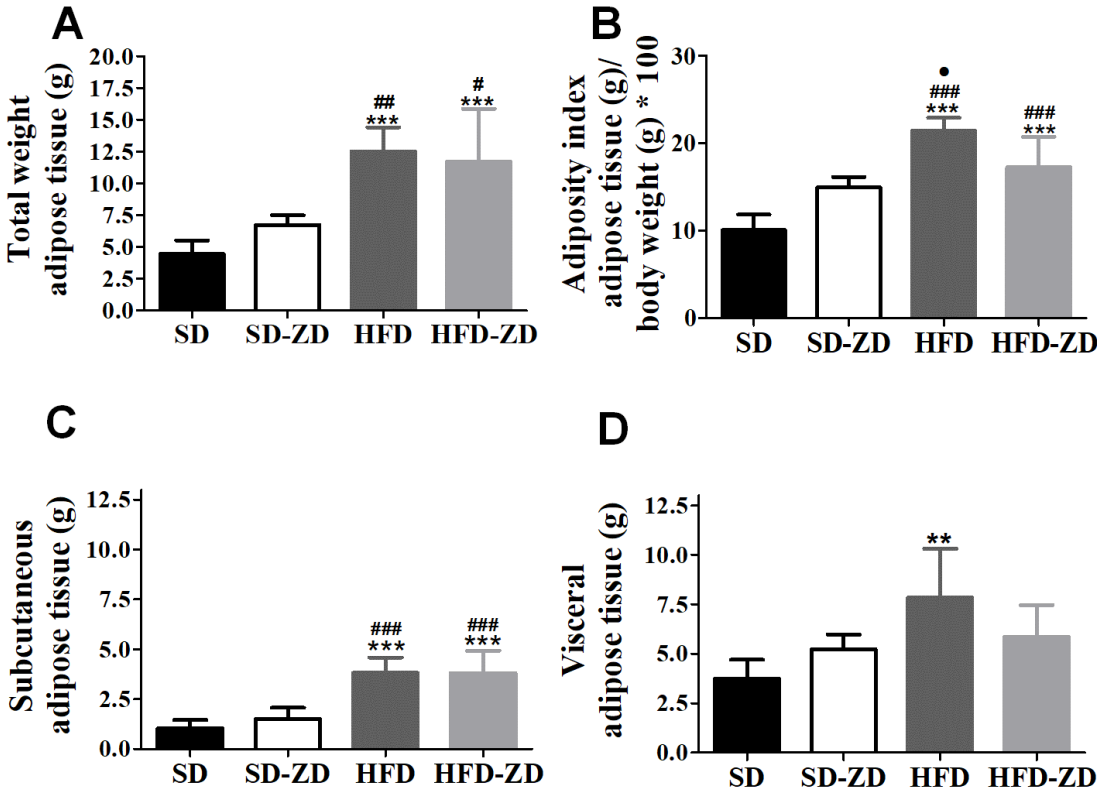

(A) Total white adipose tissue (WAT) weight, (B) adiposity index, (C) subcutaneous WAT weight, and (D) visceral WAT weight in mice. SD, standard diet; SD-ZD, standard zinc-deficient diet; HFD, high-fat diet; HFD-ZD, high-fat zinc-deficient diet. Each column represents the mean ± standard deviation of five mice per group. ** $p < 0.01$ and *** $p < 0.001$ compared with SD; # $p < 0.05$, ## $p < 0.01$, and ### $p < 0.001$ compared with SD-ZD; • $p < 0.05$ for HFD *vs.* HFD-ZD (one-way ANOVA, Bonferroni *post hoc* test).

Table 2. Organ weights (g) of mice fed experimental diets for 8 weeks

Organ	SD	SD-ZD	HFD	HFD-ZD
Liver	1.93 ± 0.11	2.02 ± 0.11	2.02 ± 0.35	2.14 ± 0.12
Lung	0.29 ± 0.09	0.27 ± 0.05	0.38 ± 0.12	0.39 ± 0.17
Heart	0.15 ± 0.10	0.17 ± 0.02	0.14 ± 0.01	0.16 ± 0.02
Spleen	0.17 ± 0.03	0.20 ± 0.02	0.16 ± 0.03	0.15 ± 0.01
Kidney	0.45 ± 0.03	0.44 ± 0.05	0.42 ± 0.03	0.40 ± 0.04
Brain	0.48 ± 0.03	0.47 ± 0.03	0.47 ± 0.04	0.46 ± 0.04

Values represents the mean ± standard deviation of five mice per group; n.s., not significantly different (one-way ANOVA, Bonferroni *post hoc* test). SD, standard diet; SD-ZD, standard Zn-deficient diet; HFD, high-fat diet; HFD-ZD, high-fat Zn-deficient diet.

Representative WAT micrographs for all groups are presented in Figs. 6A–F. The WAT of mice fed HFD and HFD-ZD was hypertrophic, with significantly lower ($p < 0.001$) adipocyte numbers (Fig. 6G), higher adipocyte volume ($p < 0.001$) (Fig. 6H), and greater ($p < 0.001$) macrophage infiltration (Fig. 6I) when compared with WAT of mice fed SD. In contrast, HFD-ZD mice showed lower ($p < 0.01$) adipocyte volume than the HFD group (Fig. 6H).

Figure 6. Impact of experimental diets on white adipose tissue morphology in mice

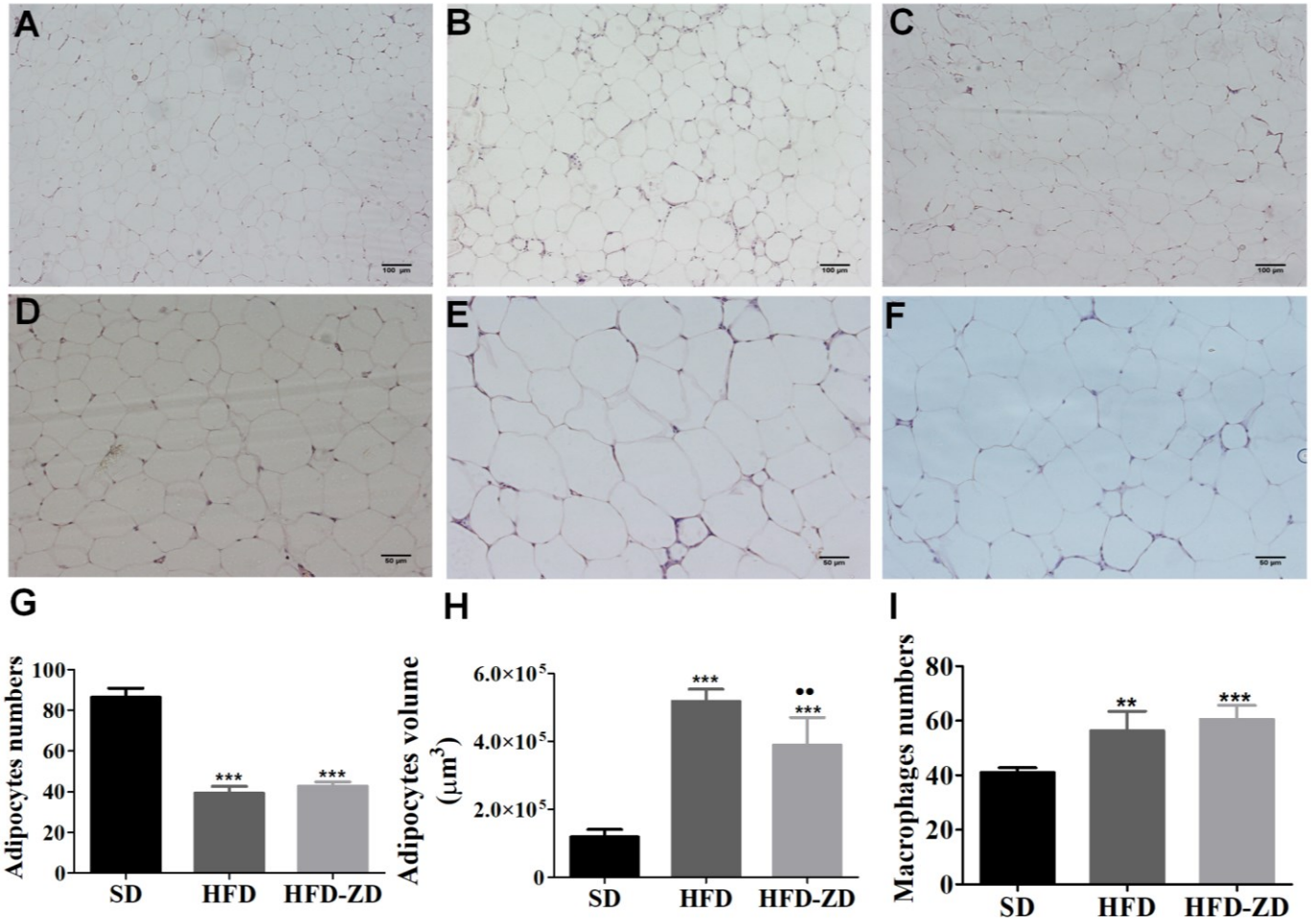

Representative light micrographs of SD (A and D), HFD (B and E), and HFD-ZD (C and F) groups. White adipose tissue (WAT) sections were stained with hematoxylin/eosin. (G) Adipocyte numbers, (H) adipocyte volume, and (I) macrophage numbers in WAT. SD, standard diet; HFD, high-fat diet; HFD-ZD, high-fat zinc-deficient diet. Each column represents the mean ± standard deviation of five fields per WAT sample from three mice per group. ** $p < 0.01$ and *** $p < 0.001$ compared with SD, •• $p < 0.01$ for HFD *vs.* HFD-ZD (one-way ANOVA, Bonferroni *post hoc* test).

5.1.3 Hematological parameters and serum adipokine levels

Administration of SD-ZD, HFD, and HFD-ZD for 8 weeks did not affect hematological parameters (Table 3). As mentioned above, HFD and HFD-ZD groups had a higher proportion of total WAT weight, attributed to increased macrophage infiltration, and, as shown in Fig. 7A, a significant increase ($p < 0.001$) in serum leptin levels compared with the respective controls (Fig. 7A). However, serum leptin and adiponectin levels were not significantly altered by Zn deficiency (Fig. 7A and B). No significant changes in serum adiponectin levels were observed between groups (Fig. 7B).

Table 3. Effect of experimental diets on hematological parameters of mice

Parameter	Diet			
	SD	SD-ZD	HFD	HFD-ZD
Red blood cells ($\times 10^{12}$/L)	7.55 ± 0.65	6.77 ± 1.41	7.69 ± 0.35	7.84 ± 0.40
Hemoglobin (g/L)	120.88 ± 8.05	116.20 ± 11.39	123.90 ± 8.05	120.60 ± 4.55
Hematocrit (%)	38.32 ± 2.75	36.57 ± 5.20	39.89 ± 2.27	39.12 ± 2.35
MCV (fL)	50.85 ± 1.71	49.60 ± 1.23	51.87 ± 1.09	49.92 ± 0.73
MCH (pg)	15.96 ± 0.60	15.12 ± 0.47	16.05 ± 0.24	15.34 ± 0.89
MCHC (g/L)	315.11 ± 7.04	306.00 ± 4.50	301.21 ± 24.75	308.92 ± 20.07
RDW (%)	14.84 ± 0.30	14.85 ± 1.27	15.17 ± 0.50	14.92 ± 0.47
White blood cells ($\times 10^9$/L)	7.26 ± 2.61	9.21 ± 2.45	7.91 ± 2.33	6.17 ± 1.78
Lymphocytes ($\times 10^9$/L)	5.37 ± 1.79	6.45 ± 1.30	5.61 ± 1.72	4.69 ± 1.23
Monocytes ($\times 10^9$/L)	0.24 ± 0.15	0.26 ± 0.30	0.32 ± 0.12	0.18 ± 0.06
Granulocytes ($\times 10^9$/L)	1.64 ± 0.77	1.71 ± 0.66	2.01 ± 0.79	1.31 ± 0.17
Lymphocytes (%)	74.35 ± 5.79	78.62 ± 2.60	71.12 ± 5.49	76.32 ± 3.46
Monocytes (%)	3.37 ± 0.97	3.05 ± 0.35	3.66 ± 0.65	3.17 ± 0.54
Granulocytes (%)	22.15 ± 4.77	18.32 ± 2.59	25.22 ± 4.87	20.51 ± 3.05
Platelet count ($\times 10^9$/L)	431.66 ± 229.10	376.25 ± 88.36	543.91 ± 158.49	519.22 ± 77.47
Mean platelet volume (fL)	6.11 ± 0.39	5.28 ± 0.27	5.92 ± 0.17	5.87 ± 0.42
PDW	15.62 ± 0.37	14.91 ± 0.47	15.47 ± 0.19	15.33 ± 0.36

Values are the mean ± standard deviation of five mice per group. n.s., not significantly different (one-way ANOVA, Bonferroni *post hoc* test). SD, standard diet; SD-ZD, standard zinc-deficient diet; HFD, high-fat diet; HFD-ZD, high-fat zinc-deficient diet; MCV, mean corpuscular volume; MCH, mean corpuscular hemoglobin; MCHC, mean corpuscular hemoglobin concentration; RDW, red cell distribution width; PDW, platelet distribution width.

Figure 7. Effect of experimental diets on serum leptin and adiponectin levels

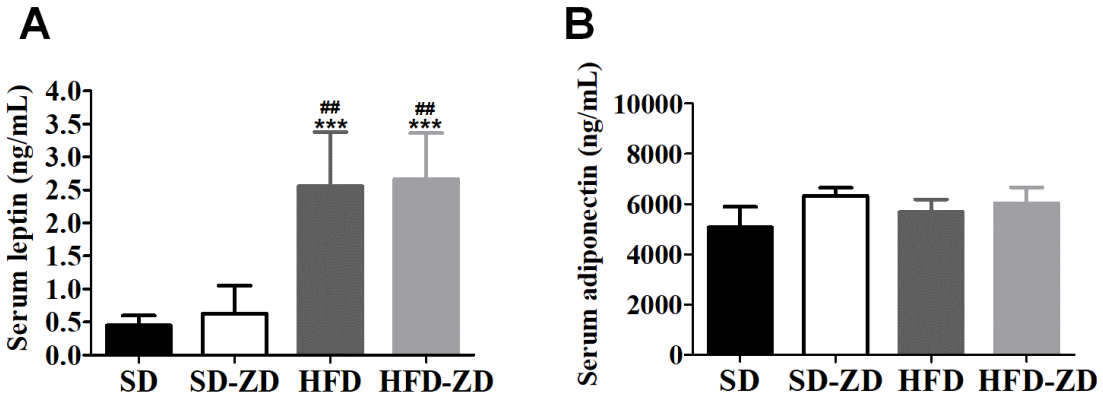

(A) Serum leptin, (B) serum adiponectin. SD, standard diet; SD-ZD, standard zinc-deficient diet; HFD, high-fat diet; HFD-ZD, high-fat zinc-deficient diet. Each column represents the mean ± standard deviation of five mice per group. *** $p < 0.001$ compared with SD; ## $p < 0.01$ compared with SD-ZD (one-way ANOVA, Bonferroni *post hoc* test).

5.1.4 Splash test

The anhedonic behavior of mice fed HFD (Zn-sufficient diet) and SD-ZD and HFD-ZD (Zn-deficient diets) was analyzed by determining the latency to initiate grooming behavior (Fig. 8A) and the time spent grooming (Fig. 8B). Splash test results showed an increased latency in mice fed SD-ZD and HFD-ZD compared with mice fed SD ($p < 0.05$) (Fig. 8A). However, no significant differences were observed between HFD and SD groups (Fig. 8A and B). Mice fed HFD-ZD spent less time grooming, which is an anhedonic-like behavior ($p < 0.05$) (Fig. 8B).

Figure 8. Anhedonia in mice fed experimental diets for 8 weeks

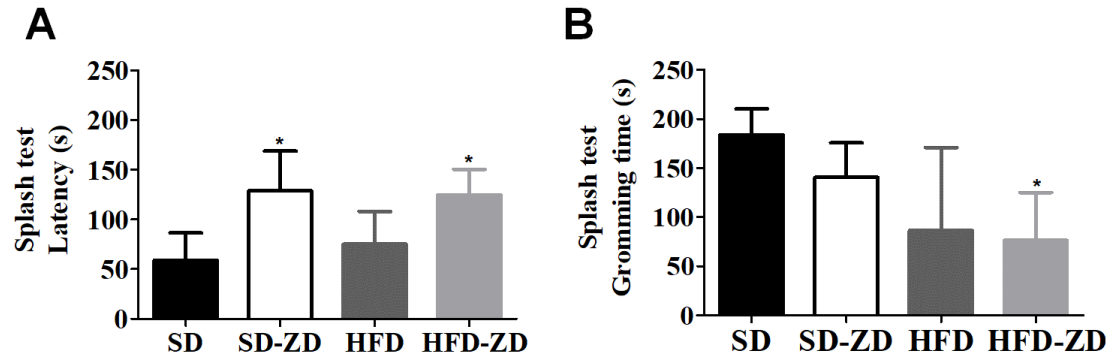

(A) Latency to initiate grooming, (B) time spent grooming. SD, standard diet; SD-ZD, standard zinc-deficient diet; HFD, high-fat diet; HFD-ZD, high-fat zinc-deficient diet. Each column represents the mean ± standard deviation of five mice per group. * $p < 0.05$ (one-way ANOVA, Bonferroni *post hoc* test).

5.1.5 Serum Trp and Kyn levels and Kyn/Trp ratio

Considering that HFD (rich in SFA) and HFD-ZD (rich in SFA and Zn-deficient) may lead to behavioral disturbances, it was hypothesized that Kyn levels and Kyn/Trp ratio would be enhanced in the serum of mice fed HFD or HFD-ZD. Serum Trp and Kyn levels of mice fed HFD or HFD-ZD were significantly lower than those of the SD group (Fig. 9A and B). The SD-ZD group samples were insufficient to be determined serum Kyn levels using HPLC; consequently, the Kyn/Trp ratio was not calculated. No significant differences in Kyn/Trp ratio, which reflects Trp catabolism, were observed (Fig. 9C).

Figure 9. Effect of experimental diets on serum tryptophan, kynurenine, and kynurenine/tryptophan ratio

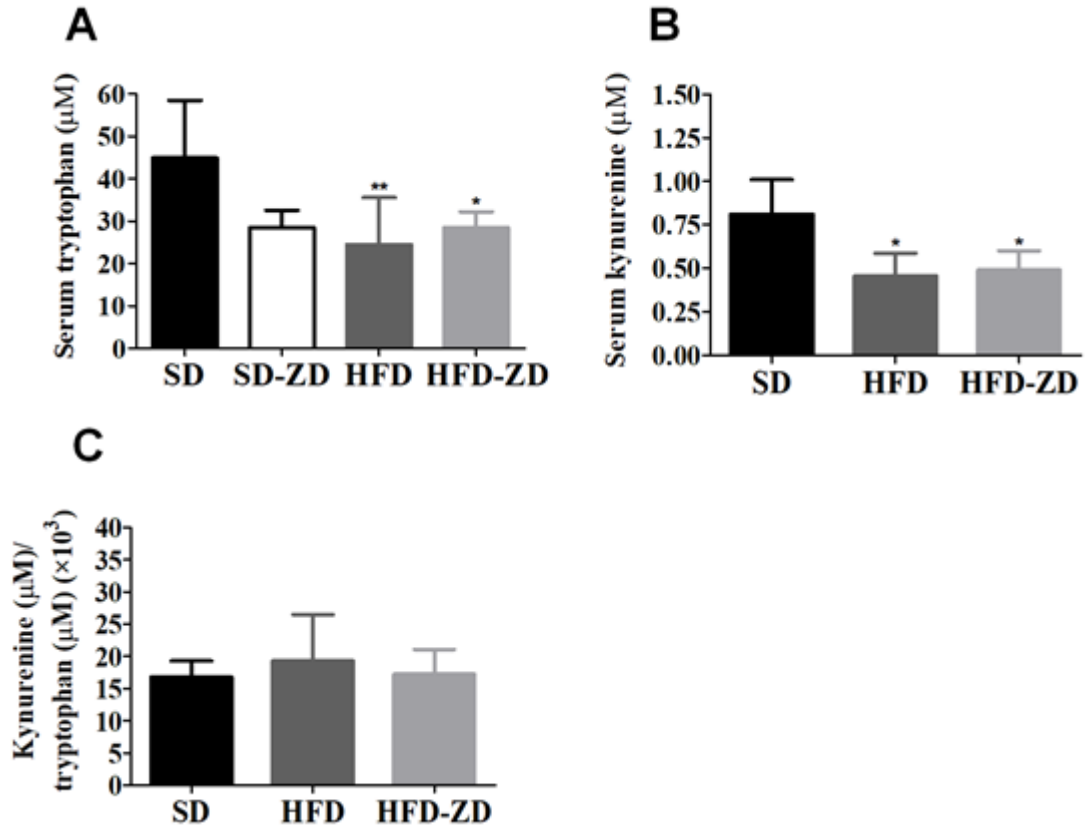

(A) Serum tryptophan, (B) kynurenine, (C) kynurenine/tryptophan ratio. SD, standard diet; SD-ZD, standard zinc-deficient diet; HFD, high-fat diet; HFD-ZD, high-fat zinc-deficient diet. Each column represents the mean ± standard deviation of five mice per group. * $p < 0.05$; ** $p < 0.01$ (one-way ANOVA, Bonferroni *post hoc* test).

5.1.6 Assessment of obesity parameters and motivation behaviors after fluoxetine treatment

In the second part of the *in vivo* experiment, mice were treated daily with fluoxetine for 2 weeks following the 8 weeks of chronic exposure to experimental diets (SD-ZD, HFD, and HFD-ZD). Fluoxetine is a selective serotonin reuptake inhibitor widely prescribed for the treatment of depression and anxiety disorders. We investigated the ability of fluoxetine to alter biochemical parameters and reverse behavioral alterations of chronic exposure to SD-ZD or HFD-ZD in the splash test. At the end of fluoxetine treatment, the HFD-ZD group showed a lower energy intake than the SD-ZD group ($p < 0.001$) (Fig. 10A). Adiposity index (Fig. 10B) was not altered by fluoxetine treatment in comparison with pretreatment levels (Fig. 5B). Interestingly, fluoxetine treatment decreased serum leptin levels and significantly increased serum adiponectin levels in HFD-ZD mice (Fig. 10C and D) compared with pretreatment values (Fig. 7A and B).

Figure 10. Energy intake, adiposity index, serum leptin, and serum adiponectin in mice treated with fluoxetine (10 mg/kg for 2 weeks) and fed experimental diets

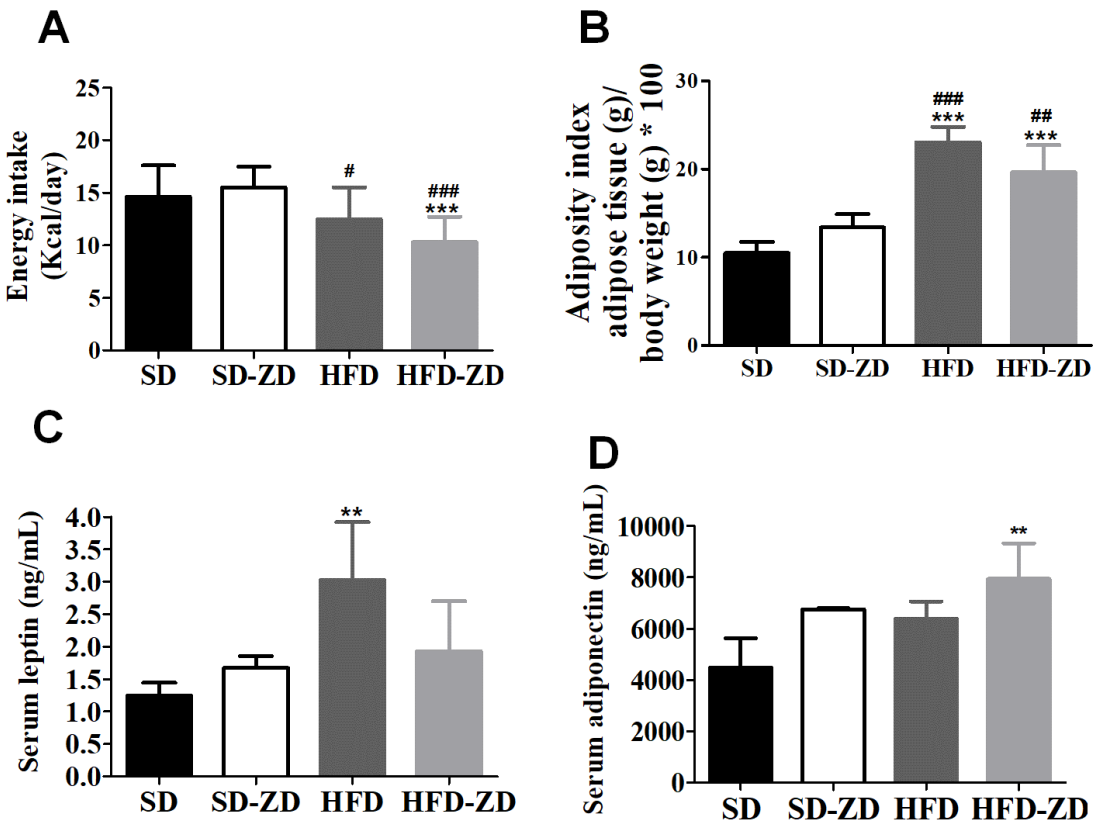

(A) Energy intake, (B) adiposity index, (C) serum leptin, and (D) serum adiponectin. SD, standard diet; SD-ZD, standard zinc-deficient diet; HFD, high-fat diet; HFD-ZD, high-fat zinc-deficient diet. Each column represents

the mean ± standard deviation of five mice per group. Adiposity index was calculated as adipose tissue weight divided by body weight times 100. ** $p < 0.01$ and *** $p < 0.001$ compared with SD; # $p < 0.05$, ## $p < 0.01$, and ### $p < 0.001$ compared with SD-ZD (two-way ANOVA, Bonferroni *post hoc* test).

The groups did not differ in latency or grooming time in the splash test, as depicted in Fig. 11A and B, demonstrating the ability of fluoxetine to revert anhedonic-like behaviors induced by HFD-ZD.

Figure 11. Splash test results of mice treated with fluoxetine (10 mg/kg) for 2 weeks and fed experimental diets for 10 weeks

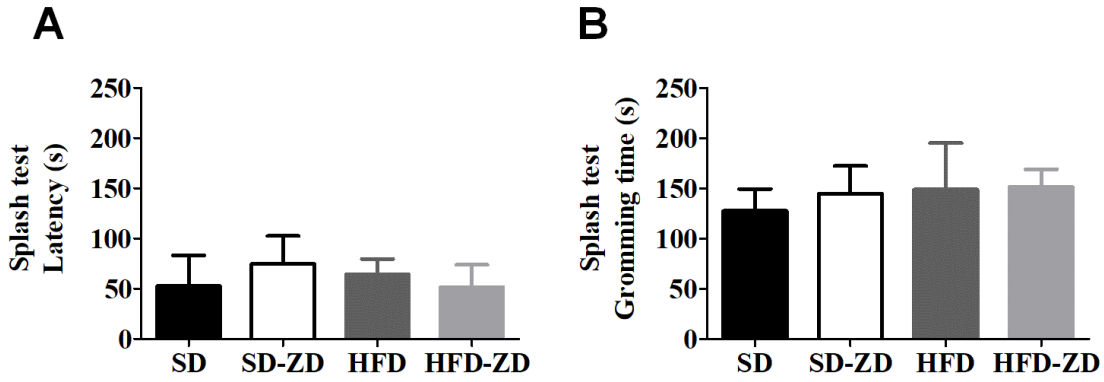

(A) Latency and (B) grooming time. SD, standard diet; SD-ZD, standard zinc-deficient diet; HFD, high-fat diet; HFD-ZD, high-fat zinc-deficient diet. Each column represents the mean ± standard deviation of five mice per group.

The ability of fluoxetine treatment to alter serum Trp, Kyn, or Kyn/Trp ratio was assessed, but no significant differences were found between groups (Fig. 12A–C). The SD-ZD group samples were insufficient to be determined serum Kyn levels using HPLC; consequently, the Kyn/Trp ratio was not calculated.

Figure 12. Serum tryptophan, kynurenine, and kynurenine/tryptophan ratio in mice treated with fluoxetine (10 mg/kg) for 2 weeks and fed experimental diets for 10 weeks

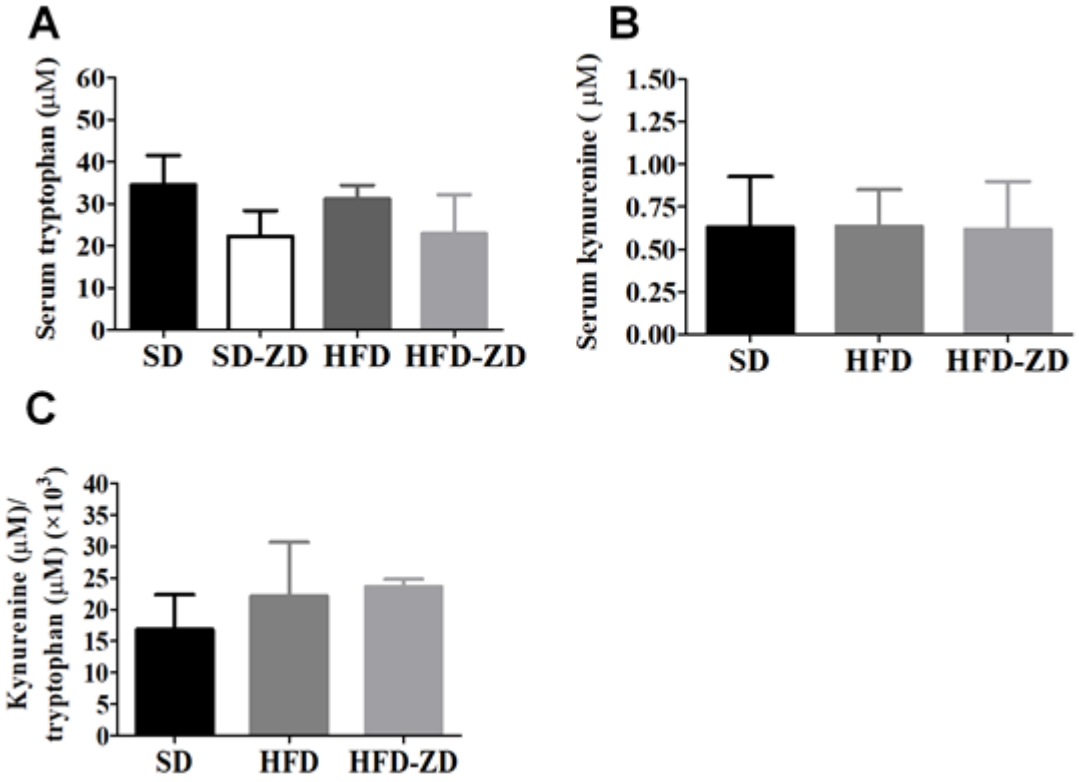

(A) Tryptophan, (B) kynurenine, and (C) kynurenine/tryptophan ratio. SD, standard diet; SD-ZD, standard zinc-deficient diet; HFD, high-fat diet; HFD-ZD, high-fat zinc-deficient diet. Each column represents the mean ± standard deviation of five mice per group.

5.2 *IN VITRO* STUDY

5.2.1 Determination and quantification of Trp and Kyn in cell supernatant by HPLC

First, we established and validated an HPLC analytical method for determination and quantification of Trp and Kyn in cell culture supernatant, the method was validated and described previously by Júlio (2015). The linearity of the method (Table 4) was assessed using three standard calibrations. Calibration curves were constructed using standard Trp and Kyn solutions at nine nominal concentrations (0.5, 1, 2.5, 5, 7.5, 10, 25, 50, and 100 μM). In the development of HPLC methods, matrix effects constitute a significant issue that should be minimized as much as possible (van de STEENE and LAMBERT, 2008). With this in mind, a series of standards solutions were prepared in BSA solution in Milli-Q water, which corresponds to the average protein content in DMEM FCS + Penstrep medium. Both the standard solutions and the samples analyzed had the same preparation conditions (protein precipitation followed by dilution) and chromatography separation conditions. As result, this protocol can minimize the effect of different matrix considering that DMEM FCS+ Penstrep medium contained 80 μM of Trp.

Table 4. Linearity of the developed HPLC analytical method for quantification of tryptophan and kynurenine in cell culture supernatant

Analyte	**Calibration curve**	R^2	**Retention time (min)**
Trp	$y = 1207.2x + 993.9$	0.99	11
	$y = 1207x + 1527.4$	0.99	
	$y = 1088.8x + 263.3$	0.99	
	$y = 998.7x + 1522.7$	0.99	
Kyn	$y = 989.5x + 1902.7$	0.99	6
	$y = 998.4x + 1008.1$	0.99	

The coefficient of determination (R^2) was used as a measure of linearity. Validation assays were performed in triplicate using standard solutions prepared and analyzed on different days.

5.2.2 Differentiation of THP-1 monocytes into macrophage-like cells and LPS stimulation

Cell culture supernatants enriched in proinflammatory cytokines were obtained by using the methodological setup described by Takashiba *et al*. (1999), with minor modifications. The human monocyte cell line THP-1 was differentiated into macrophage-like cells by exposure to 200 nM PMA, which promotes cellular adhesion. Then, THP-1 macrophages were stimulated with a 100 ng/mL LPS solution for 4 h. As described in the literature, upon binding to TLR-4 membrane receptors, LPS activates the NF-κB signaling cascade, resulting in the production and secretion of proinflammatory cytokines into the culture medium (TREDE *et al*., 1995). Indeed, LPS-stimulated THP-1 macrophages released a significant amount of the proinflammatory cytokines IL-6 and TNF-α ($p < 0.05$ and $p < 0.01$, respectively) into culture medium, as determined by specific ELISA assays (Fig. 13).

Figure 13. Levels of the proinflammatory cytokines in the supernatant of lipopolysaccharide-stimulated THP-1 macrophages

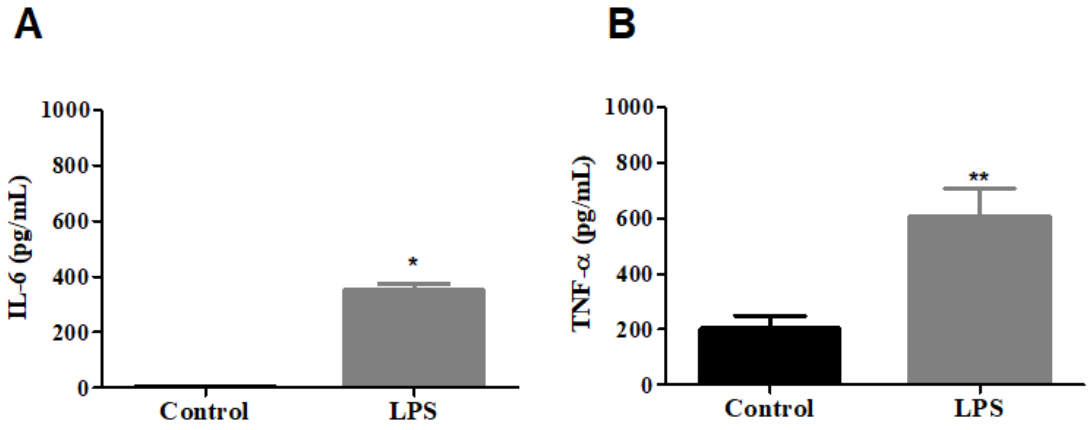

(A) Interleukin 6 (IL-6), (B) tumor necrosis factor-alpha (TNF-α) in LPS-stimulated THP-1 macrophages supernatant, as determined by ELISA. Each column represents the mean ± standard deviation of three independent experiments. Control cells were cultivated in DMEM only; * $p < 0.05$ and ** $p < 0.01$ (Mann–Whitney *U*-test).

5.2.3 Effect of proinflammatory THP-1 supernatant on human glioma cell viability and Trp–Kyn pathway regulation

The human adherent glioma cells A172 and T98G were chosen because they express IDO (GRANT *et al*., 2000; MIYAZAKI *et al*., 2009). IDO catalyzes the first enzymatic reaction of the Kyn–Trp pathway (oxidation of the essential amino acid Trp). IDO expression and activation result in accumulation of downstream metabolites, such as Kyn. Trp and Kyn levels

were measured in the culture supernatant of A172 and T98G cells. Cells were seeded at 2×10^4 cells/500 µL and incubated for 24 h until reaching 60% confluency. Then, T98G and A172 cells were treated or not with different concentrations of proinflammatory THP-1 supernatant, as described in Section 4.2.2.2.

Kyn levels were significantly higher ($p < 0.001$) in the supernatant of A172 cells treated with 25 (10.88 ± 1.24 *vs*. 6.75 ± 1.22 µM), 50 (11.92 ± 2.87 *vs*. 7.14 ± 0.74 µM), or 100% (11.24 ± 1.48 *vs*. 6.99 ± 0.91 µM) proinflammatory THP-1 supernatant as compared with the control (6.03 ± 1.43) (Fig. 14A). The same was true for T98G cells 25 (3.16 ± 0.84 *vs*. 1.07 ± 0.50 µM), 50 (3.51 ± 0.48 *vs*. 0.98 ± 0.27 µM), and 100% (3.93 ± 0.63 *vs*. 1.04 ± 0.25 µM) *vs* control (1.18 ± 0.87, $p < 0.001$) (Fig. 15A). A reduction in Trp levels was also observed in both cell lines after treatment with 25, 50, or 100% proinflammatory THP-1 supernatant (Fig. 14B and 15B).

The Kyn/Trp ratio provides a measure of Trp breakdown and can be used as an indicator of IDO activity in conjunction with other immune activation markers (ARNONE *et al*., 2018). This parameter was significantly higher ($p < 0.001$) in treated supernatant from A172 cells (Fig. 14C) and T98G cells (Fig. 15C) compared with the control.

According to Figs. 14A and 15A, the baseline levels of Kyn produced and released by A172 cells were notably higher than those released by T98G cells. After treatment with proinflammatory THP-1 supernatant, A172 cells had a nearly 2-fold increase in Kyn levels compared with the control. For stimulated T98G cells, Kyn production was nearly 3-fold that of control cells.

Figure 14. Effect of different concentrations of proinflammatory THP-1 supernatant on kynurenine levels, tryptophan levels, and kynurenine/tryptophan ratio in the culture supernatant of A172 cells

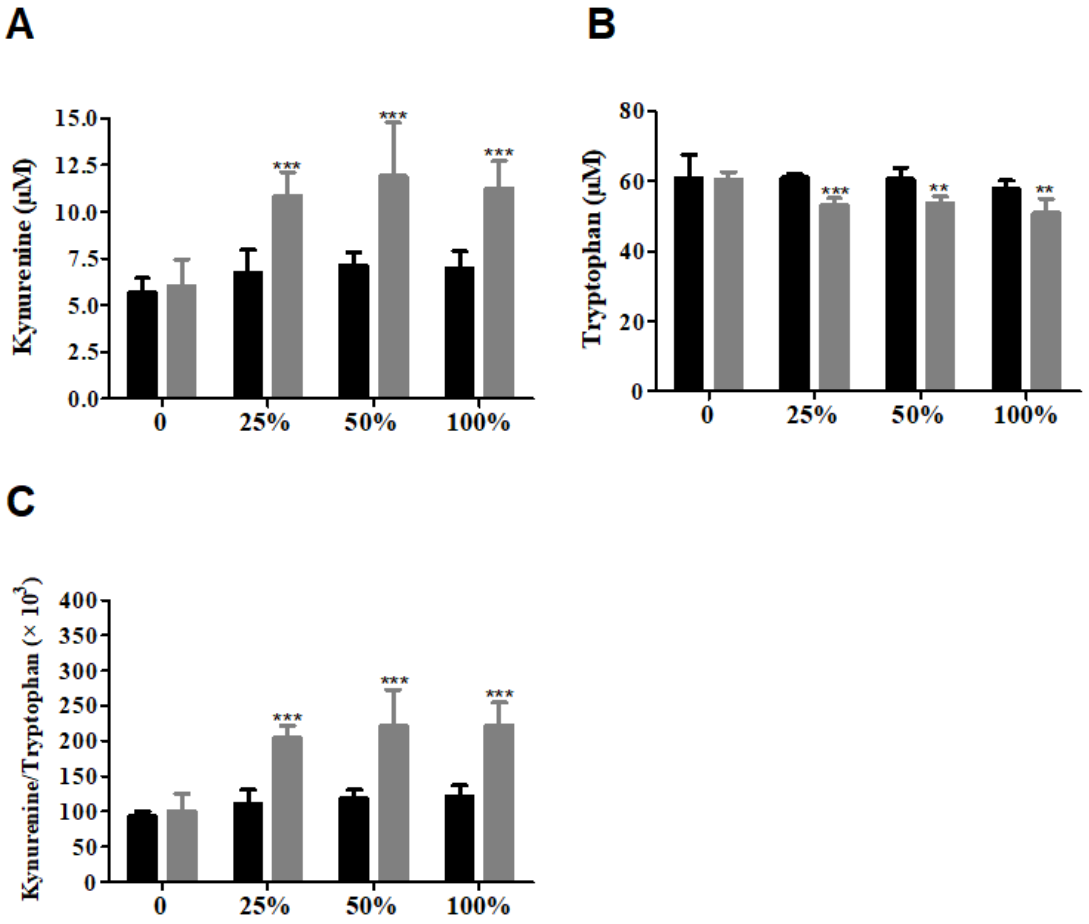

(A) Kynurenine levels, (B) tryptophan levels, and (C) kynurenine/tryptophan ratio. A172 cells were treated with increasing concentrations (0, 25, 50, and 100%) of the supernatant of lipopolysaccharide (LPS)-stimulated THP-1 macrophages or DMEM containing corresponding LPS levels (control, black bars). Columns represent the mean ± standard deviation of three independent biological replicates, each performed in triplicate. ** $p < 0.01$, *** $p < 0.001$ (two-way ANOVA, *post hoc* Bonferroni).

Figure 15. Effect of different concentrations of proinflammatory THP-1 supernatant on kynurenine levels, tryptophan levels, and kynurenine/tryptophan ratio in the culture supernatant of T98G cells

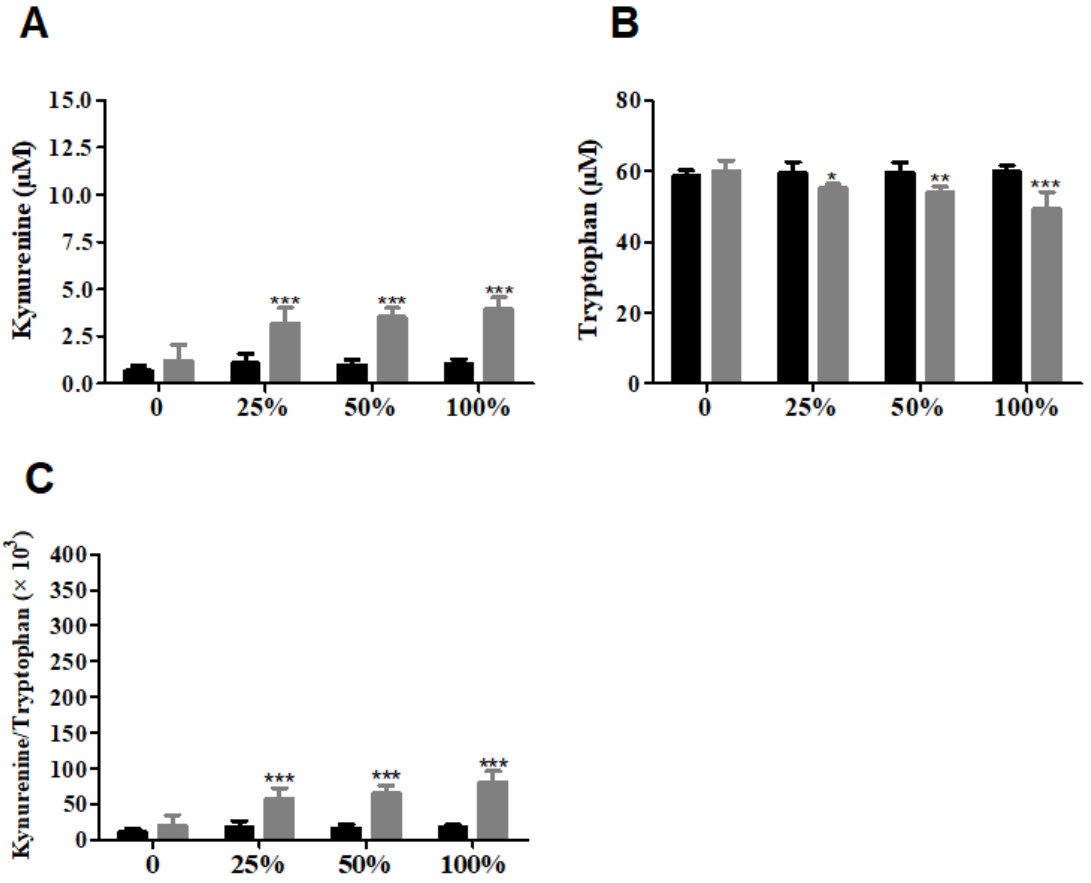

(A) Kynurenine levels, (B) tryptophan levels, and (C) kynurenine/tryptophan ratio. T98G cells were treated with increasing concentrations (0, 25, 50, and 100%) of the supernatant of lipopolysaccharide (LPS)-stimulated THP-1 macrophages or DMEM containing corresponding LPS levels (control, black bars). Columns represent the mean ± standard deviation of three independent biological replicates, each performed in triplicate. * $p < 0.05$, ** $p < 0.01$, *** $p < 0.001$ (two-way ANOVA, Bonferroni *post hoc* test).

5.2.4 Viability of A172 and T98G cells treated with TPEN

Before investigating the effect of Zn deficiency on Kyn/Trp breakdown in T98G cells treated with supernatant of LPS-stimulated THP-1 macrophages, it was first necessary to determine the viability of A172 and T98G cells treated with different concentrations of TPEN. Cell viability was assessed using an MTT viability assay. Different from EDTA, which is a membrane-impermeable chelator (RICHARDSON and BAKER, 1994), TPEN is a well-described membrane-permeable chelating agent that primarily depletes intracellular free Zn (femtomolar affinity of 15.6 L/mol, pH 7.2) (MARET, 2015). Fig. 16A and B presents the dose–response curve of TPEN (0.5, 1, 1.5, 2, 2.5, 3, 3.5, 4, 4.5, 5, and 7.5 µM) on A172 and T98G

cells, respectively. Both cell lines showed similar sensitivity to TPEN. Viability decreased substantially between extracellular TPEN concentrations of 2 and 3.5 µM.

Figure 16. Viability of A172 and T98G cells treated with different concentrations of TPEN for 24 h

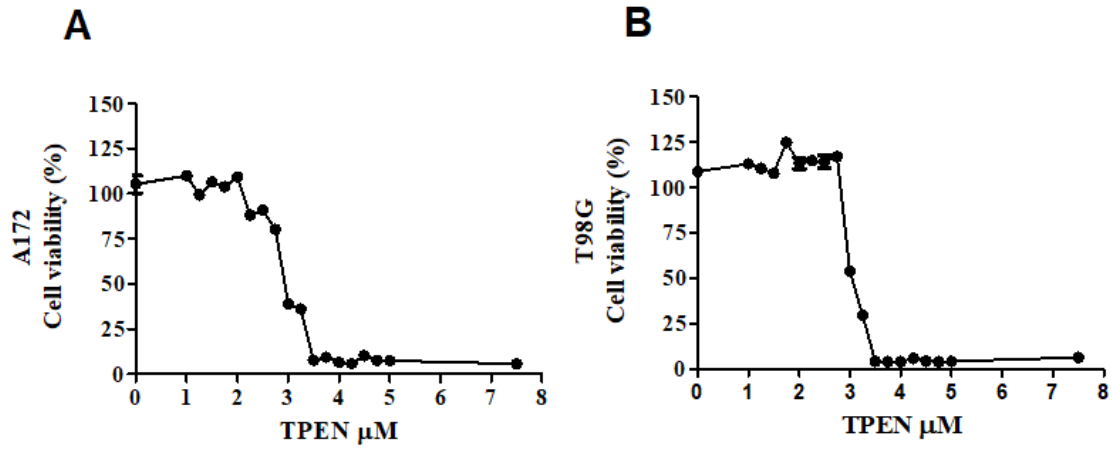

(A) A172 and (B) T98G cells. Cell viability was quantified using an MTT assay. Results (mean ± standard deviation) were obtained from two independent experiments, each performed in triplicate.

As described above, T98G cells showed lower basal levels of Kyn but a stronger response to treatment with proinflammatory supernatant. Because of these results, subsequent experiments on the Zn-dependency of the Kyn pathway were performed with this cell line only.

5.2.5 Impact of Zn status and proinflammatory THP-1 supernatant on Trp–Kyn pathway regulation in T98G cells

After defining nontoxic TPEN concentrations for T98G cells, we subjected cells to the second incubation regime, as described in Section 4.2.2.2. Briefly, T98G cells were seeded at 2×10^4 cells/500 µL and incubated for 24 h until reaching 60% confluency. Next, cells were preincubated for 2, 4, or 24 h with either $DMEM_{FCS+P/S}$ or $DMEM_{FCS+P/S}$ + 3 µM TPEN. Pretreatment solutions were removed, and cells were incubated for 24 h with one of the following solutions: $DMEM_{FCS+P/S}$ + 100 ng/mL LPS (control), proinflammatory THP-1 supernatant, $DMEM_{FCS+P/S}$ + 3 µM TPEN, or proinflammatory THP-1 supernatant + 3 µM TPEN. Solutions that contained TPEN were Zn-deficient and those without TPEN were Zn-adequate. After this period, cell viability was assessed by an MTT method and Trp and Kyn levels in cell supernatants were determined by HPLC.

Under Zn-deficient conditions, 3 µM TPEN was toxic to T98G cells. Viability was reduced by about 30% in T98G cells preincubated for 2 or 4 h with $DMEM_{FCS+P/S}$ + 3 µM TPEN, followed by incubation with proinflammatory THP-1 supernatant + 3 µM TPEN for 24 h (Fig. 17A and B).

Figure 17. Cell viability in the culture supernatant of T98G cells pretreated for 2, 4, or 24 h in DMEM with or without TPEN followed by 24 h of incubation with supernatant from lipopolysaccharide-stimulated THP-1 macrophages with or without TPEN

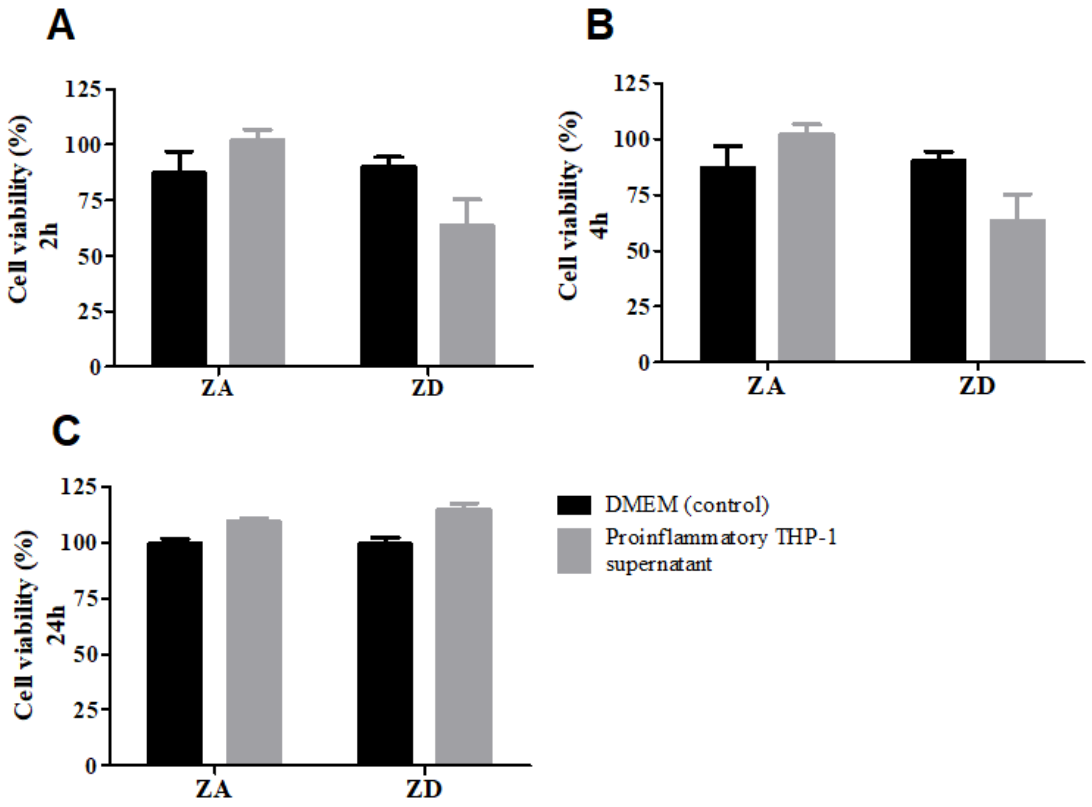

(A) Cell viability 2h, (B) cell viability 4h, and (C) cell viability 24h. ZA, zinc-adequate conditions (without TPEN); ZD, zinc-deficient conditions (with TPEN). T98G cells were preincubated with $DMEM_{FCS+P/S}$ with or without 3 µM TPEN (Zn chelator) for 2, 4, or 24h h followed by incubation with proinflammatory THP-1 culture supernatant or DMEM (control) with or without 3 µM TPEN for 24 h. Columns represent the mean ± standard deviation of three independent biological replicates, each performed in triplicate.

Because of the reduction in viability, T98G cells did not release Kyn in the supernatant (Figs. 18A and 19A). Under Zn-adequate conditions, on the other hand, cells preincubated for 4 h with fresh medium, followed by incubation with proinflammatory THP-1 supernatant for 24 h, released higher concentrations of Kyn ($p < 0.05$) (Fig. 19A), resulting in a higher Kyn/Trp ratio ($p < 0.01$) (Fig. 19C). The increased Kyn levels can be explained by the high viability

(~100%) of Zn-adequate cells (Fig. 17B) compared with the reduced viability (~70%) of Zn-deficient cells.

Figure 18. Kynurenine levels, tryptophan levels, and kynurenine/tryptophan ratio in the culture supernatant of T98G cells pretreated for 2 h in DMEM with or without TPEN followed by 24 h of incubation with supernatant from lipopolysaccharide-stimulated THP-1 macrophages with or without TPEN

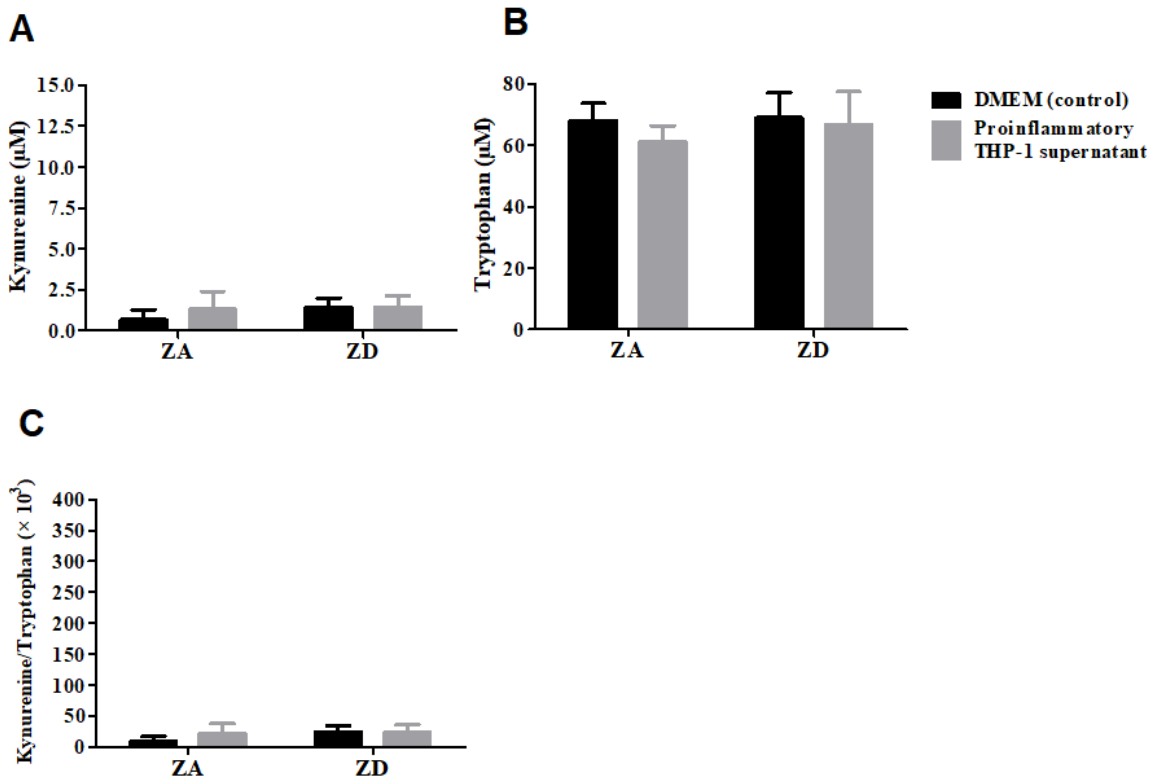

(A) Kynurenine levels, (B) tryptophan levels, and (D) kynurenine/tryptophan ratio. ZA, zinc-adequate conditions (without TPEN); ZD, zinc-deficient conditions (with TPEN). T98G cells were preincubated with $DMEM_{FCS+P/S}$ with or without 3 µM TPEN (Zn chelator) for 2 h followed by incubation with proinflammatory THP-1 culture supernatant or DMEM (control) with or without 3 µM TPEN for 24 h. Columns represent the mean ± standard deviation of three independent biological replicates, each performed in triplicate.

Figure 19. Kynurenine levels, tryptophan levels, and kynurenine/tryptophan ratio in the culture supernatant of T98G cells pretreated for 4 h in DMEM with or without TPEN followed by 24 h of incubation with supernatant from lipopolysaccharide-stimulated THP-1 macrophages with or without TPEN

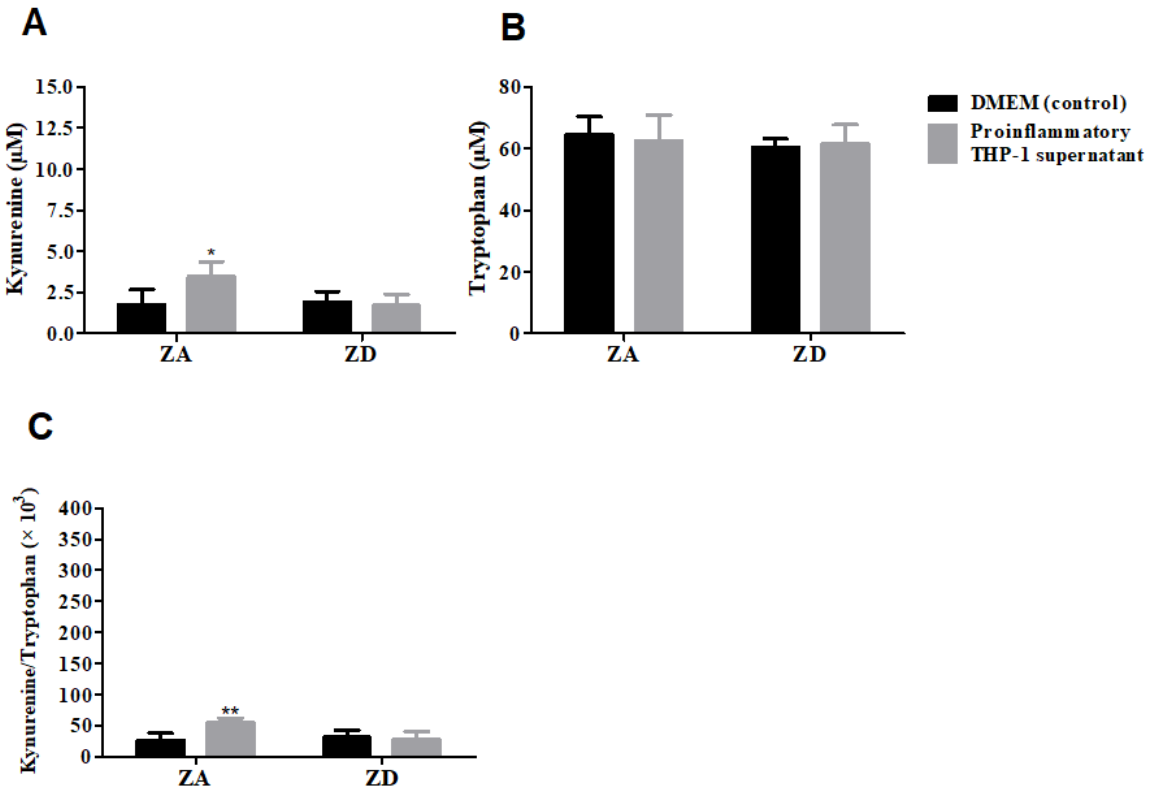

(A) Kynurenine levels, (B) tryptophan levels, and (C) kynurenine/tryptophan ratio. ZA, zinc-adequate conditions (without TPEN); ZD, zinc-deficient conditions (with TPEN). T98G cells were preincubated with $DMEM_{FCS+P/S}$ with or without 3 µM TPEN (Zn chelator) for 4 h followed by incubation with proinflammatory THP-1 culture supernatant or DMEM (control) with or without 3 µM TPEN for 24 h. Columns represent the mean ± standard deviation of three independent biological replicates, each performed in triplicate. * $p < 0.05$, ** $p < 0$ .01 (two-way ANOVA, Bonferroni *post hoc* test).

Interestingly, preincubation of T98G cells for 24 h with TPEN, followed by incubation for 24 h with proinflammatory THP-1 supernatant + 3 µM TPEN, resulted in 100% cell viability (Fig. 17C). Supernatant Kyn concentrations and, consequently, Kyn/Trp ratio ($p < 0.05$) (Fig. 20A) were increased ($p < 0.05$) (Fig. 20C) under both Zn-adequate and -deficient conditions. There was a decrease in Trp supernatant levels of T98G cells treated with Zn-deficient proinflammatory THP-1 supernatant ($p < 0.05$) (Fig. 20B). However, no differences in Kyn concentration or Kyn/Trp ratio were observed between the supernatants of T98G cells treated with Zn-deficient and -adequate proinflammatory THP-1 supernatant, as shown in Fig. 20A and C. Overall, these findings suggested that Zn did not participate in Kyn/Trp breakdown.

Figure 20. Kynurenine levels, tryptophan levels, and kynurenine/tryptophan ratio in the culture supernatant of T98G cells pretreated for 24 h in DMEM with or without TPEN followed by 24 h of incubation with supernatant from lipopolysaccharide-stimulated THP-1 macrophages with or without TPEN

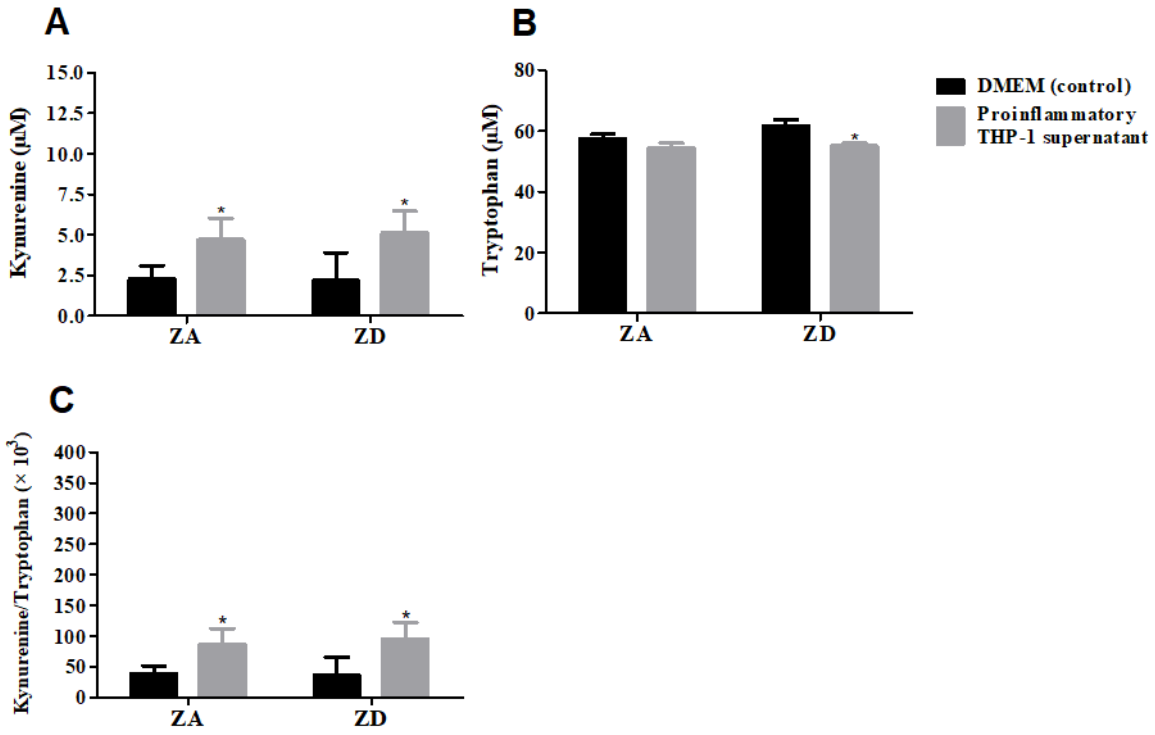

(A) Kynurenine levels, (B) tryptophan levels, and (C) kynurenine/tryptophan ratio. ZA, zinc-adequate conditions (without TPEN); ZD, zinc-deficient conditions (with TPEN). T98G cells were preincubated with $DMEM_{FCS+P/S}$ with or without 3 µM TPEN (Zn chelator) for 24 h followed by incubation with proinflammatory THP-1 culture supernatant or DMEM (control) with or without 3 µM TPEN for 24 h. Columns represent the mean ± standard deviation of three independent biological replicates, each performed in triplicate. * $p < 0.05$ (two-way ANOVA, Bonferroni *post hoc* test).

5.2.6 Impact of Zn status on the production of inflammatory mediators of the Trp–Kyn pathway in T98G cells

This next part of the *in vitro* study was aimed at understanding the influence of Zn on LPS-stimulated THP-1 macrophages. As mentioned in Section 2, one of the most exciting findings in Zn biochemistry is the compound's molecular role as a second messenger in immune cells. A variety of signaling pathways were found to involve Zn signals, including activation of immune cells (HAASE and RINK, 2014a). Several reports investigated the ability of intracellular free Zn to influence signaling and production of proinflammatory cytokines *in vitro* (VON BULOW *et al.*, 2007; BAO *et al.*, 2003). Here, Zn-deficient conditions were induced by pretreating THP-1 macrophages prior to LPS stimulation.

THP-1 cells were treated for 4 h with one of the following solutions: (i) $DMEM_{FCS+P/S}$ alone, (ii) $DMEM_{FCS+P/S}$ + 100 ng/mL LPS, (iii) $DMEM_{FCS+P/S}$ + 3 µM TPEN, or (iv) $DMEM_{FCS+P/S}$ + 100 ng/mL LPS + 3 µM TPEN. After incubation, supernatants were collected and applied to T98G cells for stimulation (third incubation regime, Section 4.2.2.2).

T98G cells were seeded at 2×10^4 cells/500 µL and incubated for 24 h until reaching 60% confluency. Then, T98G cells were treated with the respective supernatants (i–iv) and subjected to Kyn and Trp determination. As shown in Fig. 21A, no differences in Kyn levels were observed between the supernatants of T98G cells treated with LPS, TPEN, or LPS + TPEN and the control with 100% cell viability for all conditions (Fig. 21B). This indicates that T98G cells were not activated by treatment with proinflammatory THP-1 supernatant.

Figure 21. Kynurenine levels in the supernatant of T98G cells treated with zinc-adequate or -deficient lipopolysaccharide-stimulated THP-1 macrophage supernatant and cell viability

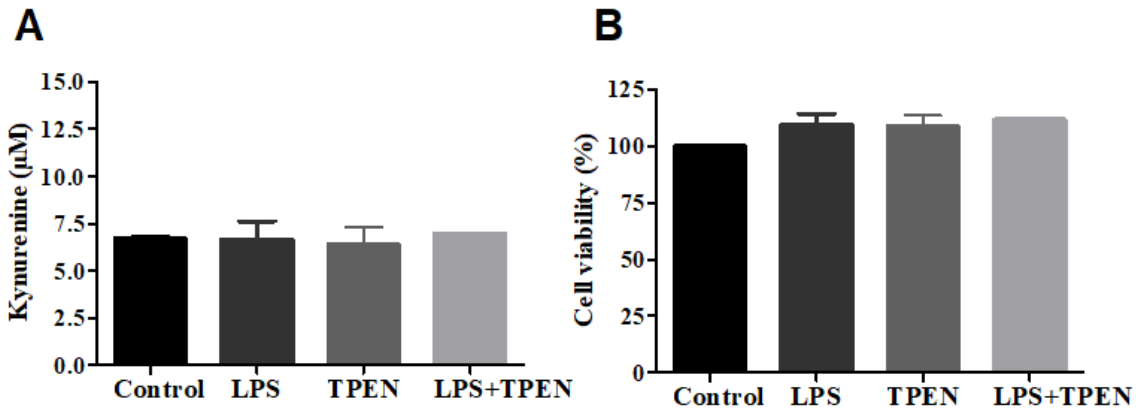

(A) Kynurenine and (B) cell viability. T98G cells were treated with supernatant from THP-1 macrophages (control), supernatant from lipopolysaccharide (LPS)-stimulated THP-1 macrophages, supernatant from THP-1 macrophages treated with 3 µM TPEN, or supernatant from LPS-stimulated THP-1 macrophages treated with 3 µM TPEN. Columns are the mean ± standard deviation of three independent biological replicates, each performed in triplicate.

Next, cells were subjected to the first incubation regime described in Section 4.2.2.2. The results of the first incubation regime, showing that incubation with proinflammatory THP-1 supernatant did not increase Kyn levels (Fig. 22), confirmed these findings (Fig. 21A)

Figure 22. Effect of different concentrations of proinflammatory THP-1 supernatant on kynurenine levels in the culture supernatant of T98G cells

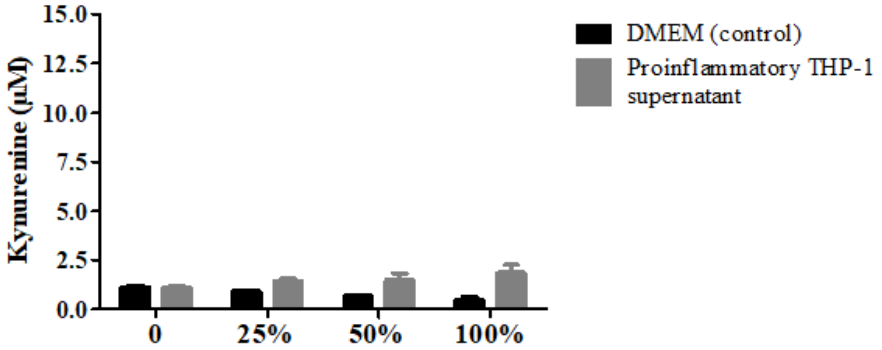

Kynurenine levels in the supernatant of T98G cells treated with increasing concentrations (0, 25, 50, and 100%) of the proinflammatory THP-1 supernatant (gray bars) or DMEM containing corresponding LPS levels (control, black bars). Columns represent the mean ± standard deviation of three independent biological replicates, each performed in triplicate.

The following step was to increase T98G cell density. Five seeding densities were tested, and T98G cells were treated with proinflammatory THP-1 supernatant or DMEM (control) to investigate why T98G cells did not respond to treatment with proinflammatory THP-1 supernatant. As depicted in Fig. 23, the increase in Kyn levels was proportional to T98G cell seeding density. In the following experiments, cells were seeded at 6×10^4 cells/500 µL instead of 2×10^4 cells/500 µL.

Figure 23. Kynurenine levels in the culture supernatant of T98G cells seeded at different densities.

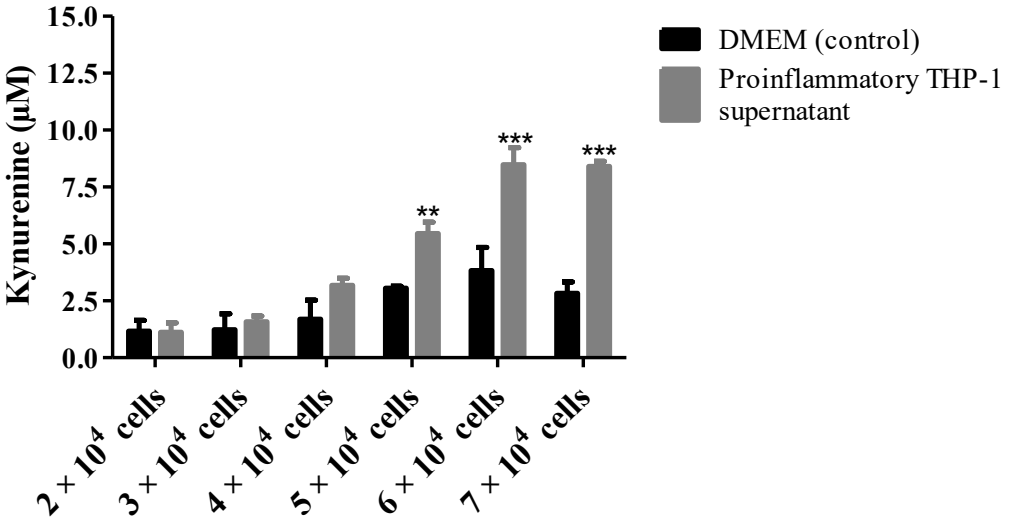

Kynurenine levels in the supernatant of T98G cells seeded at different densities (cells/500 µL) and treated with proinflammatory THP-1 supernatant (gray bars) or DMEM containing corresponding LPS levels (control, black bars). Columns are the mean ± standard deviation of three independent biological replicates, each performed in triplicate. ** $p < 0.01$, *** $p < 0.001$ (two-way ANOVA, Bonferroni *post hoc* test).

As shown in Fig. 24B, T98G cells were almost 100% viable, regardless of treatment. Kyn levels released by T98G cells were significantly higher ($p < 0.05$) after treatment with proinflammatory THP-1 supernatant (Fig. 24A); as a result, Trp concentrations decreased ($p < 0.001$) (Fig. 24D) and Kyn/Trp ratio increased ($p < 0.05$) (Fig. 24C).

This experiment aimed to determine the role of Zn deficiency in LPS-stimulated THP-1 macrophages and in the stimulation of Kyn/Trp breakdown in T98G cells. Interestingly, Kyn levels were much higher in T98G supernatant incubated with LPS/TPEN-treated THP-1 supernatant than in T98G supernatant incubated with LPS-stimulated THP-1 supernatant (10.83 ± 1.48 *vs*. 6.87 ± 0.94 µM, $p < 0.01$) (Fig. 24A), as was the Kyn/Trp ratio (274.41 ± 11.34 *vs*. 166.97 ± 23.60, $p < 0.05$) (Fig. 24C). Overall, these results indicate that Zn deficiency in LPS-stimulated THP-1 supernatant increased Kyn/Trp breakdown in T98G cells.

Figure 24. Kynurenine levels, cell viability, kynurenine/tryptophan ratio, and tryptophan levels in the supernatant of T98G cells treated with zinc-adequate or -deficient lipopolysaccharide-stimulated THP-1 macrophage supernatant

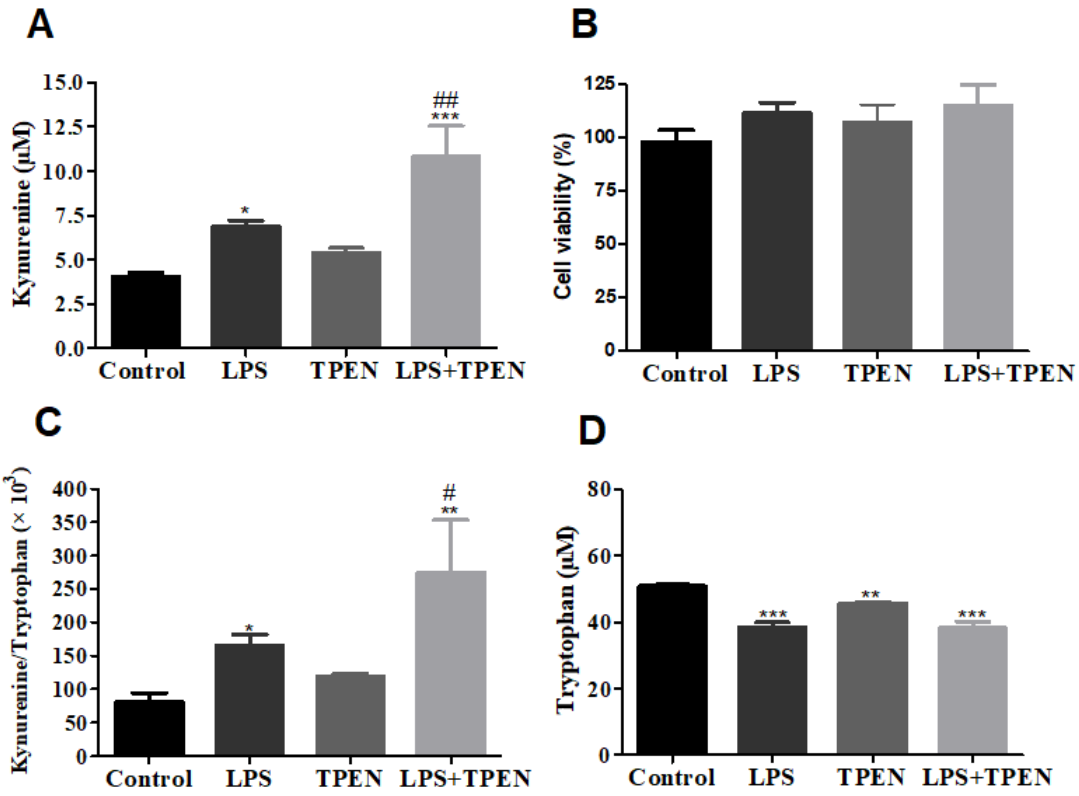

(A) Kynurenine, (B) cell viability, (C) kynurenine/tryptophan ratio, and (D) tryptophan. T98G cells were treated with supernatant from THP-1 macrophages (control), supernatant from lipopolysaccharide (LPS)-stimulated THP-1 macrophages, supernatant from THP-1 macrophages treated with 3 μM TPEN, or supernatant from LPS-stimulated THP-1 macrophages treated with 3 μM TPEN. Columns are the mean ± standard deviation of three independent biological replicates, each performed in triplicate. * $p < 0.05$, ** $p < 0.01$, and *** $p < 0.001$, compared with the control; # $p < 0.05$ and ## $p < 0.01$ for LPS + TPEN *vs*. LPS (two-way ANOVA, Bonferroni *post hoc* test).

5.2.7 Determination of intracellular free Zn in THP-1 macrophages

The effects of LPS and/or TPEN incubation on intracellular free Zn levels in THP-1 cells were estimated by using the Zn fluorescent sensor Zinpyr-1 (WALKUP *et al*., 2000). Zinpyr-1-bound Zn in THP-1 macrophages was determined after application of different inducers. According to the results of Fig. 25, LPS stimulation slightly increased intracellular free Zn levels in THP-1 macrophages compared with LPS + TPEN stimulation. In LPS-stimulated THP-1 macrophages, the maximum Zn signal occurred within less than 2 min, followed by 12 min of gradual reduction compared with the control (Fig. 25). Treatment with LPS did not change the patterns of intracellular free Zn distribution in THP-1 macrophages but rather increased free Zn in the entire cell.

Figure 25. Effects of lipopolysaccharide (LPS) and/or TPEN on intracellular free Zn concentrations in THP-1 macrophages, as determined using the fluorescent Zn sensor Zinpyr-1

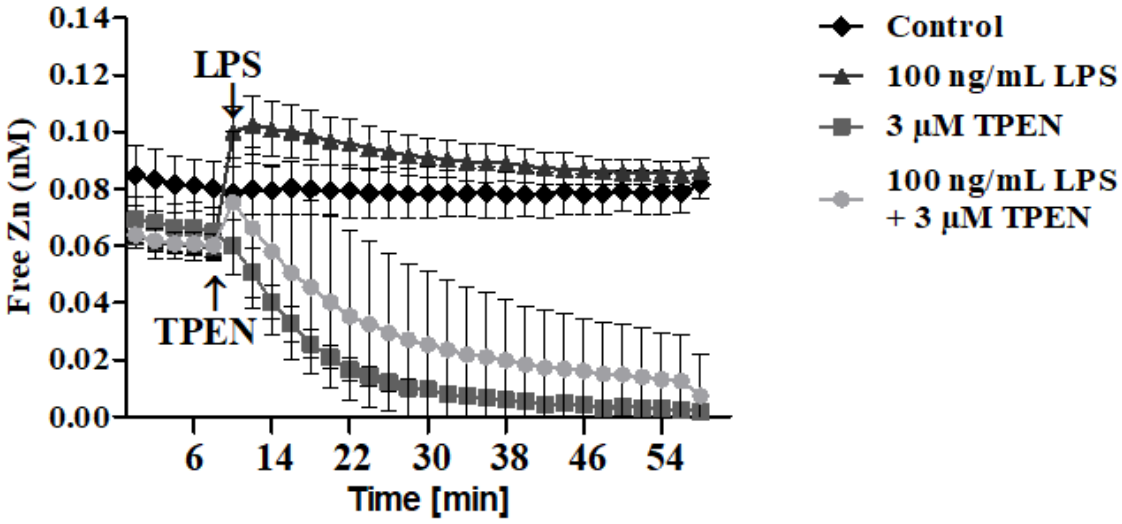

(A) THP-1 macrophages were loaded with Zinpyr-1 (2.5 µM), incubated, and washed twice with assay buffer. Minimal (F_{min}) and maximal (F_{max}) fluorescence signals were determined by adding 100 µL of assay buffer containing 20 µM TPEN or 600 µM $ZnSO_4 \cdot 7H_2O$, respectively, to a subset of wells used for calibration. Fluorescence was recorded at 2-min intervals. After 10 min of baseline fluorescence determination, cells were treated with buffer (control), 100 ng/mL LPS, 3 µM TPEN, or 100 ng/mL LPS + 3 µM TPEN. Fluorescence was recorded for an additional 50 min. Intracellular labile Zn was calculated using the equation $[Zn] = K_d \times [(F - F_{min})/(F_{max} - F)]$ (GRYNKIEWICZ *et al*., 1985), assuming a dissociation constant (K_d) of 0.7 nM for the Zn–Zinpyr-1-complex (WALKUP *et al*., 2000; BURDETTE *et al*., 2001). Data from a representative experiment are shown as the mean of triplicates ± standard deviation of three experiments.

A similar experiment was carried out using the Zn fluorophore FluoZin-3AM (HAUGLAND, 2000). The Zinpyr-1 demonstrated a relatively increased free Zn in the entire cell, while FluoZin-3AM exclusively labeled cellular ornganelles which contained storage free Zn (KALTENBERG *et al*., 2010).

LPS stimulation led to a maximal Zn signal within the first 2 min, followed by a gradual reduction compared with the control for the following 30 min (Fig. 26A). Even though LPS was applied at different concentrations, Zn signals in THP-1 macrophages were found to not be dose-dependent. However, free Zn levels increased 1.5-fold compared with the control after 2 min with addition of LPS solutions at different concentrations (Fig. 26B). Treatment with the Zn chelator TPEN (at 3 or 20 µM) confirmed the specificity of the FluoZin-3AM signal within 2 min of treatment, inducing a sharp decline (Fig. 26A).

Figure 26. Effects of lipopolysaccharide (LPS) and/or TPEN on intracellular free Zn concentrations in THP-1 macrophages, as determined using the Zn fluorophore FluoZin-3AM

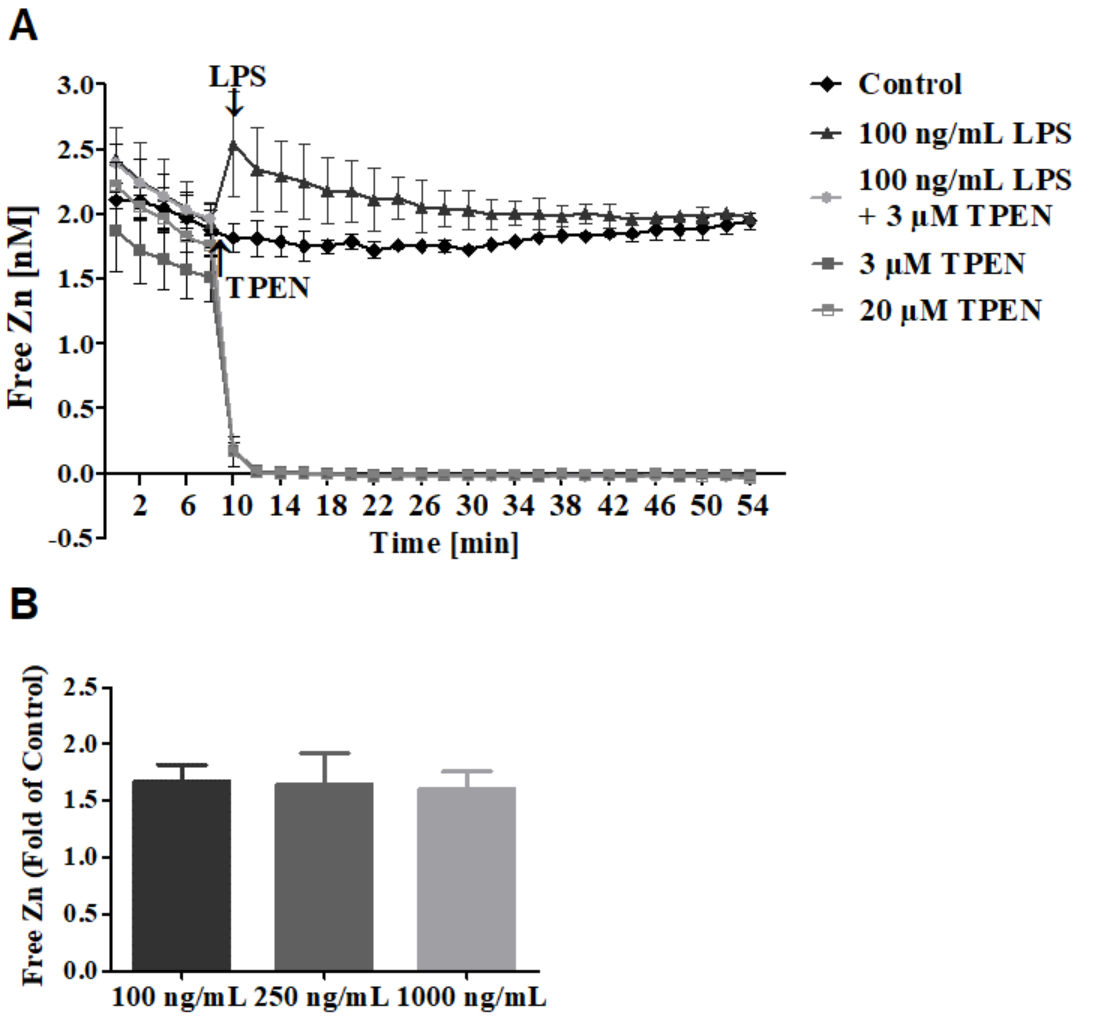

(A) THP-1 macrophages were loaded with FluoZin-3AM (1 µM), incubated, and washed twice with assay buffer. Minimal (F_{min}) and maximal (F_{max}) fluorescence signals were determined by adding 100 µL of assay buffer containing 20 µM TPEN or 600 µM $ZnSO_4 \cdot 7H_2O$, respectively, to a subset of wells used for calibration. Fluorescence was recorded at 2-min intervals. After 10 min of baseline fluorescence determination, cells were treated with buffer (control), 100 ng/mL LPS, 3 µM TPEN, or 100 ng/mL LPS + 3 µM TPEN. Fluorescence was recorded for an additional 50 min. Intracellular labile Zn was calculated using the equation $[Zn] = K_d \times [(F - F_{min})/(F_{max} - F)]$ (GRYNKIEWICZ *et al*., 1985), assuming a dissociation constant (K_d) of 8.9 nM for the Zn–FluoZin 3-AM complex (KRĘŻEL and MARET, 2006). (B) Free zinc in cells treated with 100, 250 or 1000 ng/mL LPS was expressed as the fold of control after 2 min. Data from a representative experiment are shown as the mean of triplicates ± standard deviation of three experiments.

5.2.8 Impact of Zn status on the production of inflammatory mediators of the Trp–Kyn pathway in T98G cells before RT-PCR assays

RT-PCR gene expression analyses were performed to investigate which proinflammatory cytokines are expressed in LPS-stimulated and unstimulated THP-1 macrophages under Zn-adequate and -deficient conditions. However, before carrying out RT-

PCR, it was necessary to evaluate whether the cells used for transcript analysis were effectively stimulated by LPS.

The results of Fig. 27 confirm those demonstrated in Fig. 24. One-way ANOVA revealed significant differences in Kyn levels and Kyn/Trp ratio in the supernatant of T98G cells treated with proinflammatory THP-1 supernatant + TPEN (Zn-deficient) compared with supernatant of proinflammatory THP-1 (Zn-adequate). The results of RT-PCR gene expression analysis of proinflammatory cytokines in LPS-stimulated THP-1 under Zn-adequate or -deficient conditions are comparable to the results of Kyn/Trp breakdown in T98G cells (Fig. 27), as the evaluated cells and supernatant were obtained from the same three independent biological replicates.

Figure 27. Kynurenine, tryptophan, and kynurenine/tryptophan ratio in the culture supernatant of T98G cells stimulated with supernatant of lipopolysaccharide (LPS)-stimulated THP-1 macrophages under zinc-adequate or -deficient conditions

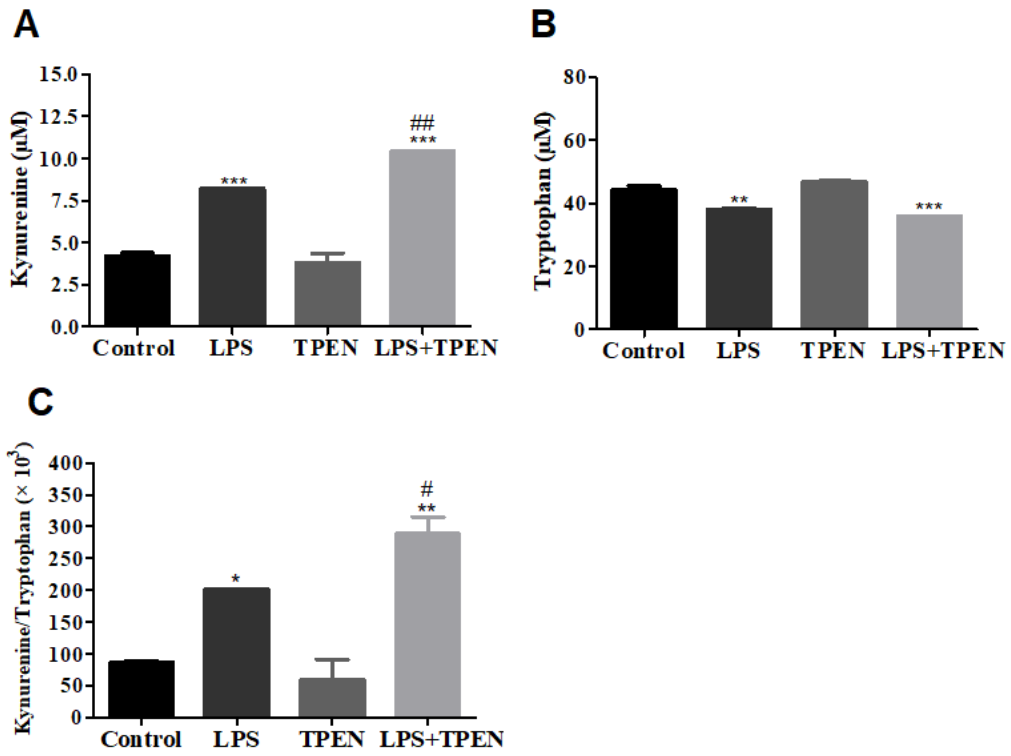

(A) Kynurenine, (B) tryptophan, and (C) kynurenine/tryptophan ratio. T98G cells were treated with supernatant from THP-1 macrophages (control), supernatant from LPS-stimulated THP-1 macrophages, supernatant from THP-1 macrophages treated with 3 µM TPEN, or supernatant from LPS-stimulated THP-1 macrophages in the presence of TPEN. Columns are the mean ± standard deviation of three independent biological replicates, each performed in triplicate. * $p < 0.05$, ** $p < 0$ .01, and *** $p < 0.001$ compared with the control; # $p < 0.05$ and ## $p < 0.01$ for LPS + TPEN *vs*. LPS (one-way ANOVA, Bonferroni *post hoc* test).

5.2.9 Gene expression profiling of proinflammatory cytokines in LPS-stimulated THP-1 macrophages under Zn-adequate and -deficient conditions

RT-PCR was used to assess the expression of *IL6*, *TNFA*, *IFNA*, *IFNB*, and *IFNG* in THP-1 macrophages incubated with either fresh medium (control), medium containing 100 ng/mL LPS, medium containing 3 µM TPEN, or medium containing LPS/TPEN (LPS and TPEN were added simultaneously). The analysis revealed that *IL6* expression in LPS-stimulated THP-1 macrophages under both Zn-adequate (7.53 ± 1.46) and Zn-deficient (10.27 ± 0.43) conditions was significantly higher than in the control ($p < 0.001$, Fig. 28A).

However, no significant differences in *IL6* expression were observed between LPS- and LPS/TPEN-treated cells. Thus, the labile Zn status of THP-1 macrophages seemed to be less influenced by *IL*6 expression. *TNFA* expression was also higher in LPS-stimulated THP-1 macrophages under both Zn-adequate (2.82 ± 0.31) and Zn-deficient conditions (2.64 ± 0.35) ($p < 0.01$, Fig. 28B).

Figure 28. Influence of TPEN on lipopolysaccharide (LPS)-induced expression of *IL6* and *TNFA* by THP-1 macrophages

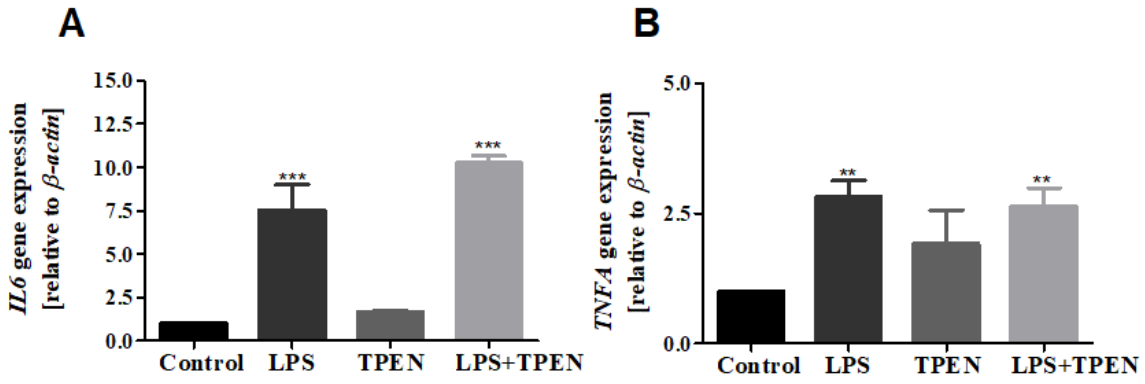

(A, B) Relative mRNA expression of *IL6* and *TNFA* genes in THP-1 macrophages, as determined by RT-PCR. Expression levels are relative to those of untreated THP-1 macrophages and normalized to that of the β-actin gene. THP-1 cell cultures were treated with fresh medium (control), 100 ng/mL LPS (Zn-adequate condition), 3 µM TPEN (Zn-deficient condition), or 100 ng/mL LPS + 3 µM TPEN (Zn-deficient condition) for 4 h. Columns are the mean ± standard deviation of three independent biological replicates, each performed in triplicate. ** $p < 0.01$, *** $p < 0.001$ (two-way ANOVA, Bonferroni *post hoc* test).

IL-6 and TNF-α levels in the supernatant of LPS stimulated THP-1 macrophages were determined by ELISA. In line with RT-PCR results, IL-6 levels were significantly higher in Zn-adequate and -deficient LPS-stimulated THP-1 supernatant than in unstimulated THP-1 supernatant ($p < 0.001$) (Fig. 29A). The same was observed for TNF-α levels ($p < 0.05$) (Fig. 29B). Of note, there was a significant difference in IL-6 levels between supernatant from LPS-

stimulated THP-1 macrophages incubated under Zn-deficient and Zn-adequate conditions ($p < 0.05$) (Fig. 29A).

Figure 29. Levels of interleukin 6 and tumor necrosis factor-alpha in the supernatants of differentiated THP-1, lipopolysaccharide (LPS)-stimulated differentiated THP-1, differentiated THP-1 treated with TPEN, and differentiated THP-1 treated with TPEN/LPS

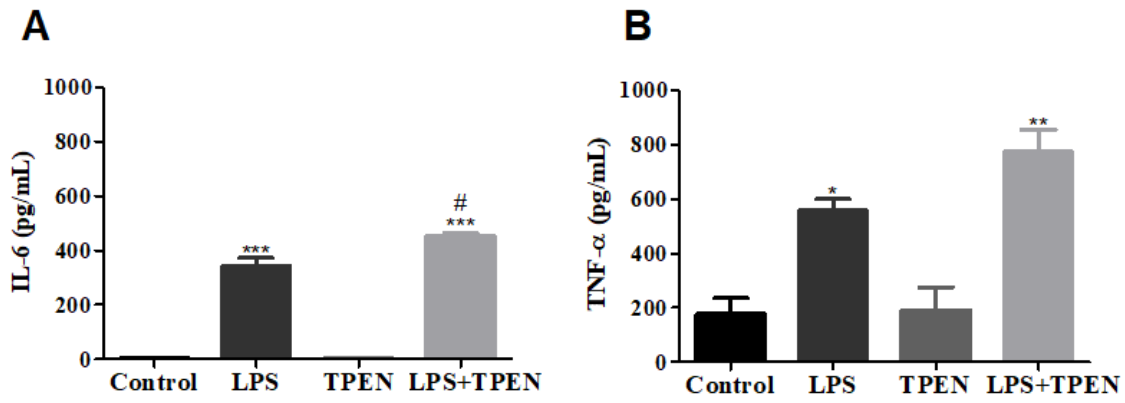

(A, B) interleukin 6 (IL-6) and tumor necrosis factor-alpha (TNF-α) levels determined using ELISA. THP-1 cell cultures were treated with fresh medium (control), 100 ng/mL LPS (Zn-adequate condition), 3 µM TPEN (Zn-deficient condition), or 100 ng/mL LPS + 3 µM TPEN (Zn-deficient condition) for 4 h. Columns are the mean ± standard deviation of three independent biological replicates, each performed in triplicate. * $p < 0.05$, ** $p < 0.01$, *** $p < 0.001$; # $p < 0.05$ (one-way ANOVA, Bonferroni *post hoc* test).

IFNA and *IFNB* mRNA levels in THP-1 macrophages did not differ between treatments (Fig. 30A and B). LPS/TPEN treatment substantially enhanced *IFNG* transcription by about 4-fold compared with LPS treatment. Thus, the labile Zn status of THP-1 macrophages is greatly influenced by *IFNG* expression ($p < 0.01$) (Fig. 30C).

Figure 30. Impact of TPEN on lipopolysaccharide-induced expression of interferon genes in THP-1 macrophages.

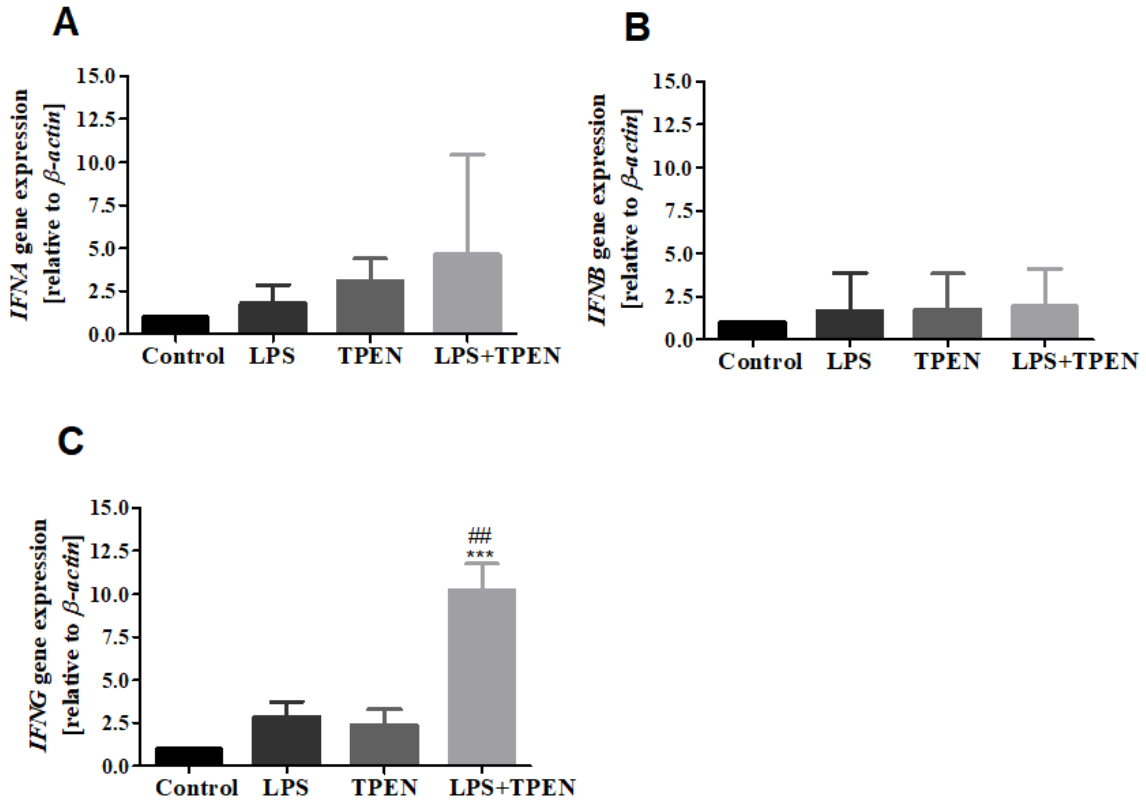

(A, B, and C) Relative mRNA expression of *IFNA*, *IFNB*, and *IFNG* in THP-1 macrophages, as assessed by RT-PCR. Expression levels are relative to those of untreated THP-1 macrophages and normalized to that of the β-actin gene. THP-1 macrophages were treated with fresh medium (control), 100 ng/mL LPS (Zn-adequate condition), 3 µM TPEN (Zn-deficient condition), or 3 µM TPEN + 100 ng/mL LPS (Zn-deficient condition) for 4 h. Columns are the mean ± standard deviation of three independent biological replicates, each performed in triplicate. *** $p < 0.001$, ## $p < 0.01$ (one-way ANOVA, Bonferroni *post hoc* test).

Taken together, the *in vitro* data demonstrated that Zn deficiency may enhance LPS-induced proinflammatory responses in THP-1 macrophages, as evidenced by the increase in *IFNG* expression and IL-6 levels. Higher levels of proinflammatory cytokines in THP-1 macrophage supernatant increased Kyn/Trp breakdown in T98G cells, as shown by the higher Kyn levels.

6 DISCUSSION

6.1 *IN VIVO* EXPERIMENTS

Modern Western diets are characterized by high SFA intake, a well-known risk factor for obesity, and limited intake of micronutrients such as Zn **(**COSTARELLI *et al*., 2010; RIOS-LUGO *et al*., 2020). Numerous animal and human studies have concluded that individuals with dietary Zn deficiency are more prone to behavioral alterations (SWARDFAGER *et al*., 2013). Furthermore, obesity significantly contributes to the development of neuropsychiatric comorbidities (PAN *et al*., 2012; ZHAO *et al*., 2011). In this thesis, we sought to investigate the role of Zn in DIO and adipose tissue hypertrophy in mice and assess to what extent Zn deficiency is linked with behavioral disturbances. This was achieved by evaluating the effects of different diets on the Kyn–Trp pathway and the ability of fluoxetine treatment to reverse behavioral alterations and biochemical parameters.

Various animal studies used the C57Bl/6J inbred mouse strain as a DIO model, as the strain is highly susceptible to developing obesity (SURWIT and COLLINS, 2001). However, C57BL/6J mice are resistant to the development of dietary Zn deficiency compared with other rodents (LUECKE and FRAKER, 1979). Thus, for the experiments carried out in this thesis, we used outbred Swiss albino mice, which are metabolically sensitive to HFD and whose wide genetic variability is similar to that found in humans (WHITE *et al*., 2013; MAREI *et al*., 2020). Notably, obesity and depression are more prevalent in adult women than in men, which is why experiments were performed with adult female Swiss albino mice only (WONG and LICINIO, 2001; BLÜHER, 2019). Behavioral assays are frequently performed using Swiss albino mice, with reliable results when using antidepressants (CAN *et al*., 2012). In the present thesis, female Swiss albino mice were susceptible to DIO, and obese mice had a greater feed efficiency (weight gain divided by energy intake). The results showed that energy conversion from HFD resulted in body composition changes, such as increased body weight, Lee index, and abdominal circumference, in obese mice with equal or lower energy intake than their respective controls. Our experimental model provided results that agreed with those of other DIO studies (PORTOVEDO *et al*., 2015; MAREI *et al*., 2020).

Total serum Zn concentration was assessed using a Randox Zn colorimetric assay and the results confirmed that mice fed SD-ZD and HFD-ZD achieved a Zn-deficient state. Waqar Rabbani *et al*. (2013) used the same kit on an auto-analyzer to determine total serum Zn in children presenting with febrile seizures. Other methods have been used to assess total serum

or plasma Zn levels in humans and rodents, including atomic absorption spectrometry and inductively coupled plasma optical emission spectroscopy (ZALEWSKI *et al*., 2006; OMU *et al*., 2015). Liu *et al*. (2013) used inductively coupled plasma optical emission spectrometry for Zn quantification and found that C57BL/6 mice fed Zn-deficient diets for 3 weeks had significantly lower total serum Zn concentrations.

Less than 1% of total body Zn is found in the serum. About 80–90% of serum Zn is bound to serum albumin, 10–20% is strongly bound to α2-macroglobulin, and the remainder is known as free Zn (ZALEWSKI *et al*., 2006; KAMBE *et al*., 2015). The free Zn pool is biologically active and involved in numerous signaling pathways (FUKADA *et al*., 2011; MARET, W. 2015). Changes in its homeostasis can lead to a diversity of abnormalities in humans and animal models (FUKADA *et al*., 2011). Motivated by the importance of determining serum free Zn, Alker *et al*. (2019) have been developing reliable biomarkers of free Zn status.

The fat content of HFD resembles the fat intake of the US adult population (US NHANES, 2012). HFD and HFD-ZD, composed of 30% lard (rich in SFA), effectively induced obesity in mice. According to the review study carried out by Buettner *et al.* (2007), the best method to induce obesity in animals is to use HFDs containing lard. SFA was more effective in promoting obesity and insulin resistance than polyunsaturated fat (BUETTNER *et al*., 2007). Hariri and Thibault (2010), in a review study, showed that SFAs are highly obesogenic because they are inadequately used for energy production, resulting in acylation to triglycerides and storage in WAT. Increased lipid storage in WAT has been reported as a characteristic feature of obesity in both humans and animals (GREENBERG *et al*., 2011). The results of *in vivo* experiments showed that obese mice (HFD and HFD-ZD groups) had a marked increase in the proportions of visceral and subcutaneous WAT, resulting from increased lipid storage and adipocyte volume. Huang *et al.* (2017) reported that C57BL/J mice supplemented with Zn sulfate for 20 weeks showed increased visceral WAT, greater adipocyte size, and higher leptin and IL-6 expression in visceral WAT. The authors suggested that leptin may stimulate the expression of proinflammatory cytokines in adipocytes and macrophages (HUANG *et al.*, 2017).

Furthermore, obese mice showed increased macrophage infiltration in WAT, increased serum leptin, and decreased serum adiponectin. These results are in agreement with those of other studies showing that serum leptin is proportional to WAT and macrophage number and that adipocytes contribute to the production of proinflammatory adipokines, such as leptin (FRIEDMAN and HALAAS, 1998; MAKKI *et al*., 2013). WAT expansion and dysfunction is

associated with chronic obesity and results in altered immune function and systemic inflammation. Leptin has been implicated in the aggravation of systemic inflammation for its role in the secretion of the proinflammatory cytokines TNF-α and IL-6 and its function as a chemoattractant for macrophages (LOFFREDA *et al.*, 1998; GRUEN *et al.*, 2007; POPKO *et al*., 2010). A previous study (LIU *et al*., 2013) reported that Zn deficiency increased serum leptin levels and macrophage infiltration in WATs of Zn-deficient obese C57BL/6J mice. Liu *et al.* (2013) argued that Zn deficiency can contribute to exacerbation of a proinflammatory state in WAT. In contrast, in the present experiments, differences in leptin levels between Swiss albino mice fed HFD and HFD-ZD were not observed. Such discrepancies may be due to the inbred strain C57BL/6J used in Liu *et al*. (2013); these animals are known to develop a more severe form of obesity (KLEINERT *et al*., 2018; MAREI *et al*., 2020) than outbred Swiss albino mice, whose wide genetic variability is similar to that found in humans (WHITE *et al*., 2013; MAREI *et al*., 2020). Moreover, treatment duration and dietary fat levels differed between studies. Mice subjected to the feeding protocol developed in the current study mimicked human obesity more closely than C57BL/6J mice in the study of Liu *et al*. (2013).

Obesity is associated with several comorbidities, including psychiatric and psychosocial problems. Depressive symptoms are observed in obese individuals at higher rates than symptoms of other disorders (COHEN, 2010). Recent reports showed that depression is associated with increased levels of proinflammatory cytokines in peripheral blood and the CNS (BAUNE *et al*., 2012; PAPAKOSTAS *et al*., 2013). A study performed using a rodent model showed that increased cytokine expression in the hippocampus, which is involved in mood regulation and memory formation, is associated with emotional behavior disturbances and cognitive impairments (PISTELL *et al*., 2010). Obesity t is strongly linked to an increase in leptin, TNF-α, and IL-6 levels in adipose tissue and serum (CINTI, 2005). Notably, Zn deficiency was shown to increase proinflammatory cytokine (IL-1β and TNF-α) synthesis in the HL-60 promyelocytic cell line (WESSELS *et al*., 2013). Low serum Zn in depressed patients was correlated with immune–inflammatory responses and neuroprogression (MAES *et al*., 1997). In a previous clinical study, the proinflammatory cytokines IL-1α, IL-1β, and IL-6 were upregulated in peripheral blood mononuclear cells of overweight and obese Zn-deficient adults (with low dietary Zn intake) compared with overweight and obese subjects with adequate dietary Zn intake (COSTARELLI *et al*., 2010). In the referred study, dietary micronutrient intake was estimated using a semiquantitative food frequency questionnaire. The authors suggested that hypozincemia can aggravate obesity-related disturbances, such as insulin resistance and inflammation, thereby worsening the preexisting obesity status (COSTARELLI

et al., 2010). In an *in vivo* study conducted by De Oliveira *et al*., a cafeteria diet promoted metabolic disturbances and impaired recognition memory in Wistar rats after 20 weeks. The cafeteria diet increased plasma glucose and triglyceride levels, visceral WAT, weight gain, and TNF-α levels. Animals were then supplemented with Zn for 4 weeks. Zn reduced hyperglycemia and decreased IL-6 levels. The authors demonstrated that Zn supplementation of obese animals can reverse obesity-related metabolic dysfunction, reduce neuroinflammation, and ameliorate memory impairment induced by the cafeteria diet (DE OLIVEIRA *et al*., 2021).

Therefore, obesity, Zn deficiency, and depression might share a crucial, pivotal mediator: the inflammatory process. Indeed, obesity-related proinflammatory cytokines contribute to increased IDO expression and activity, leading to a shift in the Kyn pathway (JENKINS *et al*., 2016). Recently, an association was proposed between enhanced IDO expression and activity and obesity genesis and development (MANGGE *et al*., 2014). High IDO expression/activation induced peripherally by proinflammatory cytokines might play an important role in emotional and cognitive alterations in obesity.

Serum Trp, Kyn, and Kyn/Trp ratio were determined in mice models. Kyn/Trp ratio can be used as an indicator of IDO activity, together with immune activation markers, as it provides a measure of Trp breakdown (ARNONE *et al*., 2018). Obese mice had lower serum Trp and Kyn levels. Studies have shown that excess dietary fats and carbohydrates in mice can induce hepatic steatosis and alter Trp metabolism (NAGANO *et al*., 2013). This fact suggests involvement of the Kyn pathway in liver lipid metabolism. The changes in gut microbiota associated with metabolic syndrome and obesity are at least partially mediated by impaired Trp metabolism (AGUS *et al*., 2018). No differences in peripheral Kyn/Trp were observed in the experiments. However, in a prior *in vivo* study, LPS-challenged C57Bl/6 mice fed a Western diet showed exacerbated expression of proinflammatory cytokines and IDO activation in the hippocampus and hypothalamus (ANDRÉ *et al*., 2014).

Anhedonia is one of two symptoms required for diagnosis of depression in humans (DUNLOP and NEMEROF, 2007). In mice, anhedonic behavior is frequently determined as a high latency and short time spent grooming in the splash test (ISINGRINI *et al*., 2010; d'AUDIFFRET *et al*., 2010; MACHADO *et al*., 2012). A previous rodent study demonstrated that intake of HFD (60% of fat from lard) for 16 weeks induced depressive behaviors, as assessed in sucrose preference and forced-swim tests (YAMADA *et al.*, 2011). However, in the present experiments, mice fed HFD did not show altered behaviors. These differences may be due to the short duration of dietary treatment or the lower fat levels used in the present experiments (30% compared with 60% used by Yamada *et al*., 2011). Noteworthy, 8 weeks of

Zn-deficient diets were sufficient to increase latency to initiate grooming in the splash test, but only mice fed HFD-ZD exhibited anhedonic-like behavior (increased latency and reduced grooming time). In most studies using the splash test, total grooming time and frequency are the only parameters used to measure anhedonic behavior as a model of depression (DETANICO *et al*., 2009; YALCIN *et al*., 2005).

In the second part of the *in vivo* experiment, the ability of fluoxetine to reverse behavioral changes and biochemical parameters in Zn-deficient obese mice was evaluated. Fluoxetine, a selective serotonin reuptake inhibitor, is the most widely antidepressant prescribed for psychiatric patients. In a preclinical study, fluoxetine was administered daily at 10 to 18 mg/kg to mice for 24 days; plasma levels of the drug were comparable to those observed in patients taking 20–80 mg/day (DULAWA *et al*., 2004). Here, fluoxetine was administered orally at 10 mg/kg once a day for 14 days to study its antidepressant action at a clinically relevant concentration. The anhedonic behavior of Zn-deficient obese mice induced by HFD-ZD was reversed by fluoxetine treatment. These findings corroborate a preclinical study showing that treatment with fluoxetine for 2 weeks reduces depressive-like behavior caused by 4-week dietary Zn restriction (DOBOSZEWSKA *et al*., 2015).

Fluoxetine, in addition to having antidepressant properties, exerts anti-inflammatory effects (ROUMESTAN *et al*., 2007). In an *in vitro* study, fluoxetine inhibited LPS-induced expression and production of proinflammatory cytokines (TNF-α and IL-6) in microglial cells (LIU *et al*., 2011). In rodents, TNF-α administration induced an anhedonic effect in the sucrose preference test, which was reversed by administration of anti-TNF-α antibody or fluoxetine, showing that anhedonic effects promoted by this cytokine are sensitive to fluoxetine treatment (KASTER *et al*., 2012). Previous *in vitro* studies showed that adiponectin suppresses TNF-α production in macrophages (YOKOTA *et al*., 2000). Here, fluoxetine treatment reduced energy intake and serum leptin and increased serum adiponectin in Zn-deficient obese mice. These results are in agreement with literature data reporting that fluoxetine can decrease energy intake and promote weight loss both in mice and humans as a result of an elevation in serotonin levels in the synaptic cleft. These effects induce a feeling of satiety, resulting in hypophagia and decreased plasma leptin levels (LAUZURICA *et al*., 2013).

The results of *in vivo* experiments suggest that obesity and Zn deficiency increase leptin levels and consequently aggravate systemic inflammation by enhancing secretion of proinflammatory cytokines, such as TNF-α. These effects may be associated with the anhedonic behavior observed in HFD-ZD mice. The ability of fluoxetine to reverse anhedonic behavior could be due to a reduction in serum leptin levels and an increase in adiponectin levels, which

consequently reduces TNF-α production. Proinflammatory cytokines are involved in mood regulation through activation of Trp catabolism; however, no differences in peripheral Kyn/Trp breakdown were observed. It is possible that HFD-ZD elevates proinflammatory cytokines and IDO expression and activity in the brain, particularly in microglial cells. To the best of our knowledge, no previous study, whether clinical or experimental, has examined Zn deficiency in obese individuals with psychiatric disorders such as depression. Thus, further studies are needed to elucidate the mechanisms underlying neuroinflammatory responses to Zn deprivation and HFD.

The present study constitutes an important step toward a better understanding of Zn deficiency and its association with obesity and neuropsychiatric alterations. Overall, the results demonstrated the effects of obesity combined with Zn deficiency on anhedonic behavior, associated with exacerbation of the inflammatory state. Fluoxetine treatment was able to reverse behavioral and adipokine alterations, in agreement with the potential anti-inflammatory effects of the drug. The findings provide evidence that obesity associated with Zn deficiency may increase vulnerability to immune-mediated depressive symptoms.

6.2 *IN VITRO* EXPERIMENTS

Several studies reported a relationship between Zn deficiency and obesity in humans (SWARDFAGER *et al.*, 2013; NAZEM *et al*., 2016). Obesity is characterized by disproportionate WAT distribution, adipocyte hypertrophy, inflammation, and increased circulating levels of proinflammatory cytokines (CINTI, 2005). Excessive production of proinflammatory cytokines can result in greater expression and activity of IDO in the Trp pathway, leading to Trp depletion and increased Kyn levels (MIYAZAKI *et al*., 2009). The current *in vitro* study examined the interrelation between Zn deficiency and the Trp–Kyn pathway under proinflammatory conditions.

This study developed an *in vitro* cell culture model suitable for investigation of the effects of Zn deficiency on Trp–Kyn pathway under proinflammatory conditions by combining two human cell line subsets: THP-1 macrophages, capable of synthesizing proinflammatory mediators upon LPS stimulation, and A172/T98G glioma cells, active in the Trp–Kyn pathway cascade. As recently demonstrated by Ozawa *et al*. (2020), IDO1 is greatly expressed in glioma stem cells. Acute monocytic leukemia THP-1 cells were differentiated into macrophages by treatment with PMA (LUND *et al*., 2016). Differentiation of THP-1 monocytes by PMA or other stimuli makes these cells acquire a macrophage-like phenotype that mimics primary human macrophages (TEDESCO *et al*., 2018). Takashiba *et al.* (1999) showed that, following incubation with 200 nM PMA for 20 h, THP-1 cells adhered and expressed morphological characteristics of macrophages; then, cells were washed and received the addition of 100 ng mL^{-1} LPS. The authors evaluated the kinetics of TNF-α secretion during 6 h and observed a peak at 4 h, followed by a decline. NF-κB in the cytoplasm of differentiated THP-1 cells was translocated into the nucleus within 30 min of LPS stimulation. Translocation preceded the peak in TNF-α transcription rate (TAKASHIBA *et al*., 1999). LPS acts as a prototypical M1 stimulus (inflammatory stimulus) *in vitro*, causing macrophage activation and polarization, resulting in stimulation of proinflammatory mediators and high levels of proinflammatory cytokines (DIERICHS *et al*., 2018). Kim and collaborators (2010) used THP-1 cells that were differentiated with 100 nM PMA for 72 h and stimulated with 1000 ng/mL LPS for 24 h. The authors observed an increase in TNF-α, IL-1β, and IL-6 levels and gene expression. In accordance with literature data, the results of the current study showed an increase in *IL6* and *TNFA* expression in THP-1 macrophages after 4 h of LPS treatment as well as an increase in IL-6 and TNF-α levels in proinflammatory THP-1 supernatant.

HPLC-UV analysis showed that Kyn levels were increased in the culture supernatant of A172 and T98G cells treated with proinflammatory THP-1 supernatant. This result agrees partially with a previous *in vitro* study showing that IDO expression and activity is mediated by combined IL-6, TNF-α, and IL-1β action (FUJIGAKI *et al*., 2006).

Control solutions were prepared by addition of LPS at concentrations used to stimulate THP-1 cells to investigate whether LPS can induce IDO activity in A172 and T98G cells, which would lead to the release of Kyn in culture medium. Previous *in vitro* studies demonstrated that LPS induces IDO expression in dendritic cells and primary murine microglial cells (JUNG *et al*., 2007; WANG *et al.*, 2010). Addition of LPS to culture medium did not influence Kyn/Trp ratio or Kyn levels, thus, it was used as negative control.

It has been demonstrated that A172 and T98G cells express IDO-1/2 and respond to IFN-γ dependently or independently, resulting in Kyn accumulation in cell supernatants (TOURINO *et al*., 2013; MIYAZAKI *et al*., 2009). A high supernatant Kyn/Trp ratio is indicative of increased intracellular IDO expression and activation; this enzyme catalyzes Trp oxidation, as observed here in both glioma cell lines. We found that basal Kyn levels were markedly higher in A172 cells than in T98G cells. This might be attributed to TDO expression and activity in A172 cells, contributing to the formation of a pool of Kyn (YANG *et al*., 2019). T98G cells, on the other hand, only express IDO, explaining the lower basal levels of Kyn (JULIO, 2016). Thus, further experiments on the Zn-dependency of the Kyn pathway were carried out using T98G cells only.

The following investigations were aimed at determining the sensitivity of the two human glioma cell lines to intracellular free Zn depletion, induced by TPEN. In the current study, the toxic concentration of TPEN to A172 and T98G cells was found to be 3 μM. These findings are similar to those reported by Münnich *et al*. (2016), who found EC_{50} values of 2.5 μM for TPEN on A172 cells incubated for 24 h. Different from these findings, Ollig *et al*. (2016) observed that 3 μM TPEN was nontoxic to THP-1 monocytes.

Cousins *et al*. (2003) remarked that acute Zn deprivation is commonly used to identify genes directly regulated by intracellular free Zn in THP-1 cells. In an effort to investigate the indirect effects of Zn on THP-1 gene expression and monocyte function, Mazzatti *et al*. (2008) developed a method that relies on longer incubation times to deplete labile Zn. In this study, the goal was to investigate the role of Zn deprivation in acute and long-term metabolic and behavioral processes and its effects on the Kyn–Trp pathway in T98G human glioma cells. It was found that 2 and 4 h of preincubation of T98G cells with TPEN produced a considerable decrease in cell viability; therefore, the results of Kyn release and Trp consumption for the acute

incubation period were discarded. T98G cells preincubated for 24 h showed a viability comparable to that of controls; thus, Kyn and Trp data were considered valid. The results indicated that Zn depletion had no effect on T98G Kyn/Trp breakdown. Because IDO is an iron-containing enzyme, reduced iron levels may downregulate IDO expression and activity (JOHNSON, 2001). A study conducted by Tanaka *et al*. (2013) examined the association of peripheral IDO activity with serum Kyn/Trp ratio and levels of trace elements such as selenium and Zn in hemodialysis patients. No relationship was found between peripheral Kyn/Trp ratio (an indicator of IDO activity) and total serum Zn.

The next phase of the *in vitro* study was designed to investigate the effects of Zn on LPS-stimulated THP-1 macrophages. As mentioned in the literature review, the most exciting findings in Zn biochemistry is perhaps its role as a second messenger in immune cells. A growing number of signaling pathways were found to involve Zn signals, including pathways for immune cell activation (HAASE and RINK, 2014a). Several *in vitro* studies investigated the ability of intracellular free Zn to modulate the effects and production of numerous proinflammatory cytokines (von BULOW *et al*., 2007; BAO *et al*., 2003). Experiments including a Zn deprivation step, in which THP-1 macrophages were treated with TPEN and activated with LPS, demonstrated that Kyn concentrations and Kyn/Trp ratio were significantly higher in T98G medium following treatment with supernatant from LPS-stimulated Zn-deficient THP-1 macrophages as compared with medium from cells treated with supernatant from LPS-stimulated Zn-adequate macrophages.

Given the importance of signals mediated by free Zn^{2+} for signal transduction in monocytes and macrophages (HAASE and RINK, 2007), fluorescent probe assays were performed to investigate the impact of intracellular free Zn on THP-1 macrophages. The functional principle of fluorescent probes is based on the binding of the analyte to a metal-specific binding site, which alters the optical properties of the attached fluorophore (ALKER and HAASE, 2020). Free Zn concentrations in the high picomolar to low nanomolar range are sufficiently high to allow detection by membrane-permeable fluorescent Zn probes (MARET, 2015). In this study, the free Zn concentration of THP-1 cells was determined using two Zn-selective fluorescent probes, Zinpyr-1 and FluoZin3-AM. Zinpyr-1 is a membrane-permeant fluorescent sensor for Zn with high selectivity and affinity (BURDETTE *et al*., 2001). FluoZin-3AM is a well-suited probe because it is easily loaded into cells in the form of an acetoxymethyl ester and is retained during measurements (LI *et al*., 2009). The formula introduced by Grynkiewicz and coworkers (GRYNKIEWICZ *et al*., 1985) allows estimating F_{max} and F_{min} from the concentration of free Zn detected when Zn and TPEN are used, respectively (HAASE

et al., 2006; ALKER and HAASE, 2020). Thus, even though FluoZin3-AM (K_d = 8.9 nM) has a lower affinity for Zn than Zinpyr-1 (K_d = 0.7 ± 0.1 nM).

Calculated free Zn levels were about 2.5 nM in THP-1 cells incubated with FluoZin-3AM and about 0.08 nM in cells incubated with Zinpyr-1. These results are consistent with previous findings that showed free Zn concentrations of 2.5 nM and 4.4 nM in peripheral blood monocytes and lymphocytes, respectively, incubated with FluoZin-3AM (HAASE *et al*., 2008). As intracellular free Zn participates in signal transduction and acts as a second messenger in immune cells, alterations in intracellular free Zn concentrations are expected to occur in response to LPS stimulation. Accordingly, THP-1 macrophages loaded with Zinpyr-1 or FluoZin-3AM showed a rapid rise in free Zn after 2 min of LPS exposure. Treatment with the Zn chelator TPEN at 3 or 20 μM confirmed the specificity of the FluoZin-3AM signal observed at 2 min after treatment, inducing a fast decline in free Zn levels. These results are in agreement with those reported by Haase *et al*. (2008), who found that the maximal Zn signal in RAW 264.7 murine macrophages occurred within 2 min of LPS stimulation.

Zn plays an essential role in the release of proinflammatory cytokines. Free Zn has been found to act either as a negative or a positive regulator of NF-κB activation depending on the cell model (FOSTER and SAMMAN, 2012). von Bülow *et al*. (2007) investigated the mechanism by which Zn-mediated elevation of cellular cGMP affects signal transduction to suppress TNF-α synthesis in human monocytes. Upon binding to LPS, TLR4 complexes with CD-14 and MD-2 and triggers the initiation of two pathways, one dependent and the other independent of MyD88 (ZHOU *et al.*, 2020). The MyD88-indepdent pathway leads to the production of proinflammatory cytokines via NF-κB and is activated by fast Zn signals, which occur within seconds to minutes of receptor binding (HAASE and RINK, 2014). Induction of the MyD88-dependent pathway involves phosphorylation and activation of IRAK. IRAK-1, together with TNF receptor-associated factor 6, activates the IκB–IKK complex, which phosphorylates NF-κB. NF-κB then forms a heterodimer with p65/p50 and is translocated to the cell nucleus, where it binds to promoters of inflammatory genes, increasing the expression and release of inflammatory cytokines such as IL-6 and TNF-α (JIALAL *et al.*, 2014). In agreement with these findings, the current results showed an increase in both *IL6* and *TNFA* gene expression in THP-1 macrophages at 4 h after LPS-treatment. Subsequently, TLR4–TIRAP–MyD88 the receptor complex is internalized and binds to TRAM and TRIF, inducing the delayed activation of NF-κB and the phosphorylation of interferon regulatory factor 3 (IRF3). Zn signaling can inhibit IRF3 phosphorylation and thus prevent IFN-β secretion. A study using RAW 264.7 murine macrophages showed that the transcription of TRIF-dependent

genes, such as *Ifnb* and the *Ifnb*–induced genes *Cd80* and *Cd86*, are enhanced by TPEN chelation of intracellular Zn^{2+} (BRIEGER *et al.*, 2013). This investigation showed that *IFNB* was expressed both in Zn-deficient and -adequate LPS-stimulated THP-1 macrophages. Previous observations revealed that Zn deficiency reduces IL-6 and TNF-α production in peripheral human monocytes (MAYER *et al*., 2014). On the other hand, Wong *et al.* (2013) found that Zn deficiency increased the production of TNF-α and IL-1β in LPS-stimulated Zn-deficient THP-1 cells (WONG *et al.*, 2013). In the present study, supernatant from LPS-stimulated Zn-deficient THP-1 macrophages had significantly higher levels of IL-6 than supernatant from Zn-adequate cells. Overall, findings of proinflammatory cytokine release in Zn-insufficient states are controversial and may depend on the cell line, experimental conditions, and duration of Zn depletion (MAARES and HAASE, 2016).

One of the most interesting results was the increase in *IFNG* expression in LPS-stimulated Zn-deficient THP-1 macrophages. IFN-γ is the predominant proinflammatory cytokine implicated in the induction of IDO, as shown in monocytes, macrophages, and microglial cells (CAMBPELL *et al*., 2014). It is suggested that increased *IFNG* expression and increased IL-6 supernatant levels in LPS-stimulated Zn-deficient THP-1 macrophages may be potential stimulators of the Kyn/Trp pathway by promoting IDO expression and activity in T98G cells, leading to the conversion of Trp into Kyn. This study reports, for the first time, an increase in Kyn/Trp breakdown in T98G cells induced by supernatant obtained from LPS-stimulated THP-1 macrophages maintained under Zn-deficient conditions. This study also demonstrated the relationship between changes in proinflammatory cytokine expression, particularly in *IFNG* expression and increased IL-6 protein release at the metabolite level. These results can provide essential insights into the role of Zn in the Kyn–Trp pathway and its association with inflammation and neurological pathogenesis.

7 CONCLUSIONS

In conclusion, *in vivo* experiments showed that mice fed fat-rich diets (HFD and HFD-ZD) had increased body weight gain, WAT hypertrophy and expansion, and, as a consequence, increased serum leptin levels and exacerbated macrophage infiltration into WAT. HFD groups also showed lower serum Trp and Kyn levels, but no differences were observed in peripheral Kyn/Trp breakdown. In the splash test, mice fed HFD-ZD exhibited abnormalities in motivational behaviors suggestive of anhedonia, a core symptom of depression. Two weeks of fluoxetine treatment reversed anhedonic-like behaviors, decreased serum leptin, and increased serum adiponectin in mice fed HFD-ZD. The first conclusion drawn from the *in vivo* study was that Zn did not have a direct effect on peripheral Kyn/Trp breakdown. However, exposure of glioblastoma cells to supernatant from LPS-stimulated THP-1 macrophages in a Zn-deficient state produced secondary effects on the Trp–Kyn pathway, as indicated by an increase in Kyn levels and Kyn/Trp ratio in T98G cell supernatant. RT-PCR revealed that *IL6*, *TNFA*, and *IFNG* were expressed in LPS-stimulated THP-1 macrophages, both under Zn-adequate and -deficient conditions. Another finding was that Zn deficiency promoted an increase in IL-6 levels in supernatant from LPS-stimulated Zn-deficient THP-1 macrophages as compared Zn-adequate conditions. It is suggested that these cytokines are involved in potentiating IDO expression and activation in T98G cells.

Overall, the *in vivo* results demonstrated that Zn deficient-HFD mice showed anhedonic-like behaviors, and fluoxetine treatment reversed such behaviors. Moreover, the *in vitro* study revealed an increase in Kyn/Trp breakdown in T98G cells induced by supernatant obtained from LPS-stimulated THP-1 macrophages maintained under Zn-deficient conditions. The current results provide evidence that obesity associated with Zn deficiency may increase vulnerability to immune-mediated depressive symptoms.

8 OUTLOOK

Further investigations of the relationship between Zn deficiency and low-grade inflammation, a well-characterized state of obesity, are needed to bridge the knowledge gaps on the topic. In line with the *in vivo* and *in vitro* findings of this thesis, future studies should aim to:

- Investigate the impact of HFD-ZD on the hippocampus and hypothalamus of mice by determining the expression of *Il6*, *Ifng*, *Tnfa*, and *Ido1*.
- Determine Kyn and Trp levels and Kyn/Trp ratio in T98G cells treated with monoclonal anti-IFN-γ antibody and supernatant from LPS-stimulated Zn-deficient THP-1 macrophages.
- Quantify Kyn catabolites, such as KYNA and QUIN, in culture medium using the model developed in this *in vitro* study, which requires LC–mass spectrometry.
- Determine KYNA/QUIN ratio in culture medium using the developed *in vitro* model and investigate its potential as a neuroprotective index, in which low values indicate inflammation-induced pathology.

GRAPHICAL ABSTRACT

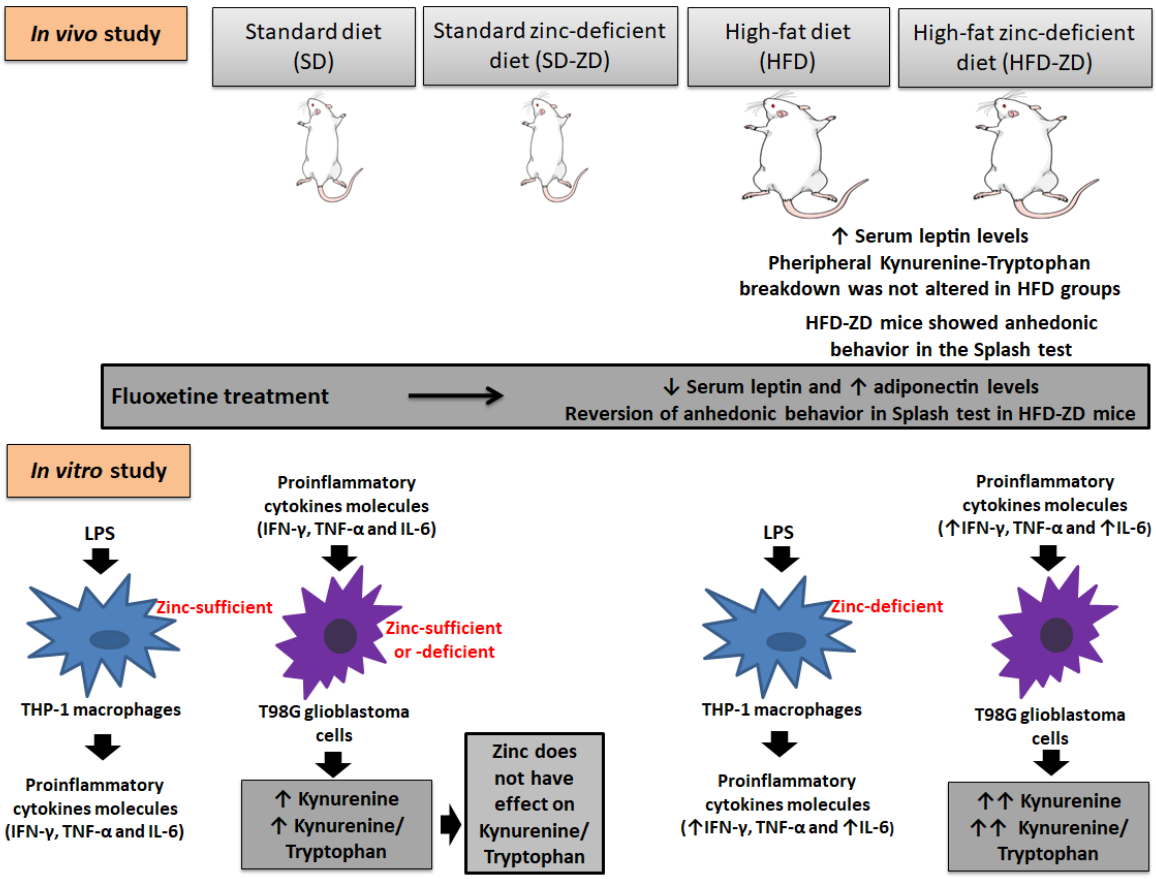

SUPPLEMENTAL INFORMATION

Supplemental Table 1. Ingredient composition (g/kg diet) of experimental diets fed to mice in the *in vivo* study

Ingredient	**SD**	**SD-ZD**	**HFD**	**HFD-ZD**
Corn starch	533	533	193.4	193.4
Sugar cane	100	100	133.6	133.6
Albumin	220	220	187	187
Corn oil	40	40	53	53
Pork fat	-	-	300	300
Cellulose	50	50	66.8	66.8
Minerals	42.2	42.2	46.8	46.8
Vitamins	10.5	10.5	13.4	13.4
L-Cystine	1.8	1.8	2.4	2.4
Choline bitartrate	2.5	2.5	3.6	3.6
Energy (kcal/g)	3.5	3.5	5.2	5.2

SD, standard diet; SD-ZD, standard zinc-deficient diet; HFD, high-fat diet; HFD-ZD, high-fat zinc-deficient diet. Diets were formulated in accordance with American Institute of Nutrition guidelines (REEVES *et al*., 1993).

Supplemental Table 2. Vitamin composition of experimental diets fed to mice in the *in vivo* study

Vitamin	**Content (g/kg diet)**
Nicotinic acid	3.00
Calcium pantothenate	1.60
Pyridoxine-HCl	0.70
Thiamine-HCl	0.60
Riboflavin	0.60
Folic acid	0.20
D-Biotin	2.00
Vitamin B12	2.50
Vitamin E	5.00
Vitamin A	0.80
Vitamin D_3	0.25
Vitamin K	0.70
Excipient	974.85

Supplemental Table 3. Mineral composition (g/kg diet) of experimental diets fed to mice in the *in vivo* study

Mineral salt	**SD and HFD**	**SD-ZD and HFD-ZD**
Anhydrous calcium carbonate	142.9	142.9
Potassium phosphate monobasic	102.8	102.8
Sodium chloride	29.4	29.4
Potassium citrate	39.0	28.0
Potassium sulphate	46.6	46.6
Magnesium oxide	24.0	24.0
Ferric citrate	6.0	6.0
Zinc carbonate	1.65	<0.004
Manganese carbonate	0.6	0.6
Cupric carbonate	0.3	0.3
Potassium iodate	0.01	0.01
Sodium metasilicate nonahydrate	1.4	1.4
Potassium and chromium sulfate	0.2	0.2
Lithium chloride	0.002	0.002
Boric acid	0.02	0.02
Sodium fluoride	0.03	0.03
Nickel carbonate	0.02	0.02
Ammonium vanadate	0.02	0.02
Excipient	212.646	209.8

SD, standard diet; HFD, high-fat diet; SD-ZD, standard zinc-deficient diet; HFD-ZD, high-fat zinc-deficient diet.

Supplemental Table 4. Leptin, adiponectin, tryptophan and kynurenine calibration curves of the *in vivo* study

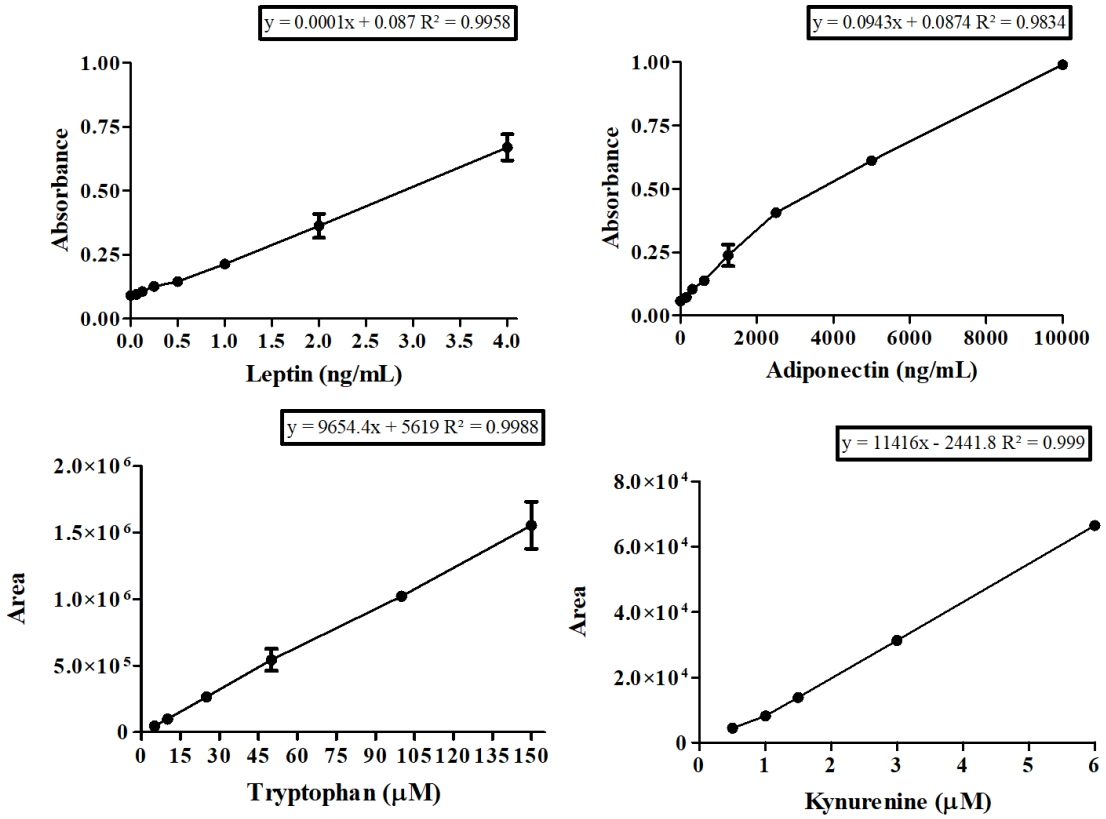

Supplemental Table 5. Tryptophan, kynurenine, IL-6 and TNF-α calibration curves of the *in vitro* study

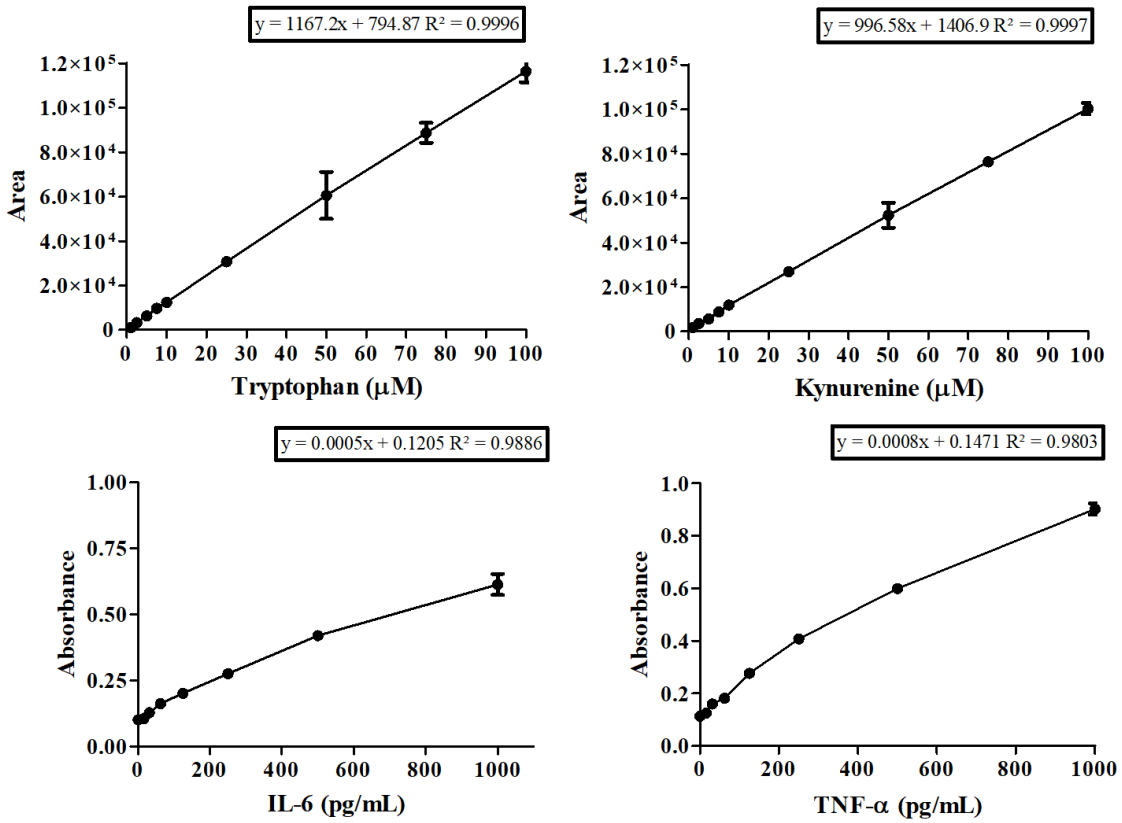

DECLARATION OF AUTHORSHIP

I hereby declare that this thesis has been written by myself, independently and without the help of third parties. I have not used any other tools or references except for those cited in this work.

The work has not been presented in the context of any other examination procedure.

I have read and understood the underlying doctoral degree regulation of the Faculty III Process Science of the Technische Universität Berlin and Post-graduation Program in Pharmacy of the Federal University of Santa Catarina.

Florianópolis, 29.01.2021

_____

Louise Rubia Probst Purnhagen

REFERENCES

AGUDELO, L. Z., T. *et al*. Skeletal muscle PGC-1α1 modulates kynurenine metabolism and mediates resilience to stress-induced depression. *Cell,* v. 159, i. 1, p. 33-45, sept/2014. Available from: <https://doi.org/10.1016/j.cell.2014.07.051>.

AGUS, A. *et al*. Gut Microbiota Regulation of Tryptophan Metabolism in Health and Disease. *Cell Host & Microbe*, v. 23, i. 6, p. 716-724, 2018. Available from: <https://doi.org/10.1016/j.chom.2018.05.003>.

ALKER, W. *et al*. A Zinpyr-1-based Fluorimetric Microassay for Free Zinc in Human Serum. *International journal of molecular sciences,* v. 20, i. 16, p. 4006, Aug/2019. Available from: <https://doi.org/10.3390/ijms20164006>.

ALKER, W., HAASE, H. Comparison of Free Zinc Levels Determined by Fluorescent Probes in THP1 Cells Using Microplate Reader and Flow Cytometer. *Biol Trace Elem Res*. 2020. Available from: <https://doi.org/10.1007/s12011-020-02355-w>.

AL-SUHAIMI, E. A.; SHEHZAD, A. Leptin, resistin and visfatin: the missing link between endocrine metabolic disorders and immunity. *Eur J Med Res*, v.18, i. 1, p.12, may/2013. Available from: <https://doi.org/10.1186/2047-783X-18-12>.

AMITANI, M. *et al*. The role of leptin in the control of insulin-glucose axis. *Frontiers in Neuroscience*, v. 7, p. 51, 2013. Available from: <https://doi.org/ 10.3389/fnins.2013.00051>.

ANDRÉ, C., *et al*. Diet-induced obesity progressively alters cognition, anxiety-like behavior and lipopolysaccharide-induced depressive-like behavior: focus on brain indoleamine 2,3-dioxygenase activation. *Brain Behav Immun,* v. 41, p.10-21. 2014. Available from: <https://doi.org/10.1016/j.bbi.2014.03.012>.

APPARI, M., K. M. CHANNON, AND E. MCNEILL. Metabolic Regulation of Adipose Tissue Macrophage Function in Obesity and Diabetes. *Antioxid Redox Signal*, v. 29, i. 3, p. 297-312. 2018. Available from: <https://doi.org/10.1089/ars.2017.7060>.

ARNONE, D., S. Role of Kynurenine pathway and its metabolites in mood disorders: A systematic review and meta-analysis of clinical studies. *Neurosci Biobehav Rev,* v. 92, p. 477-485. 2018. Available from: <https://doi.org/10.1016/j.neubiorev.2018.05.031>.

ASAKAWA, A., *et al*. Antagonism of ghrelin receptor reduces food intake and body weight gain in mice. *Gut*, v. 52, i., 7, p. 947-52. 2003. Available from: <https://doi.org/10.1136/gut.52.7.947>.

ATKINSON, R. L., *et al*. Plasma zinc and copper in obesity and after intestinal bypass. *Ann Intern Med,* v. 89, i. 4, p. 491-3. 1978.

AVTANSKI, D. *et al*. Characterization of inflammation and insulin resistance in high-fat diet-induced male C57BL/6J mouse model of obesity. *Animal Model Exp Med*, v. 2, p.252– 258, 2019. Available from: <https://doi.org/10.1002/ame2.12084>.

BADAWY, A. and KYNURENINE, A. Pathway of Tryptophan Metabolism: Regulatory and Functional Aspects. *Int J Tryptophan Res*., v.10 2017. Available from: <https://doi.org/10.1177/1178646917691938>.

BAI, Y., and SUN, Q. Macrophage recruitment in obese adipose tissue. *Obes Rev,* v. 16, i. 2, p. 127-36. 2015. Available from: <https://doi.org/10.1111/obr.12242>.

BAO, B., *et al*. Zinc modulates mRNA levels of cytokines. *Am J Physiol Endocrinol Metab,* v. 285, i.5, p. 1095-102. 2003. Available from: <https://doi.org/10.1152/ajpendo.00545.2002>.

BARRETT, P. MERCER, J. G. MORGAN, P. J. Preclinical models for obesity research. *Disease Models & Mechanisms*, v. 9, p.1245-1255, 2016. Available from: <https://doi.org/10.1242/dmm.026443>.

BAQAI N., WILDING J.P.H. Pathophysiology and aetiology of obesity. *Medicine United Kingdom*, v. 43, i.2, p. 73-76, 2015. Available from: <https://doi.org/10.1016/j.mpmed.2014.11.016>.

BAUNE BT., *et al*. Inflammatory biomarkers predict depressive, but not anxiety symptoms during aging: the prospective Sydney Memory and Aging Study. *Psychoneuroendocrinology*, v. 37, p. 1521–1530. 2012.

BAY-RICHTER, *et al*. A role for inflammatory metabolites as modulators of the glutamate N-methyl-D-aspartate receptor in depression and suicidality. *Brain Behav Immun,* v. 43, p.110-7. 2015. Available from: <https://doi.org/10.1016/j.bbi.2014.07.012>.

BEDIZ, C. S., BALTACI A. K., and MOGULKOC R. 2003. Both zinc deficiency and supplementation affect plasma melatonin levels in rats. *Acta Physiol Hung,* v. 90, i. 4, p. 335-9. 2015. Available in: <https://doi.org/10.1556/APhysiol.90.2003.4.7.>.

BENOMAR Y., and TAOUIS M. Molecular Mechanisms Underlying Obesity-Induced Hypothalamic Inflammation and Insulin Resistance: Pivotal Role of Resistin/TLR4 Pathways. *Front Endocrinol (Lausanne*), v. 10, i.140, Mar/2019 Available in: <https://doi.org/10.3389/fendo.2019.00140>.

BERRY, D. C., *et al.* The developmental origins of adipose tissue. *Development,* v. 140, i. 19, p.3939-49. 2017. Available from: <https://doi.org/10.1242/dev.080549>. 2013.

BHAT, Z. F. *et al*. Obesity and neurological disorders: Dietary perspective of a global menace. *Crit Rev Food Sci Nutr*, p. 1-17, Available from: <https://doi.org/10.1080/10408398.2017.1404442>.

BIJLAND, S., MANCINI S. J., and SALT I. P. Role of AMP-activated protein kinase in adipose tissue metabolism and inflammation. *Clin Sci (Lond),* v. 124, i. 8, p. 491-507. 2013. Available from: <https://doi.org/10.1042/CS20120536>.

BLÜHER, M. Obesity: global epidemiology and pathogenesis. *Nat Rev Endocrinol*. 2019. Available from: <https://doi.org/10.1038/s41574-019-0176-8>.

BRANDACHER, G., *et al.* Bariatric Surgery Cannot Prevent Tryptophan Depletion Due to

Chronic Immune Activation in Morbidly Obese Patients. *OBES SURG,* v. 16, p. 541–548, 2006. Available from: <https://doi.org/10.1381/096089206776945066>.

BRASIL, MINISTÉRIO DA SAÚDE SECRETARIA DE VIGILÂNCIA EM SAÚDE. Vigitel: vigilância de fatores de risco e proteção para doenças crônicas por inquérito telefônico. edited by Vigitel. Brasília. 2016.

BRIEGER, A., RINK L., and HAASE H. Differential regulation of TLR-dependent MyD88 and TRIF signaling pathways by free zinc ions. *J Immunol*, v 191, i. 4, p. 1808-17. 2013. Available from: <https://doi.org/10.4049/jimmunol.1301261>.

BUETTNER, R., J. SCHÖLMERICH, and L. C. BOLLHEIMER. High-fat diets: modeling the metabolic disorders of human obesity in rodents. *Obesity (Silver Spring)***,** v. 15, i.4, p.798-808, 2007. Available from: <https://doi.org/10.1038/oby.2007.608>.

BURDETTE, S. C., *et al*. Fluorescent sensors for Zn (2^{+}) based on a fluorescein platform: synthesis, properties and intracellular distribution. *J Am Chem Soc, v.* 123, i. 32, p.7831-41. 2001. Available from: <https://doi.org/10.1021/ja010059l>.

CABALLERO, B. The global epidemic of obesity: an overview. *Epidemiol Rev*, v. 29, i.1-5. 2007. Available from: <https://doi.org/10.1093/epirev/mxm012>.

CAMPBELL, B. M, *et al*. Kynurenines in CNS disease: regulation by inflammatory cytokines. *Front Neurosci,* v. 8, i.12. 2014. Available from: <https://doi.org/10.3389/fnins.2014.00012>.

CAN, A., *et al*. The mouse forced swim test. *J Vis Exp,* v. 59, p. 36-38. 2012. Available from: <https://doi.org/10.3791/3638>.

CAPURON, L. MILLER, A. H. Immune system to brain signaling: Neuropsychopharmacological implications. *Pharmacology & Therapeutics*, v. 130, i. 2, p. 226-238. 2011. Available from: <https://doi.org/10.1016/j.pharmthera.2011.01.014>.

CAPURON, L., RAVAUD, A., NEVEU, P. *et al.* Association between decreased serum tryptophan concentrations and depressive symptoms in cancer patients undergoing cytokine therapy. *Mol Psychiatry*, v. 7, p. 468–473, 2002. Available from: <https://doi.org/10.1038/sj.mp.4000995>.

CASTANON, N., J. LASSELIN, and L. CAPURON. Neuropsychiatric comorbidity in obesity: role of inflammatory processes. *Front Endocrinol (Lausanne),* v. 5, i.74, 2014. Available from: <https://doi.org/10.3389/fendo.2014.00074>.

CARTER, K.P. *et al*. Fluorescent sensors for measuring metal ions in living systems. *Chem Rev,* v. 114, i. 8, p. 4564– 4601. 2014. Available from: <https://doi.org/10.1021/cr400546e>.

CASTOLDI, A., *et al*. The Macrophage Switch in Obesity Development. *Front Immunol*, v. 6, i. 637. 2015. Available from: <https://doi.org/10.3389/fimmu.2015.00637>.

CAWLEY, J. MEYERHOEFER, C. The medical care costs of obesity: An instrumental variables approach. *Journal of Health Economics*, v. 31, i.1, p. 219-230, 2012.

CHASAPIS, C. T., *et al*. Zinc and human health: an update. *Arch Toxicol,* v. 86, v. 4, p. 521-534. 2012. Available from: <https://doi.org/10.1007/s00204-011-0775-1>.

CHAURAND, P. *et al*. Imaging Mass Spectrometry of Intact Proteins from Alcohol-Preserved Tissue Specimens: Bypassing Formalin Fixation. *Journal of Proteome Research*, v. 7, i. 8, p. 3543-3555. 2008. Available from: <https://doi.org/10.1021/pr800286z>.

CHAVES FILHO, A. J. M. *et al*. IDO chronic immune activation and tryptophan metabolic pathway: A potential pathophysiological link between depression and obesity. *Prog Neuropsychopharmacol Biol Psychiatry*, v. 80, p.234-249, 2018. Available from: <https://doi.org/10.1016/j.pnpbp.2017.04.035>.

CHEN, M. *et al.* Zinc in hair and serum of obese individuals in Taiwan. *Am J Clin Nutr.,* v. 48, i. 5, p. 1307-9. 1988. Available from: <https://doi.org/10.1093/ajcn/48.5.1307>.

CINTI, S. The adipose organ. *Prostaglandins Leukot Essent Fatty Acids*, v.73, i.1, p.9-15. 2005. Available from: <https://doi.org/10.1016/j.plefa.2005.04.010>.

COHEN, R. A. Obesity-associated cognitive decline: excess weight affects more than the waistline. *Neuroepidemiology*, v. 34, i.4, p.230-1. 2010. Available from: <https://doi.org/10.1159/000297745>.

COPE, E. C., *et al*. Microglia Play an Active Role in Obesity-Associated Cognitive Decline. *J Neurosci.,* v. 38, i. 41, p. 8889-8904. 2018. Available from: <https://doi.org/10.1523/JNEUROSCI.0789-18.2018>.

COSTARELLI, L. *et al*. Distinctive modulation of inflammatory and metabolic parameters in relation to zinc nutritional status in adult overweight/obese subjects. *J Nutr Biochem*, v. 21 i.5, p. 432-7, 2010. Available from: <https://doi.org/10.1016/j.jnutbio.2009.02.001>.

COUSINS, R. J., *et al*. A global view of the selectivity of zinc deprivation and excess on genes expressed in human THP-1 mononuclear cells. *Proc Natl Acad Sci U S A,* v. 100, i. 12, p.6952-7. 2003. Available from: <https://doi.org/10.1073/pnas.0732111100>.

CUI, H., LÓPEZ, M. and RAHMOUNI, K. The cellular and molecular bases of leptin and ghrelin resistance in obesity. *Nat Rev Endocrinol*, v. 13, p. 338–351 2017. Available from: <https://doi.org/10.1038/nrendo.2016.222>.

CYPESS, A. M. *et al*. Identification and importance of brown adipose tissue in adult humans. *N Engl J Med***,** v. 360, i. 15, p. 1509-17, 2009. Available from: <https://doi.org/10.1056/NEJMoa0810780>.

D'AUDIFFRET, A.C., *et al*. Depressive behavior and vascular dysfunction: a link between clinical depression and vascular disease. *Journal of Applied Physiology*., v. 108, p. 1041-1051. 2010.

DANTZER R, *et al*. From inflammation to sickness and depression: when the immune system subjugates the brain. *Nat Rev Neurosci*., v. 9, i. 1, p. 46-56. 2008. Available from: <https://doi.org/10.1038/nrn2297>.

DANTZER, R. *et al*. Inflammation-associated depression: From serotonin to kynurenine. *Psychoneuroendocrinology*, v. 36, i. 3, p. 426-436, 2011. Available from: <https://doi.org/10.1016/j.psyneuen.2010.09.012>.

DANTZER, R., and WALKER A. K. Is there a role for glutamate-mediated excitotoxicity in inflammation-induced depression? *J Neural Transm (Vienna),* v. 121, i. 8, p. 925-32. 2014. Available from: <https://doi.org/10.1007/s00702-014-1187-1>.

DARCY, C. J., *et al*. An observational cohort study of the kynurenine to tryptophan ratio in sepsis: association with impaired immune and microvascular function. *PLoS One,* v., i. 6. 2011. Available from: <https://doi.org/10.1371/journal.pone.0021185>.

DE GIT, K.C.G. and ADAN, R.A.H. Leptin resistance and inflammation. *Obes Rev*, v 16, p. 207-224. 2015. Available from: <https://doi.org/10.1111/obr.12243>.

DE LUIS, D. A., *et al*. Micronutrient status in morbidly obese women before bariatric surgery. *Surg Obes Relat Dis,* v. 9, i. 2, p. 323-7. 2013. Available from: <https://doi.org/10.1016/j.soard.2011.09.015>.

DE OLIVEIRA, M. L., SANTOS L. M., and da SILVA E. N. Direct healthcare cost of obesity in brazil: an application of the cost-of-illness method from the perspective of the public health system in 2011. *PLoS One,* v. 10, i. 4. 2015. Available from: <https://doi.org/10.1371/journal.pone.0121160>.

DE OLIVEIRA, S., *et al.* Zinc Supplementation Decreases Obesity-Related Neuroinflammation and Improves Metabolic Function and Memory in Rats. *Obesity*, v. 29, p. 116-124. 2021. Available from: <https://doi.org/10.1002/oby.23024>.

DE SOUZA, C. T., *et al*. Consumption of a fat-rich diet activates a proinflammatory response and induces insulin resistance in the hypothalamus. *Endocrinology,* v. 146, i. 10, p. 4192-9. 2005. Available from: <https://doi.org/10.1210/en.2004-1520>.

DETANICO, B.C., *et al*., Antidepressant-like effects of melatonin in the mouse chronic mild stress model. *European Journal of Pharmacology*, v. 607, p. 121-125. 2009.

DI MARTINO, G., *et al*. Relationship between zinc and obesity. *J Med,* v. 24, i. 2-3, p.177-83. 1993.

DIERICHS, L., KLOUBERT V., and RINK L. Cellular zinc homeostasis modulates polarization of THP-1-derived macrophages. *Eur J Nutr.,* v. 57, i. 6, p. 2161-2169. 2018. Available from: <https://doi.org/ 10.1007/s00394-017-1491-2>.

DOBOSZEWSKA, U. *et al.* Antidepressant activity of fluoxetine in the zinc deficiency model in rats involves the NMDA receptor complex. *Behav Brain Res*, v. 287, p. 323-30, 2015. Available from: https://www.ncbi.nlm.nih.gov/pubmed/25845739>.

DREWNOWSKI, A. SPECTER, SE. Poverty and obesity: the role of energy density and energy costs. *The American Journal of Clinical Nutrition*. v. 79, i. 1, p. 6–16, 2004. Available from: <https://doi.org/10.1093/ajcn/79.1.6>.

DULAWA, S.C., *et al*., Effects of chronic fluoxetine in animal models of anxiety and depression. *Neuropsychopharmacology,* v. 29, p.1321–1330. 2004.

DUNLOP B. W, and NEMEROFF, C. B. The role of dopamine in the pathophysiology of depression. *Arch Gen Psychiatry*, v. 64, p. 327–37, 2007. Available from: <https://doi.org/10.1001/archpsyc.64.3.327>.

ENRIORI, P. J., *et al*. Leptin resistance and obesity. *Obesity (Silver Spring),* v. 14, Suppl 5, p. 254S-258S, 2006. Available from: <https://doi.org/10.1038/oby.2006.319>.

FAROOQI, S., and O'RAHILLY, S. Genetics of Obesity in Humans. *Endocrine Reviews*, v. 27, i. 7, p. 710–718, December 2006. Available from: <https://doi.org/10.1210/er.2006-0040>.

FOSTER, M., and SAMMAN, S. Zinc and regulation of inflammatory cytokines: implications for cardiometabolic disease. *Nutrients,* v. 4, i. 7, p. 676-94. 2012. Available from: <https://doi.org/10.3390/nu4070676>.

FREDERICKSON, C. J., KOH, J. Y. and BUSH A. I. The neurobiology of zinc in health and disease. *Nat Rev Neurosci., v.* 6, i. 6, p. 449-62. 2005. Available from: <https://doi.org/10.1038/nrn1671>.

FREITAS, A. E., *et al*. Fluoxetine modulates hippocampal cell signaling pathways implicated in neuroplasticity in olfactory bulbectomized mice. *Behav Brain Res,* v. 237, p.176-84. 2013. Available from: <https://doi.org/10.1016/j.bbr.2012.09.035>.

FRIEDMAN, J. M., and HALAAS, J. L. Leptin and the regulation of body weight in mammals. *Nature, v.* 395, i. 6704, p. 763-70. 1998. Available from: <https://doi.org/10.1038/27376>.

FUJIGAKI, H., *et al.* The signal transducer and activator of transcription 1alpha and interferon regulatory factor 1 are not essential for the induction of indoleamine 2,3-dioxygenase by lipopolysaccharide: involvement of p38 mitogen-activated protein kinase and nuclear factor-kappaB pathways, and synergistic effect of several proinflammatory cytokines. *J. Biochem*., v. 139, p. 655–662. 2006. Available from: <https://doi.org/10.1093/jb/mvj072>.

FRUH, S. M. Obesity: Risk factors, complications, and strategies for sustainable long-term weight management. *J Am Assoc Nurse Pract,* v. 29, i. 1, p. 3-14. 2017. Available from: <https://doi.org/10.1002/2327-6924.12510>.

FUKADA, *et al*. Zinc homeostasis and signaling in health and diseases: Zinc signaling. *J Biol Inorg Chem.,* v. 16, i. 7, p. 1123-34. 2011. Available from: <https://doi.org/10.1007/s00775-011-0797-4>.

FUKADA, T., & KAMBE, T. Welcome to the World of Zinc Signaling. *International journal of molecular sciences*, v. 19, i. 3, p. 785. 2018. Available from: <https://doi.org/10.3390/ijms19030785>.

FULTON, S. Appetite and reward. *Front. Neuroendocrinol*. v. 31, p.85–103, 2010. Available from: <https://doi.org/10.1016/j.yfrne.2009.10.003>.

GAO, H. *et al*. The Role of Zinc and Zinc Homeostasis in Macrophage Function. *Journal of*

Immunology Research, v. 11 2018. Available from: <https://doi.org/10.1155/2018/6872621>.

GARCÍA, O. P. *et al*. Impact of micronutrient deficiencies on obesity. *Nutr Rev*, v. 67, i.10, p. 559-72, 2009. Available from: <https://doi.org/10.1111/j.1753-4887.2009.00228.x>.

GIARD, D. J., *et al*. *In vitro* cultivation of human tumors: establishment of cell lines derived from a series of solid tumors. *J Natl Cancer Inst.,* v. 51, i. 5, p. 1417-23. 1973. Available from: <https://doi.org/10.1093/jnci/51.5.1417>.

GOLDE, W. T., GOLLOBIN, P. and RODRIGUEZ, L. L. A rapid, simple, and humane method for submandibular bleeding of mice using a lancet. *Lab Anim (NY),* v. 34, i. 9, p. 39-43. 2005. Available from: <https://doi.org/10.1038/laban1005-39>.

GOMES, D. C. K., *et al.* Trends in obesity prevalence among Brazilian adults from 2002 to 2013 by educational level. *BMC Public Health*, v. 19, i.1, p. 965. 2019. Available from: <https://doi.org/10.1186/s12889-019-7289-9>.

GONZÁLEZ-MUNIESA, P., *et al*. Obesity. *Nat Rev Dis Primers,* v. 3. 2017. Available from: <https://doi.org/10.1038/nrdp.2017.34>.

GOSTNER, J. M., *et al*. Tryptophan Metabolism and Related Pathways in Psychoneuroimmunology: The Impact of Nutrition and Lifestyle. *Neuropsychobiology* , v. 79, i. 1, p. 89-99. 2020. Available from: <https://doi.org/10.1159/000496293>.

GRANT, R. S., *et al.* Induction of indolamine 2,3-dioxygenase in primary human macrophages by human immunodeficiency virus type 1 is strain dependent. *J Virol,* v. 74, i. 9, p.4110-5. 2000. Available from: <https://doi.org/10.1128/jvi.74.9.4110-4115.2000>.

GREENBERG, A. S., *et al*. The role of lipid droplets in metabolic disease in rodents and humans. *J Clin Invest*, v. 121, i. 6, p. 2102-10. 2011. Available from: <https://doi.org/10.1172/JCI46069>.

GRØNLI, O. *et al*. Zinc deficiency is common in several psychiatric disorders. *PloS One,* v. 8,12 e82793. 2013. Available from: <doi:10.1371/journal.pone.0082793>.

GRUEN M.L., HAO M., PISTON D.W., HASTY A.H. Leptin requires canonical migratory signaling pathways for induction of monocyte and macrophage chemotaxis. *Am J Physiol Cell Physiol*., v. 293, i. C, p. 1481–8. 2007

GRYNKIEWICZ, G., POENIE, M., and TSIEN, R. Y. A new generation of Ca2+ indicators with greatly improved fluorescence properties. *J Biol Chem,* v. 260, i. 6, p.3440-50. 1985.

GU, Z., *et al.* Body mass index, waist circumference, and waist-to-height ratio for prediction of multiple metabolic risk factors in Chinese elderly population. *Sci Rep,* v. 8, i. 1, p. 385. 2018. Available from: <https://doi.org/10.1038/s41598-017-18854-1>.

GU, K., *et al*. The association between serum zinc level and overweight/obesity: a meta-analysis. *Eur J Nutr* v. 58, p. 2971–2982, 2019. Available from: <https://doi.org/10.1007/s00394-018-1876-x>.

GUILLEMOT-LEGRIS, O., and MUCCIOLI, G. G. Obesity-Induced Neuroinflammation: Beyond the Hypothalamus. *Trends Neurosci,* v. 40, i. 4, p. 237-253. 2017. Available from: <https://doi.org/10.1016/j.tins.2017.02.005>.

GUSTAFSON, B., *et al*. Inflammation and impaired adipogenesis in hypertrophic obesity in man. *Am J Physiol Endocrinol Metab,* v. 297, i. 5, p. E999-E1003. 2009. Available from: <https://doi.org/10.1152/ajpendo.00377.2009>.

HAASE, H., *et al*. Flow cytometric measurement of labile zinc in peripheral blood mononuclear cells. *Anal Biochem,* v. 352, i. 2, p. 222-30. 2006. Available from: <https://doi.org/10.1016/j.ab.2006.02.009>.

HAASE, H., *et al.* Zinc signals are essential for lipopolysaccharide-induced signal transduction in monocytes. *J Immunol*, v. 181, i. 9, p. 6491-502. 2008. Available from: <https://doi.org/10.4049/jimmunol.181.9.6491>.

HAASE, H., and RINK L. Signal transduction in monocytes: the role of zinc ions. *Biometals,* v. 20, i. 3-4, p. 579-85. 2007. Available from: <https://doi.org/10.1007/s10534-006-9029-8>.

HAASE, H., and RINK L. Multiple impacts of zinc on immune function. *Metallomics,* v. 6, i. 7, p. 1175-80. 2014a. Available from: <https://doi.org/10.1039/c3mt00353a>.

HAASE, H., and RINK L. Zinc signals and immune function. *Biofactors,* v. 40, i. 1, p. 27-40. 2014b. Available from: <https://doi.org/10.1002/biof.1114>.

HAASE, H. *et al*. Revised D-A-CH-reference values for the intake of zinc. *Journal of Trace Elements in Medicine and Biology*, v 61. 2020. Available from: <https://doi.org/10.1016/j.jtemb.2020.126536>.

HARIRI, N., GOUGEON, R. and THIBAULT, L. A highly saturated fat-rich diet is more obesogenic than diets with lower saturated fat content. *Nutr Res***,** v. 30, i.9, p.632-43, 2010. Available from: <https://doi.org/10.1016/j.nutres.2010.09.003>.

HARIRI, N. and THIBAULT, L. High-fat diet-induced obesity in animal models. *Nutr Res Rev,* v.23, i.2, p.:270-99, 2010. Available from: <https://doi.org/10.1017/S0954422410000168>.

HAROON, E., *et al.* Associations among peripheral and central kynurenine pathway metabolites and inflammation in depression. *Neuropsychopharmacol*., v. 45, p. 998–1007, 2020. Available from: <https://doi.org/10.1038/s41386-020-0607-1>.

HAUGLAND, R. P. *Handbook of Fluorescent Probes and Research Products*, 8th Ed. Eugene, Oregon, Molecular Probes, 2001.

HEINONEN, Sini. *Adipose Tissue Metabolism in Acquired Obesity*. DOCTORAL PROGRAMME IN BIOMEDICINE, Research Programs Unit, Diabetes and Obesity,University of Helsinki Finland, University of Helsinki. 2016.

HEENEY, D., *et al.* Lactobacillus plantarum bacteriocin is associated with intestinal and systemic improvements in diet-induced obese mice and maintains epithelial barrier integrity in vitro. *Gut Microbes*, v. 10, i. 3, p. 382-397, 2019. Available from:

<https://doi.org/10.1080/19490976.2018.1534513>.

HOTAMISLIGIL, G. S., SHARGILL, N. S., and SPIEGELMAN, B. M. Adipose expression of tumor necrosis factor-alpha: direct role in obesity-linked insulin resistance. *Science,* v. 259, i. 5091, p. 87-91. 1993.

HRUBY, A., and F. B. HU. The Epidemiology of Obesity: A Big Picture. *Pharmacoeconomics*, v.33, i.7, p. 673-89, 2015. Available from: <https://doi.org/10.1007/s40273-014-0243-x>.

HUANG, X. *et al.* Chronic High Dose Zinc Supplementation Induces Visceral Adipose Tissue Hypertrophy without Altering Body Weight in Mice. *Nutrients,* v. 9, i. 10, p. 1138. 2017. Available from: <https://doi.org/10.3390/nu9101138>.

ISINGRINI, E., *et al*. Association between repeated unpredictable chronic mild stress (UCMS) procedures with a high fat diet: a model of fluoxetine resistance in mice. *PLoS One,* v. 5, i. 4. 2010. Available from: <https://doi.org/10.1371/journal.pone.0010404>.

JACKSON, M.J. *Physiology of Zinc: General Aspects.* Edited by In: Mills C.F. (eds) Zinc in Human Biology., *ILSI Human Nutrition Reviews.* London: Springer. 1989.

JENKINS, T. A. *et al*., Influence of Tryptophan and Serotonin on Mood and Cognition with a Possible Role of the Gut-Brain Axis. *Nutrients*, v. 8, n.1, 2016. Available from: <https://doi.org/10.3390/nu8010056>.

JIALAL, I. KAUR, H. DEVARAJ, S. Toll-like Receptor Status in Obesity and Metabolic Syndrome: A Translational Perspective. *The Journal of Clinical Endocrinology & Metabolism*, v. 99, i. 1, p. 39–48, Jan/2014. Available from: <https://doi.org/10.1210/jc.2013-3092>.

JO, J., *et al.* Hypertrophy and/or Hyperplasia: Dynamics of Adipose Tissue Growth. *PLoS Comput Biol,* v. 5, i. 3. 2009. Available from: <https://doi.org/10.1371/journal.pcbi.1000324>.

JOHNSON, S. The possible crucial role of iron accumulation combined with low tryptophan, zinc and manganese in carcinogenesis. *Med Hypotheses,* v. 57. i. 5, p. :539-43. 2001. Available from: <https://doi.org/10.1054/mehy.2001.1361>.

JULIO, A. R. *Desenvolvimento e validação de métodos bioanalíticos para o monitoramento dos produtos das vias metabólicas do triptofano em linhagem celular de glioma humano*. Doctor Degree, Faculdade de Ciências Farmacêuticas São Paulo University. 2016.

JUNG, I.D., *et al*. Different regulation of indoleamine 2,3-dioxygenase by lipopolysaccharide and interferon gamma in murine bone marrow derived dendritic cells. *FEBS Lett*., v. 581, 1449–1456. 2007.

KALTENBERG, J.*et al*. Zinc signals promote IL-2-dependent proliferation of T cells. *Eur J Immunol.*v. 40, i.5, p.1496-503. 2010. doi: 10.1002/eji.200939574. PMID: 20201035

KAMBE, T., *et al*. The Physiological, Biochemical, and Molecular Roles of Zinc Transporters in Zinc Homeostasis and Metabolism. *Physiol Rev.,* v. 95, i. 3, p. 749-84. 2015. Available from: <https://doi.org/10.1152/physrev.00035.2014>.

KANOSKI S.E, *et al*. The effects of a high-energy diet on hippocampal function and blood-brain barrier integrity in the rat. *J Alzheimers Dis*.; v. 21, i. 1, p. 207-219. 2010. Available from: <https://doi.org/10.3233/JAD-2010-091414>.

KASTER, M.P. *et al*. Depressive-like behavior induced by tumor necrosis factor-α in mice. *Neuropharmacology*, v. 62, p.419-426, 2012.

KATO, A., *et al*. Lipopolysaccharide-binding protein critically regulates lipopolysaccharide-induced IFN-beta signaling pathway in human monocytes. *J Immunol*., v. 172, i. 10, p. 6185-94. 2004. Available from: <https://doi.org/10.4049/jimmunol.172.10.6185>.

KIM, J. A., *et al*. Phosphorylated glucosamine inhibits the inflammatory response in LPS-stimulated PMA-differentiated THP-1 cells. *Carbohydr Res.,* v. 345, i. 13, p. 1851-5. 2010. Available from: <https://doi.org/10.1016/j.carres.2010.06.006>.

KING, J. C., *et al*. J. H., & Raiten, D. J. Biomarkers of Nutrition for Development (BOND)-Zinc Review. *The Journal of nutrition*, v. 146, i. 4, p. 858S–885S. 2015. Available from: <https://doi.org/10.3945/jn.115.220079>.

KLEINERT, M. *et al*. Animal models of obesity and diabetes mellitus. *Nat Rev Endocrinol,* v**.** 14, p. 140–162, 2018. Available from: <https://doi.org/10.1038/nrendo.2017.161>.

KLOUBERT, V., and RINK, L. Zinc as a micronutrient and its preventive role of oxidative damage in cells. *Food Funct,* v. 6, i. 10, p. 3195-204. 2015. Available from: <https://doi.org/10.1039/c5fo00630a>.

KOLIAKI, C., LIATIS, S., DALAMAGA, M. *et al*. The Implication of Gut Hormones in the Regulation of Energy Homeostasis and Their Role in the Pathophysiology of Obesity. *Curr Obes Rep.* 2020. Available from: <https://doi.org/10.1007/s13679-020-00396-9>.

KRĘŻEL A, and MARET W. Zinc-buffering capacity of a eukaryotic cell at physiological pZn. *J Biol Inorg Chem.,* v. 11, i. 8, p. 1049/1062. 2006. Available from: <https://doi.org/10.1007/s00775-006-0150-5>.

KWOK, K. H., LAM, K. S. and XU, A. Heterogeneity of white adipose tissue: molecular basis and clinical implications. *Exp Mol Med*, v. 48, p.215, 2016. Available from: <https://doi.org/10.1038/emm.2016.5>.

LAMPRON, A., ELALI, A., and RIVEST, S. Innate immunity in the CNS: redefining the relationship between the CNS and Its environment. *Neuron,* v. 78, i. 2, p. 214.32. 2013. Available from: <https://doi.org/10.1016/j.neuron.2013.04.005>.

LANG, P. *et al*. Effects of different diets used in diet-induced obesity models on insulin resistance and vascular dysfunction in C57BL/6 mice. *Sci Rep,* v. 9, i.1, p.195-56, 2019. Available from: <https://doi.org/10.1038/s41598-019-55987-x>.

LASKEY, M. A. Dual-energy X-ray absorptiometry and body composition. *Nutrition*, v. 12, i. 1, p.45-51, 1996. Available from: <https://doi.org/10.1016/0899-9007(95)00017-8>.

LAUZURICA, N., *et al*. Hypophagia and induction of serotonin transporter gene expression in

raphe nuclei of male and female rats after short-term fluoxetine treatment. *J. Physiol. Biochem*. v. 69, p. 69–74. 2013.

LEE, M. J., WU, Y., and FRIED, S. K. Adipose tissue remodeling in pathophysiology of obesity. *Curr Opin Clin Nutr Metab Care,* v. 13, i. 4, p. 371-6. 2010. Available from: <https://doi.org/10.1097/MCO.0b013e32833aabef>.

LEE, M. J., WU, Y., and FRIED, S. K. Adipose tissue heterogeneity: implication of depot differences in adipose tissue for obesity complications. *Mol Aspects Med*, v. 34, i.1, p.1-11, 2013. Available from: <https://doi.org/10.1016/j.mam.2012.10.001>.

LEE, P., *et al*. High prevalence of brown adipose tissue in adult humans. *J Clin Endocrinol Metab,* v. 96, i. 8, p. 2450-5. 2011. Available from: <https://doi.org/10.1210/jc.2011-0487>.

LEISEGANG, K. Malnutrition and Obesity. *Oxidants, Antioxidants and Impact of the Oxidative Status in Male Reproduction***,** 2019.

Lilly. 2017. Prozac.

LIM, N.C., FREAKE, H.C., and BRÜCKNER, C. Illuminating zinc in biological systems. *Chem Eur J,* v. 11, i. 1, p. 38–49. 2004. Available from: <https://doi.org/10.1002/chem.200400599>.

LIU, M. J. *et al*. Zinc deficiency augments leptin production and exacerbates macrophage infiltration into adipose tissue in mice fed a high-fat diet. *J Nutr*, v. 143, i. 7, p.1036-45, 2013. Available from: <https://doi.org/10.3945/jn.113.175158>.

LIU, D. *et al*. Anti-inflammatory effects of fluoxetine in lipopolysaccharide(LPS)-stimulated microglial cells. *Neuropharmacology*, v. 61, i. 4, p. 592-599. 2011. Available from: <https://doi.org/10.1016/j.neuropharm.2011.04.033>.

LIVAK, K. J., and SCHMITTGEN, T. D. Analysis of relative gene expression data using real-time quantitative PCR and the 2(-Delta Delta C(T)) Method. *Methods,* v. 25, i. 4, p. 402-8. 2001. Available from: <https://doi.org/10.1006/meth.2001.1262>.

LOFFREDA S, *et al.* Leptin regulates proinflammatory immune responses. *FASEB J.,* v. 12, p. 57–65. 1998

LÓPEZ-MUÑOZ, F., and ALAMO, C. Monoaminergic neurotransmission: the history of the discovery of antidepressants from 1950s until today. *Curr Pharm Des.,* v. 15, i. 14, p. 1563-86. 2009. Available from: <https://doi.org/10.2174/138161209788168001>.

LUECKE R, and FRAKER P. The effect of varying dietary zinc levels on growth and antibody-mediated response in two strains of mice. *J Nutr,* v. 109, 1373-6. 1979.

LUO, L., and LIU, M. Adipose tissue in control of metabolism. *J Endocrinol***,** v. 231 i.3, p. R77-R99, 2016. Available from: <https://doi.org/10.1530/JOE-16-0211>.

LUTZ, T. A., and WOODS, S. C. Overview of animal models of obesity. *Current protocols in pharmacology,* Chapter 5, Unit 5.61, 2012. Available from:

<https://doi.org/10.1002/0471141755.ph0561s58>.

MAARES, M., *et al.* The impact of apical and basolateral albumin on intestinal zinc resorption in the Caco-2/HT-29-MTX co-culture model. *Metallomics,* v. 10, i. 7, p. 979-991. 2018. Available from: <https://doi.org/10.1039/c8mt00064f>.

MAARES, M., and HAASE, H. Zinc and immunity: An essential interrelation. *Arch Biochem Biophys,* v. 611, p. 58-65. 2016. Available from: <https://doi.org/10.1016/j.abb.2016.03.022>.

MACHADO, D. G. *et al*. Fluoxetine reverses depressive-like behaviors and increases hippocampal acetylcholinesterase activity induced by olfactory bulbectomy. *Pharmacol Biochem Behav,* v. 103, i. 2, p. 220-9, Dec/2012. Available from: <https://www.ncbi.nlm.nih.gov/pubmed/22960127>.

MADAN, A. K., *et al*. Vitamin and trace mineral levels after laparoscopic gastric bypass. *Obes Surg*, v. 16, i. 5, p. 603-6. 2006. Available from: <https://doi.org/10.1381/096089206776945057>.

MAES M, *et al*. Lower serum zinc in major depression is a sensitive marker of treatment resistance and of the immune/inflammatory response in that illness. *Biological Psychiatry;* v. 42, p. 349–58. 1997.

MAES, M. *et al*. Hypozincemia in depression. *Journal of Affective Disorders*, v. 31, i. 2, p. 135-140. 1994. Available from: <https://doi.org/10.1016/0165-0327(94)90117-1>.

MAHER, T. and CLEGG, M. E. Dietary lipids with potential to affect satiety: Mechanisms and evidence. *Crit Rev Food Sci Nutr*. v. 59 i. 10, p. 1619-1644, 2019. Available from: <https://doi.org/10.1080/10408398.2017.1423277>.

MAKKI, K.; FROGUEL, P.; and WOLOWCZUK, I. Adipose tissue in obesity-related inflammation and insulin resistance: cells, cytokines, and chemokines. *ISRN Inflamm***,** v. 2013, p. 139-239. Dec/2013. Available from: <https://www.ncbi.nlm.nih.gov/pubmed/24455420>.

MANGGE, H., *et al.* Obesity-related dysregulation of the tryptophan-kynurenine metabolism: role of age and parameters of the metabolic syndrome. *Obesity (Silver Spring),* v. 22, i. 1, p. 195-20. 2014. Available from: <https://doi.org/10.1002/oby.20491>.

MARET, W. Zinc and the zinc proteome. *Met Ions Life Sci,* v. 12, p. 479-501. 2013a. Available from: <https://doi.org/10.1007/978-94-007-5561-1_14>.

MARET, W. Zinc biochemistry: from a single zinc enzyme to a key element of life. *Adv Nutr, v.* 4, i. 1, p.:82-91. 2013b. Available from: <https://doi.org/10.3945/an.112.003038>.

MARET, W. 2015. Analyzing free zinc(II) ion concentrations in cell biology with fluorescent chelating molecules. *Metallomics*, v. 7, i. 2, p.202-211. 2013b. Available from: <https://doi.org/10.1039/c4mt00230j>.

MARET, W., and SANDSTEAD, H., H. Zinc requirements and the risks and benefits of zinc supplementation. *J Trace Elem Med Biol,* v. 20, i. 1, p. 3-18. 2006. Available from: <https://doi.org/10.1016/j.jtemb.2006.01.006>.

MARET, W. Zinc in Cellular Regulation: The Nature and Significance of Zinc Signals. *Int. J. Mol. Sci*, v. 18, i. 11, p. 22-85. 2017. Available from: <https://doi.org/10.3390/ijms18112285>.

MAREI, W.F.A. *et al.* Differential effects of high fat diet-induced obesity on oocyte mitochondrial functions in inbred and outbred mice. *Sci Rep*, v.10, p.98-106. 2020. Available from: <https://doi.org/https://doi.org/10.1038/s41598-020-66702-6>.

MARIC, T., WOODSIDE, B. and LUHESHI, G. N. The effects of dietary saturated fat on basal hypothalamic neuroinflammation in rats. *Brain, Behavior, and Immunity*, v. 36, p. 35-45. 2014. Available from: <https://doi.org/https://doi.org/10.1016/j.bbi.2013.09.011.>.

MARQUES, E. L., *et al*. Changes in neuropsychological tests and brain metabolism after bariatric surgery. *J Clin Endocrinol Metab,* v. 99, i. 11, p. 2347-2352. 2014. Available from: <https://doi.org/10.1210/jc.2014-2068>.

MARREIRO, D. N., FISBERG, M., and COZZOLINO, S. M. Zinc nutritional status in obese children and adolescents. *Biol Trace Elem Res,* v. 86, i. 2, p.107-122. 2002.

MARREIRO, D. N., FISBERG, M., and COZZOLINO, S. M. Zinc nutritional status and its relationships with hyperinsulinemia in obese children and adolescents. *Biol Trace Elem Res,* v. 100, i. 2, p. 137-149. 2004.

MAYER, L. S. *et al*. Uciechowski, P. Meyer, S. Schwerdtle, T. Rink, L. and Haase, H. Differential impact of zinc deficiency on phagocytosis, oxidative burst, and production of pro-inflammatory cytokines by human monocytes. *Metallomics*, vol. 6, no. 7, pp. 1288–1295. 2014.

MAZZATTI, D. J., *et al.* Effects of long-term zinc supplementation and deprivation on gene expression in human THP-1 mononuclear cells. *J Trace Elem Med Biol* 22, v. 4, p.325-336. 2008. Available from: <https://doi.org/10.1016/j.jtemb.2008.06.002>.

McGILL, A.T. Obesity-Related Metabolic Syndrome: Investigations into Novel Clinical Markers and Possible Causes. *Doctor, Sciences/Medicine and Health Science.* The University of Auckland. 2011.

McGILL Malnutritive Obesity (‘Malnubesity’): Is It Driven by Human Brain Evolution? *Metabolic Syndrome and Related Disorders*. v. 6, i. 4, p. 241-246. 2008.

MELDRUM, D. R., MORRIS, M. A. and GAMBONE, J. C. Obesity pandemic: causes, consequences, and solutions-but do we have the will? *Fertil Steril,*v. 107, i. 4, p.833-839. 2017. Available from: <https://doi.org/10.1016/j.fertnstert.2017.02.104>.

MILAGRO, I., *et al*. *Principles of Nutrigenetics and Nutrigenomics Chapter 58 Nutrients, Obesity and Gene Expression*. Edited by Elsevier Inc. 2020.

MILANSKI, M., *et al*. Saturated fatty acids produce an inflammatory response predominantly through the activation of TLR4 signaling in hypothalamus: implications for the pathogenesis of obesity. *J Neurosci,*v. 29, i. 2, p.359-370. 2009. Available from: <https://doi.org/10.1523/JNEUROSCI.2760-08.2009>.

MŁYNIEC, K. *et al*. The role of the GPR39 receptor in zinc deficient-animal model of depression. *Behavioural Brain Research*, v. 238. p 30-35. 2013. Available from: <https://doi.org/10.1016/j.bbr.2012.10.020>.

MIQUEL, E., and FARRÉ, R. Effects and future trends of casein phosphopeptides on zinc bioavailability, *Trends in Food Science & Technology,* v. 18, i. 3, p. 139-143, 2007. Available from: <https://doi.org/10.1016/j.tifs.2006.11.004>.

MIYAZAKI, T., *et al*. Indoleamine 2,3-dioxygenase as a new target for malignant glioma therapy. Laboratory investigation. *J Neurosurg,* v. 111, i. 2, p. 230-237, 2009. Available from: <https://doi.org/10.3171/2008.10.JNS081141>.

MOSMANN, T. Rapid colorimetric assay for cellular growth and survival: application to proliferation and cytotoxicity assays. *J Immunol Methods* 65, v. 1, i. 2, p. 55-63, 1983. Available from: <https://doi.org/10.1016/0022-1759(83)90303-4>.

MORRIS, D.L., and RUI L. Recent advances in understanding leptin signaling and leptin resistance. *Am J Physiol Endocrinol Metab*, v. 297, p. 1247-1259. 2009.

MOTA MARTINS L., *et al*. Influence of cortisol on zinc metabolism in morbidly obese women. *Nutr Hosp* v. 29, i. 1, p.57–63, 2014. Available from: <https://doi.org/10.3305/nh.2014.29.1.6890>.

MYLES, I. A. Fast food fever: reviewing the impacts of the Western diet on immunity. *Nutr J,* v. 13, i. 61. 2014. Available from: <https://doi.org/10.1186/1475-2891-13-61>.

MURPHY, K., and BLOOM, S. Gut hormones and the regulation of energy homeostasis. *Nature* v. 444, p. 854–859. 2006. Available from: <https://doi.org/10.1038/nature05484>.

NAGANO, J., *et al*. Effects of indoleamine 2,3-dioxygenase deficiency on high-fat diet-induced hepatic inflammation. *PLoS One* 8 v. 9. 2013. Available from: <https://doi.org/10.1371/journal.pone.0073404>.

NAZEM, M. R., *et al*. Mutual Interaction between Obesity and Zinc Deficiency. *Jacobs Journal of Obesity*, v. 2, i. 2, p. 28-36. 2016.

NGUYEN, J.C. KILLCROSS, A.S., and JENKINS, T. A. Obesity and cognitive decline: role of inflammation and vascular changes. *Front Neurosci,* v. 8, i. 375. 2014. Available from: <https://doi.org/10.3389/fnins.2014.00375>.

NGUYEN, D. M. and EL-SERAG, H. B. The epidemiology of obesity. *Gastroenterol Clin North Am.* v. 39 i.1, p.1-7. 2010. Available from: <hhttps://doi.org/10.1016/j.gtc.2009.12.014>.

NICOLAIDIS, S. Environment and obesity. *Metabolism*. i. 100, Supplement. 2019. Available from: <https://doi.org/10.1016/j.metabol.2019.07.006>.

NIHR, National Institute for Health Research. *Hydrostatic underwater weighing*. 2020.

NILSSON, C. *et al*. Laboratory animals as surrogate models of human obesity. *Acta Pharmacol*. Sin. 33, p. 173–181. 2012.

NOCON, M., KEIL, T. and WILLICH, S.N. Education, income, occupational status and health risk behaviour. *J Public Health*, v. 15, p. 401–405. 2007. Available from: <https://doi.org/10.1007/s10389-007-0120-6>.

NOVELLI, E. L., *et al*. Anthropometrical parameters and markers of obesity in rats. *Lab Anim,* v. 41, i. 1, p. 111-119. 2007. Available from: <https://doi.org/10.1258/002367707779399518>.

OKORODUDU, D. O. *et al*. Diagnostic performance of body mass index to identify obesity as defined by body adiposity: a systematic review and meta-analysis. *Int J Obes (Lond),* v. 34, in.5, p. 791-9. 2010. Available from: <https://doi.org/10.1038/ijo.2010.5>.

OLLIG, J., *et al.* Parameters Influencing Zinc in Experimental Systems in Vivo and in Vitro. *Metals*. 2016. Available from: <https://doi.org/doi:10.3390/met6030071>.

OLZA, J., *et al*. Reported Dietary Intake and Food Sources of Zinc, Selenium, and Vitamins A, E and C in the Spanish Population: Findings from the ANIBES Study. *Nutrients,* v. 9, i. 7. 2017. Available from: <https://doi.org/10.3390/nu9070697>.

OMU, A. E., *et al*. Molecular basis for the effects of zinc deficiency on spermatogenesis: An experimental study in the Sprague-dawley rat model. *Indian Journal of Urology: IJU: Journal of the Urological Society of India*, v. 31, i. 1, p. 57–64. 2015. Available from: <https://doi.org/10.4103/0970-1591.139570>.

OSBORN, O., and OLEFSKY, J. M. The cellular and signaling networks linking the immune system and metabolism in disease. *Nat Med,* v. 18, i. 3, p. 363-374. 2012. Available from: <https://doi.org/10.1038/nm.2627>.

OUCHI, N., *et al*. Adipokines in inflammation and metabolic disease. *Nat Rev Immunol* v. 11, i. 2, p.85-97. 2011. Available from: <https://doi.org/10.1038/nri2921>.

OZATA, M., *et al.* Increased oxidative stress and hypozincemia in male obesity. *Clin Biochem,* v. 35, i. 8, p. 627-631. 2002.

PAERATAKUL, S. *et al.* The relation of gender, race and socioeconomic status to obesity and obesity comorbidities in a sample of US adults. *Int J Obes***,** v. 26, p. 1205–1210. 2002. Available from: <https://doi.org/10.1038/sj.ijo.0802026>.

PALAZIDOU, E. The neurobiology of depression. *Br Med Bull,* v. 101, p.127-145. 2012. Available from: <https://doi.org/10.1093/bmb/lds004>.

PAN, A., *et al*. Bidirectional association between depression and obesity in middle-aged and older women. *Int J Obes (Lond),* v. 36, i. 4, p. 595-602. 2012. Available from: <https://doi.org/10.1038/ijo.2011.111>.

PANDIT, R. *et al.* Dietary factors affect food reward and motivation to eat. *Obes Facts*. v. 5, n.2, p.221-242, 2012. Available from: <https://doi.org/10.1159/000338073>.

PAPAKOSTAS, G. I., *et al.* Assessment of a multi-assay, serum-based biological diagnostic test for major depressive disorder: a pilot and replication study. *Mol Psychiatry* v. 18, i. 3, p. 332-9. 2013. Available from: <https://doi.org/10.1038/mp.2011.166>.

PAZ-FILHO, G., *et al.* Leptin: molecular mechanisms, systemic pro-inflammatory effects, and clinical implications. *Arq Bras Endocrinol Metabol,* v. 56, i. 9, p. 597-607. 2012.

PENDYALA S., WALKER, J.M., and HOLT, P.R. A high-fat diet is associated with endotoxemia that originates from the gut. *Gastroenterology,* v. 142, i. 5, p.:1100-1101. 2012. Available from: <https://doi.org/10.1053/j.gastro.2012.01.034>.

PESCATORI, L. C. *et al*. Quantification of visceral adipose tissue by computed tomography and magnetic resonance imaging: reproducibility and accuracy. *Radiol Bras*, v. 52, i.1, p.1–6, 2019.

PISTELL, P. J. *et al.* Cognitive impairment following high fat diet consumption is associated with brain inflammation. J Neuroimmunol, v. 219, i. 1-2, p. 25-32, Feb /2010. Available from: <https://www.ncbi.nlm.nih.gov/pubmed/20004026>.

POPKIN, B. M., and GORDON-LARSEN, P. The nutrition transition: worldwide obesity dynamics and their determinants. Int J Obes Relat Metab Disord, v. 28 Suppl 3, p. S2-9, Nov/2004. Available from: <https://www.ncbi.nlm.nih.gov/pubmed/15543214>.

POPKO, K. *et al.* Proinflammatory cytokines Il-6 and TNF-α and the development of inflammation in obese subjects. *Eur J Med Res*, v. 15 Suppl 2, p. 120-2, Nov/2010. Available from: <https://www.ncbi.nlm.nih.gov/pubmed/21147638>.

PORTOVEDO M, *et al*. Saturated Fatty Acids Modulate Autophagy's Proteins in the Hypothalamus. *PLoS ONE*, v. 10, i. 3. 2015. Available from: <https://doi.org/10.1371/journal.pone.0119850>.

PRASAD, A. S., HALSTED, J. A., and NADIMI, M. Syndrome of iron deficiency anemia, hepatosplenomegaly, hypogonadism, dwarfism and geophagia. *Am J Med* 31:532-46. 1961.

PRICE, J. L., and DREVETS, W. C. Neural circuits underlying the pathophysiology of mood disorders. *Trends Cogn Sci,* v. 16, i. 1, p. 61-71. 2012. Available from: <https://doi.org/10.1016/j.tics.2011.12.011>.

QIAN, X. *et al*. Changes in distributions of waist circumference, waist-to-hip ratio and waist-to-height ratio over an 18-year period among Chinese adults: a longitudinal study using quantile regression. *BMC Public Health***,** v.19, i.1, p.700, 2019. Available from: <https://doi.org/10.1186/s12889-019-6927-6>.

QIN, Y., *et al*. IDO and TDO as a potential therapeutic target in different types of depression. *Metab Brain Dis*. 2018. Available from: <https://doi.org/10.1007/s11011-018-0290-7>.

RADILLA-VÁZQUEZ, R. B., *et al*. Gut Microbiota and Metabolic Endotoxemia in Young Obese Mexican Subjects. *Obes Facts,* v. 9, i. 1, p. 1-11. 2016. Available from: <https://doi.org/10.1159/000442479>.

REEVES, P. G., NIELSEN, F. H., and FAHEY, G. C. AIN-93 purified diets for laboratory rodents: final report of the American Institute of Nutrition ad hoc writing committee on the reformulation of the AIN-76A rodent diet. *J Nutr,* v. 123, i. 11, p. 1939-1951. 1993.

REFAEY, M. E., et al. Kynurenine, a Tryptophan Metabolite That Accumulates With Age, Induces Bone Loss. *J Bone Miner Res,* v. 32, i. 11, p. 2182-2193. 2017. Available from: <https://doi.org/10.1002/jbmr.3224>.1993.

REILLY, S.M. and SALTIEL, A. R. Adapting to obesity with adipose tissue inflammation. *Nat Rev Endocrinol*, v. 13, i. 11, p. 633-643. 2017. Available from: <https://doi.org/10.1038/nrendo.2017.90>.

REININGHAUS, E. Z., *et al*. Tryptophan breakdown is increased in euthymic overweight individuals with bipolar disorder: a preliminary report. *Bipolar Disord,* v. 16, i. 4, p. 432-40. 2014. Available from: <https://doi.org/10.1111/bdi.12166>.

RICHARD, D. M. *et al*. L-Tryptophan: Basic Metabolic Functions, Behavioral Research and Therapeutic Indications. *Int J Tryptophan Res*, v. 2, p. 45-60. 2009.

RICHARDSON, D.R. and BAKER, E. Two saturable mechanisms of iron uptake from transferrin in human melanoma cells: The effect of transferrin concentration, chelators, and metabolic probes on transferrin and iron uptake. *J. Cell. Physiol*, v. 161, p. 160-168. 1994. Available from: <https://doi.org/10.1002/jcp.1041610119>.

RIOS-LUGO, M.J., *et al*. Association of Serum Zinc Levels in Overweight and Obesity. *Biol Trace Elem Res,* v. 198, p. 51–57. 2020. Available from: <https://doi.org/10.1007/s12011-020-02060-8>.

ROCHFORT, K., CUMMINS, D., and PHILIP M. The blood–brain barrier endothelium: a target for pro-inflammatory cytokines. *Biochem Soc Trans*, v. 43, i. 4, p. 702-706. Aug/2015. Available from: <https://doi.org/10.1042/BST20140319>.

RODRÍGUEZ E.M., BLÁZQUEZ J.L., and GUERRA M. The design of barriers in the hypothalamus allows the median eminence and the arcuate nucleus to enjoy private milieus: the former opens to the portal blood and the latter to the cerebrospinal fluid. *Peptides*, v. 31, i. 4, p.757-776. 2010. Available from: <https://doi.org/10.1016/j.peptides.2010.01.003>.

ROUMESTAN, C., *et al.* Anti-inflammatory properties of desipramine and fluoxetine. *Respir. Res,* v. 8, i. 35. 2007.

ROOHANI, N., *et al*. Zinc and its importance for human health: An integrative review. *J Res Med Sci,* v. 18, i. 2, p. 144-157. 2013.

ROSEN, E. D., and SPIEGELMAN, B. M. Adipocytes as regulators of energy balance and glucose homeostasis. *Nature,* v. 444, i. 7121, p.:847-53. 2006. Available from: <https://doi.org/10.1038/nature05483>.

ROSEN, E. D., and SPIEGELMAN, B. M. What we talk about when we talk about fat. *Cell,* v. 156, i.1-2, p.20-44. 2014. Available from: <https://doi.org/10.1016/j.cell.2013.12.012>.

ROTONDO, F., *et al*. Quantitative analysis of rat adipose tissue cell recovery, and non-fat cell volume, in primary cell cultures. *PeerJ,* v. 4, i. e2725. 2016. Available from: <https://doi.org/10.7717/peerj.2725>.

RUDDICK, J.P., *et al.* Tryptophan metabolism in the central nervous system: medical implications. *Expert Rev Mol Med*, v. 8, i. 20, p. 1-27. Ago/2006. Available from: <https://doi.org/10.1017/S1462399406000068>.

RUSH, A. J., *et al.* Acute and longer-term outcomes in depressed outpatients requiring one or several treatment steps: a STAR*D report. *Am J Psychiatry,* v. 163, i. 11, p. 1905-1917. 2006. Available from: <https://doi.org/10.1176/ajp.2006.163.11.1905>.

RUSSO, L., and LUMENG, C. N. Properties and functions of adipose tissue macrophages in obesity. *Immunology,* v. 155, i. 4, p. 407-417. 2018. Available from: <https://doi.org/10.1111/imm.13002>.

SAINIO, E. L., PULKKI, K., and YOUNG, S. N. L-Tryptophan: Biochemical, nutritional and pharmacological aspects. *Amino Acids,* v. 10, i. 1, p. 21-47. 1996. Available from: <https://doi.org/10.1007/BF00806091>.

SAITO, M. Brown adipose tissue as a regulator of energy expenditure and body fat in humans. *Diabetes Metab J,* v.37, i.1, p.22-9. 2013. Available from: <https://doi.org/10.4093/dmj.2013.37.1.22>.

SAMODIEN, E., *et al*. Diet-induced hypothalamic dysfunction and metabolic disease, and the therapeutic potential of polyphenols. *Molecular Metabolism*, v. 27, p. 1-10, 2019. Available from: <https://doi.org/10.1016/j.molmet.2019.06.022>.

SCHACHTER, J., *et al.* Effects of obesity on depression: a role for inflammation and the gut microbiota. *Brain, Behavior, and Immunity.* 2017. Available from: <https://doi.org/10.1016/j.bbi.2017.08.026>.

SCHÄFFLER, A., and SCHÖLMERICH, J. Innate immunity and adipose tissue biology. *Trends Immunol,* v. 31, i. 6, p. 228-235. 2010. Available from: <https://doi.org/10.1016/j.it.2010.03.001>.

SCHMIDT K., *et al.* Zinc-transporter genes in human visceral andsubcutaneous adipocytes: lean versus obese. *Mol Cell Endocrinol*.v. 264, p. 68–73, i.28, 2007.

SCHOETTL, T. FISCHER, I. P. and USSAR, S. Heterogeneity of adipose tissue in development and metabolic function. *J Exp Biol*. v. 221 (Pt Suppl 1). 2018. Available from: <https://doi.org/10.1242/jeb.162958>.

SELASSIE, M. and SINHA, A.C. The epidemiology and aetiology of obesity: A global challenge. *Best Practice & Research Clinical Anaesthesiology,* v. 25, i.1, p. 1-9, 2011. Available from: <https://doi.org/10.1016/j.bpa.2011.01.002>.

SEVERO, J.S., *et al*. Role of Zinc in Zinc-α2-Glycoprotein Metabolism in Obesity: a Review of Literature. *Biol Trace Elem Res* v. 193, p. 81–88, 2020. Available from: <https://doi.org/10.1007/s12011-019-01702-w>.

SHI, H., *et al*. TLR4 links innate immunity and fatty acid-induced insulin resistance. *J Clin Invest,* v. 116, i. 11, p. 3015-25. 2006. Available from: <https://doi.org/10.1172/JCI28898>.

SINGH, R.B., *et al*. Association of low plasma concentrations of antioxidant vitamins, magnesium and zinc with high body fat per cent measured by bioelectrical impedance analysis in Indian men. *Magnes Res*., v.11, i. 1, p.3-10, Mar/1998.

SMITH, D. F., and JAKOBSEN, S. Molecular Neurobiology of Depression: PET Findings on the Elusive Correlation with Symptom Severity. *Front Psychiatry,* v. 4, i.8. 2013. Available from: <https://doi.org/10.3389/fpsyt.2013.00008>.

SOHN, K. Sufficiently good measures of obesity: the case of a developing country. *J Biosoc Sci,* v. 46, i. 6, p. 797-817. 2014. Available from: <https://doi.org/10.1017/S0021932013000692>.

STATOVCI, D. *et al*. The Impact of Western Diet and Nutrients on the Microbiota and Immune Response at Mucosal Interfaces. *Front Immunol,* v. 8, i. 838. 2017. Available from: <https://doi.org/10.3389/fimmu.2017.00838>.

STEIN, G.H. T98G: An anchorage-independent human tumor cell line that exhibits stationary phase G1 arrest in vitro. *J. Cell. Physiol*., v. 99: p. 43-54. 1979. Available from: <https://doi.org/10.1002/jcp.1040990107>.

STOLARCZYK, E. Adipose tissue inflammation in obesity: a metabolic or immune response? *Curr Opin Pharmacol,* v.37, p.35-40, 2017. Available from: <https://doi.org/10.1016/j.coph.2017.08.006>.

STRANAHAN, A. M., *et al.* Blood–brain barrier breakdown promotes macrophage infiltration and cognitive impairment in leptin receptor-deficient mice. *Journal of Cerebral Blood Flow & Metabolism,* p. 36, i. 12, p. 2108–2121. 2016. Available from: <https://doi.org/10.1177/0271678X16642233>.

STYCZEŃ, K., *et al*. The serum zinc concentration as a potential biological marker in patients with major depressive disorder. *Metabolic brain disease,* v. 32, i. 1, p. 97–103. 2017. Available from: <https://doi.org/10.1007/s11011-016-9888-9>.

SURWIT, R., and COLLINS, S. Revisiting lessons from the C57BL/6J mouse. *Am J Physiol Endocrinol Metab,* v. 280, i. 6. 2001.

SULEIMAN, J. B., MOHAMED, M. and BAKAR, A. B. A. A systematic review on different models of inducing obesity in animals: Advantages and limitations. *J Adv Vet Anim Res,* v. 7, i.1, p.103-114, 2020. Available from: <https://doi.org/10.5455/javar.2020.g399>.

SUN, T., J. *et al*. [Preparation of selectively decellular xenoskin and its biocompatibility]. *Zhongguo Xiu Fu Chong Jian Wai Ke Za Zhi,* v. 24, i. 6, p. 668-672. 2010.

SUZUKI, K., JAYASENA, C.N., and BLOOM, S.R. Obesity and appetite control. *Experimental Diabetes Research*. 2012. Available from: <https://doi.org/10.1155/2012/824305>.

SWARDFAGER, W., *et al*. Potential roles of zinc in the pathophysiology and treatment of major depressive disorder. *Neurosci Biobehav Rev,* v. 37, i. 5, p. 911-929. 2013. Available from: <https://doi.org/10.1016/j.neubiorev.2013.03.018>.

TAKASHIBA, S., *et al.* Differentiation of monocytes to macrophages primes cells for lipopolysaccharide stimulation via accumulation of cytoplasmic nuclear factor kappaB. *Infect Immun,* v. 67, i. 11, p. 5573-8. 1999.

TALLMAN, D. L., and. TAYLOR, C. G. Effects of dietary fat and zinc on adiposity, serum leptin and adipose fatty acid composition in C57BL/6J mice. *J Nutr Biochem* 14 (1):17-23. 2003.

TAN, B. L., and NORHAIZAN, M. E. Effect of High-Fat Diets on Oxidative Stress, Cellular Inflammatory Response and Cognitive Function. *Nutrients*, v. 11, i. 11. 2019. Available from: <https://doi.org/10.3390/nu11112579>.

TANAKA, A., *et al.* Association of increased indoleamine 2, 3-dioxygenase with impaired natural killer cell activity in hemodialysis patients. *Ther Apher Dial,* v. 18, i. 1, p. 19-23. 2014. Available from: <https://doi.org/10.1111/1744-9987.12071>.

TANDON, P. WAFER, R., and MINCHIN, J. E. N. Adipose morphology and metabolic disease. *Journal of Experimental Biology*, mar/2018 Available from: <https://doi.org/10.1242/jeb.164970>.

TAPIERO, H., and TEW, K. D. Trace elements in human physiology and pathology: zinc and metallothioneins. *Biomed Pharmacother,* v. 57, i. 9, p. 399-411. 2003.

TASSABEHJI, N. *et al*. Zinc deficiency induces depression-like symptoms in adult rats. *Physiology & Behavior*. V. 95, i. 3, p. 365-369, 2008. Available from: <https://doi.org/10.1016/j.physbeh.2008.06.017>.

TATARANNI, P. A. and DELPARIGI, A. Functional neuroimaging: a new generation of human brain studies in obesity research. *Obesity reviews*, v. 4, 229–238. 2003.

THALER, J.P., *et al.* Obesity is associated with hypothalamic injury in rodents and humans. *J Clin Invest* v. 122, p. 153 –162, 2012.

TEDESCO S., *et al*. Convenience versus Biological Significance: Are PMA-Differentiated THP-1 Cells a Reliable Substitute for Blood-Derived Macrophages When Studying *in Vitro* Polarization? *Frontiers in Pharmacology*, v .9, p.71, 2018. Available from: <https://www.frontiersin.org/article/10.3389/fphar.2018.0007110.3389/fphar.2018.00071>.

TERRA, X., *et al*. Grape-seed procyanidins prevent low-grade inflammation by modulating cytokine expression in rats fed a high-fat diet. *J Nutr Biochem,* v. 20, i. 3, p. 210-218, 2009. Available from: <https://doi.org/10.1016/j.jnutbio.2008.02.005>.

TIMPER, K. and BRÜNING, J. C. Hypothalamic circuits regulating appetite and energy homeostasis: pathways to obesity. Dis Model Mech, v.10, i.6, p. 679-689. 2017. Available from: <https://doi.org/10.1242/dmm.026609>.

TOURINO, M. C., *et al.* Tryptamine and dimethyltryptamine inhibit indoleamine 2,3 dioxygenase and increase the tumor-reactive effect of peripheral blood mononuclear cells. *Cell Biochem Funct,* v. 31, i. 5, p.361-4. 2013. Available from: <https://doi.org/10.1002/cbf.2980>.

TREDE, N. S., *et al.* Transcriptional activation of human TNF-alpha promoter by superantigen in human monocytic cells: role of NF-kappa B. J. *Immunol.*, v. 155, p. 902–908. 1995.

TSUCHIYA, S. *et al.* Induction of Maturation in Cultured Human Monocytic Leukemia Cells by a Phorbol Diester. *Cancer Res.,* v. 42, i. 4, p. 1530-1536, Apr/1982.

TUSSING-HUMPHREYS L., NGUYEN V.T.Q. Obesity and Micronutrient Deficiencies. In: Fantuzzi G., Braunschweig C. (eds) Adipose Tissue and Adipokines in Health and Disease. *Nutrition and Health*. Humana Press, Totowa, NJ. 2014.

VAN DE STEENE, J. C., and LAMBERT, W. E. Comparison of matrix effects in HPLC-MS/MS and UPLC-MS/MS analysis of nine basic pharmaceuticals in surface waters. *J Am Soc Mass Spectrom,* v. 19, i. 5, p. 713-8. 2008. Available from: <https://doi.org/10.1016/j.jasms.2008.01.013>.

VARATHARAJ, A., and GALEA, I. The blood-brain barrier in systemic inflammation. *Brain, Behavior, and Immunity*, v. 60, p. 1-12. 2017. Available in: <https://doi.org/10.1016/j.bbi.2016.03.010>.

VIA, M. The Malnutrition of Obesity: Micronutrient Deficiencies That Promote Diabetes. *International Scholarly Research Notices,* Article ID 103472, 2012. Available from: <https://doi.org/10.5402/2012/103472>.

VIGITEL, Excess Weight and Obesity. *Vigilância de fatores de risco e proteção para doenças crônicas por inquérito telefônico.* 2014.

VIGNAU, J., *et al*. Simultaneous determination of tryptophan and kynurenine in serum by HPLC with UV and fluorescence detection. *Biomed Chromatogr,* v. 18, i. 10, p. 872-4. 2004. Available from: <https://doi.org/10.1002/bmc.445>.

VON BÜLOW, V., *et al*. Zinc-dependent suppression of TNF-alpha production is mediated by protein kinase A-induced inhibition of Raf-1, I kappa B kinase beta, and NF-kappa B. *J Immunol*, v. 179, i. 6, p. 4180-6. 2007.

WALKUP, G.K., *et al.* A New Cell-Permeable Fluorescent Probe for Zn2+. *J Am Chem Soc,* v. 122, p. 5644–5. 2000.

WANG, J.; *et al*. Zinc, Magnesium, Selenium and Depression: A Review of the Evidence, Potential Mechanisms and Implications. *Nutrients*, v. 10, i. 584. 2018.

WANG, N., LIANG, H., and ZEN, K. Molecular mechanisms that influence the macrophage M1-M2 polarization balance. *Front Immunol,* v. 5, i. 614. 2014. Available from: <https://doi.org/10.3389/fimmu.2014.00614>.

WANG, Z., *et al*. Estimation of percentage body fat by dual-energy x-ray absorptiometry: evaluation by in vivo human elemental composition. *Phys Med Biol,* v. 55, i. 9, p. 2619-35. 2010. Available from: <https://doi.org/10.1088/0031-9155/55/9/013>.

WANG, Y., *et al.* LPS-induced indoleamine 2,3-dioxygenase is regulated in an interferon-gamma-independent manner by a JNK signaling pathway in primary murine microglia. *Brain*

Behav. Immun, v. 24, p. 201–209. 2010. Available from: <https://doi.org/10.1016/j.bbi.2009.06.152>.

WAQAR R. M. Serum Zinc Level in Children Presenting with Febrile Seizures. *Pakistan journal of medical sciences*, v. 29, i. 4, p. 1008–1011. 2013.

WEISBERG, S. P., *et al*. Obesity is associated with macrophage accumulation in adipose tissue. *J Clin Invest,* v. 112, i. 12, p. 1796-808. 2003. Available from: <https://doi.org/10.1172/JCI19246>.

WELLENREUTHER, G., *et al.* The ligand environment of zinc stored in vesicles. *Biochem Biophys Res Commun,* v. 380, i. 1, p. 198-203. 2009. Available from: <https://doi.org/10.1016/j.bbrc.2009.01.074>.

WESSELS, I., *et al*. Zinc deficiency induces production of the proinflammatory cytokines IL-1β and TNFα in promyeloid cells via epigenetic and redox-dependent mechanisms. *J Nutr Biochem*, v. 24, i. 1, p.289-97. 2013. Available from: <https://doi.org/10.1016/j.jnutbio.2012.06.007>.

WHITE, P. A. *et al*. Model of high-fat diet-induced obesity associated to insulin resistance and glucose intolerance. *Arq Bras Endocrinol Metabol,* v. 57, i. 5, p. 339-45, Jul 2013. Available from: <https://www.ncbi.nlm.nih.gov/pubmed/23896799>.

WHITTEN, L.A. Functional Magnetic Resonance Imaging (fMRI): An Invaluable Tool in Translational Neuroscience. *Research Triangle Park (NC): RTI Press*, Dec/2012. Available from: <https://doi.org/10.3768/rtipress.2012.op.0010.1212>.

WHO. Nutrition, Physical Activity and Obesity Germany. 2013. Available from: <http://www.euro.who.int/__data/assets/pdf_file/0011/243299/Germany-WHO-Country-Profile.pdf?%20ua=1>.

WHO. Obesity. World Health Organization. 2016. Available from: <https://www.who.int/health-topics/obesity#tab=tab_1>.

WHO, World Health Organization. Depression and Other Common Mental Disorders. Geneva: CC BY-NC-AS 3.0 IGO. 2017.

WILLEUMIER, K. C., D. V. Taylor, and D. G. Amen. Elevated BMI is associated with decreased blood flow in the prefrontal cortex using SPECT imaging in healthy adults. *Obesity (Silver Spring),* v. 19, i.5, p. 1095-7. 2011. Available from: <https://doi.org/10.1038/oby.2011.16>.

WILLNER, P. Chronic mild stress (CMS) revisited: consistency and behavioural-neurobiological concordance in the effects of CMS. *Neuropsychobiology*, v. 52, i. 2, p. 90-110. 2005. Available from: <https://doi.org/10.1159/000087097>.

WILSON, J.L., and ENRIORI, P.J. A talk between fat tissue, gut, pancreas and brain to control body weight. *Mol Cell Endocrinol*, v. 418, p. 108–119. 2015.

WITHROW, D., and ALTER, D. A. The economic burden of obesity worldwide: a systematic

review of the direct costs of obesity. *Obes Rev,* v. 12, i. 2, p. 131-41. 2011. Available from: <https://doi.org/10.1111/j.1467-789X.2009.00712.x>.

WOHLEB, E. S., *et al*. Integrating neuroimmune systems in the neurobiology of depression. *Nat Rev Neurosci,* v. 17, i. 8, p. 497-511. 2016. Available from: <https://doi.org/10.1038/nrn.2016.69>.

WOLF, K., *et al*. Tumour necrosis factor-alpha induced CD70 and interleukin-7R mRNA expression in BEAS-2B cells. *Eur Respir J,* v. 20, i. 2, p. 369-75. 2002.

WONG, C. P., MAGNUSSON, K. R., and HO., E. Increased inflammatory response in aged mice is associated with age-related zinc deficiency and zinc transporter dysregulation. *J Nutr Biochem,* v. 24, i. 1, p. 353-9. 2013. Available from: <https://doi.org/10.1016/j.jnutbio.2012.07.005>.

WONG ML, and LICINIO J. Research and treatment approaches to depression. *Nat Rev Neurosci.*, v.2, p.343–51. 2001

WOODS, S. C., and DAVID, A. D. Central control of body weight and appetite. *The Journal of clinical endocrinology and metabolism,* v. 93, i.11, Suppl 1: S37-50. 2008. Available from: <https://doi.org/10.1210/jc.2008-1630>.

WRIGHT, S. M., and ARNONE, L. J. Causes of obesity. *Abdom Imaging.*, v.37, i. 5, p. 730-2. 2012. Available from: <https://doi.org/10.1007/s00261-012-9862-x>.

XANTHAKOS, S. A. Nutritional deficiencies in obesity and after bariatric surgery. *Pediatr Clin North Am,* v. 56, i. 5, p. 1105-21. 2009. Available from: <https://doi.org/10.1016/j.pcl.2009.07.002>.

XIAO, C., et al. A modified HPLC method improves the simultaneous determination of plasma kynurenine and tryptophan concentrations in patients following maintenance hemodialysis. *Exp Ther Med,* v. 7, i. 4, p. 907-910. 2014. Available from: <https://doi.org/10.3892/etm.2014.1512>.

YALCIN, I., AKSU, F., and BELZUNG, C. Effects of desipramine and tramadol in a chronic mild stress model in mice are altered by yohimbine but not by pindolol. *Eur J Pharmacol,* v. 514, i.2-3, p. 165-74. 2005. Available from: <https://doi.org/10.1016/j.ejphar.2005.03.029>.

YANG, L., *et al*. 4,6-Substituted-1H-Indazoles as potent IDO1/TDO dual inhibitors. *Bioorg Med Chem,* v. 27, i. 6, p. 1087-1098. 2019. Available from: <https://doi.org/10.1016/j.bmc.2019.02.014>.

YABUT, J. M. C., *et al*. Emerging Roles for Serotonin in Regulating Metabolism: New Implications for an Ancient Molecule. *Endocrine Reviews,* v. 40, i 4, p. 1092–1107, Aug/2019. Available from: <https://doi.org/10.1210/er.2018-00283>.

YAMADA, N. *et al*. Impaired CNS Leptin Action Is Implicated in Depression Associated with Obesity, *Endocrinology*, v. 152, i. 7, p. 2634–2643, Jul/2011, Available from: <https://doi.org/10.1210/en.2011-0004>.

YI, C. X., and TSCHÖP, M. H. Brain-gut-adipose-tissue communication pathways at a glance. *Dis Model Mech*, v. 5, i. 5, p. 583-587, 2012. Available from: <https://doi.org/10.1242/dmm.009902>.

YOKOTA, T., ORITANI, K., and TAKAHASHI, I., *et al.* Adiponectin, a new member of the family of soluble defense collagens, negatively regulates the growth of myelomonocytic progenitors and the functions of macrophages. *Blood*, v. 96: 1723–1732. 2000.

ZALEWSKI, P. *et al*. Use of a zinc fluorophore to measure labile pools of zinc in body fluids and cell-conditioned media. *BioTechniques*, v. 40, i. 4, p. 509-520, 2006. Available from: <https://doi.org/doi.org/10.2144/06404RR02>.

ZANCHI, D., *et al.* The impact of gut hormones on the neural circuit of appetite and satiety: A systematic review. *Neurosci Biobehav Rev.,* v. 80, p. 457-475. 2017. Available from: <https://doi.org/10.1016/j.neubiorev.2017.06.013>.

ZHAO, G., *et al*. Waist circumference, abdominal obesity, and depression among overweight and obese U.S. adults: National Health and Nutrition Examination Survey 2005-2006. *BMC Psychiatry,* v. 11, i. 130. 2011. Available from: <https://doi.org/10.1186/1471-244X-11-130>.

ZHOU, Y., and RUI L. Leptin signaling and leptin resistance. *Front Med*., v. 7, i. 2, p.207-222. Jun/2013. Available from: <https://doi.org/10.1007/s11684-013-0263-5>.

ZHOU, H., URSO, C.J., and JADEJA, V. Saturated Fatty Acids in Obesity-Associated Inflammation. *J Inflamm Res.,* v.13, p. 1-14. Jan/2020. Available from: <https://doi.org/10.2147/JIR.S229691>.